Ref:.............

MASTER THESIS

Science and Technology
Electrical Engineering
Renewable Energies

Theme

DTC control of an asynchronous propulsion engine for an electric vehicle

Submitted by	Supervised by
GHODBANE Ahmed Marouane	Dr.TERKI Amel

In front of the jury composed of :

Mr. CHERIET Ahmed	Professor	Chairman
Mrs.TERKI Amel	Lecturer class A	Supervisor
Mr. DENDOUGA Abdelhakim	Lecturer class A	Examiner

Ref:............

A dissertation submitted to electrical engineering department of Biskra university in partial fulfillment of the requirements for the degree of master in renewable energies option Photovoltaic

Theme

DTC control of an asynchronous propulsion engine for an electric vehicle

Submitted by	**Favorable opinion of the supervisor**
GHODBANE Ahmed Marouane	*Dr.TERKI Amel*　　　　*signature*

Favorable opinion of Chairman

Dr. CHERIET Ahmed　　　　　　　*Signature*

Stamp and signature

Dedication

I dedicate my dissertation work to my dear parents
To my brother Dr.Houssem
who always showed me his support in my choices
To my sisters
Dr.Ghofrane and Belkiss
To my uncle Pr.Hatem .

I also dedicate this dissertation to
Pr. Benchouia Toufik and Dr. Ammar Abdelkarim
whose helped me a lot .

A special dedication for people whose have stood with me for the past five
years in particular
Mr. Baaissi Abd El-karim,
Mrs. Messaoudi Nassima
Mr.Adjal Hamza
Without forgetting Pr. Azioun Ammar.

I dedicate this work and give special thanks to Pr. Bennis Ouafae

Last but not least I dedicate this work to my best friend
Ghilani Abd El-moumen.

Acknowledgement

First of all I would like to thank ALLAH for giving us always the strength and patience to achieve the goals that we set.

Thanks for my parents , for helping me to shape my life with positivity and passion.
Without them, I'd never been the person I am today.

I Thank my supervisor Dr. A Terki for accepting to moderate this work and helping me .

Thanks to those who helped me to complete this work.

List of tables

List of figures

Chapter III

Chapter IV

List of abbreviations and symbols

BNEF   Bloomberg New Energy Finance

BMS   Battery Management System.

HF   Hybridization Factor

DOD   Depth of Discharge

FC   Fuel Cell

EV   Electric Vehicle

ICE   Internal Combustion Engine

PHEV   Plug-in Hybrid Electric Vehicles

HEV   Hybrid Electric Vehicles

SLI   Starting Lighting Ignition

PEMFC   Polymeric Electrolyte Membrane Fuel Cells

AC   Alternating Current

DC   Direct current

BLDC   Brushless DC

VRM   Variable Reluctance Motors

PM   Permanent Magnet

Enernst   Nernst voltage.

F   Faraday constant (96.487 C / K mol).

ΔS The change in entropy (J / k.mol).

R   Gas constant (8.314 J / K.mol).

PH_2, PO_2 Respectively the partial pressures of hydrogen and oxygen (atm).

T   Operating temperature (K).

T_{ref} Reference temperature (K).

J   Current density (A / cm^2)

$[V_{SABC}]$ Stator voltage vector

$[V_{rabc}]$ Rotor voltage vector

$[i_{SABC}]$ Stator current vector.

$[i_{rabc}]$ Rotor current vector.

$[\phi_{SABC}]$ Stator flux vector.

$[\phi_{rabc}]$ Rotor flux vector.

$U_{bus}(t_0)$ Initial bus voltage

m_s: Mutual inductance between two stator phases.

L_r: Inductance specific to a rotor phase.

m_r: Mutual inductance between two rotor phases.

M_{Sr}:   Mutual inductance of the rotor on the stator.

M_{rS}:   Mutual inductance of the stator on the rotor.

T_{em} Electromagnetic torque

ρ Air density 1.2754 kg/m³

A_f Reference area.

V_0 Air velocity.

G   Reduction ratio

T_{rr} Wheel load torque

T_r Motor load torque

ω_r Rotor speed

$p\%$ Road slope percentage

r   Wheel radius

Theme

DTC control of an asynchronous propulsion engine for an electric vehicle

Directed by : Dr. TERKI Amel   **Submitted by :** GHODBANE Ahmed Marouane

Abstract :

Today, the risk of global warming has increased due to the great growth in the transportation sector globally, which necessitated serious thinking about electric cars to replace conventional cars and searching for how to develop them in order to increase their efficiency and energy independence. Controlling the speed of the propulsion engine remains an important issue and to choose a control method several aspects must be considered like: robustness, performance and no-complexity. In addition to that, the installation of the entire system is offset by negative effects on some elements the most prominent is the perturbation of DC bus voltage , which was taken into account in this work and it controlled by a battery.

The main objective of this manuscript is to present the application of DTC control method for an electric vehicle system in order to control its speed and DC bus regulation as a secondary goal , the ASM is powered by fuel cell and battery through 2-level inverter

Keywords : Electric vehicle ,DTC , Control battery, DC bus, fuel cell ,asynchronous machine .

الملخص :

إزداد اليوم خطر الإحتباس الحراري نظرًا إلى النمو الكبير الذي يعرفه قطاع النقل عالمياً، مما استوجب التفكير الجدي في السيارات الكهربائية لتعويض السيارات التقليدية والبحث عن كيفية تطويرها من أجل زيادة كفاءتها و استقلاليتها الطاقوية ، و يبقى التحكم في سرعة محرك الدفع قضية مهمة ، ومن أجل اختيار طريقة التحكم يجب النظر في العديد من الجوانب كصلابة التقنية ، خصائصها و عدم تعقيدها، إضافة الى ذلك فان تركيب النظام كامل يقابله تأثيرات سلبية على بعض المكونات أبرزها تغير التوتر ين طرفي جامع التيار المستمر عند مدخل العاكس و التي اخذت بعين الاعتبار في هذا العمل حيث تم التحكم في توتره عن طريق البطارية .

ان الهدف الرئيسي لهذه المذكرة هو تطبيق طريقة التحكم المباشر في العزم على محرك الدفع للسيارة الكهربائية من أجل التحكم في سرعته و التحكم في جهد جامع التيار المستمر عند مدخل العاكس كهدف ثانوي ،النظام مكون من بطارية تحكم و محرك دفع غير متزامن مغذى بخلية وقودية عن طريق عاكس بطبقتين.

الكلمات المفتاحية : سيارة كهربائية ، التحكم المباشر للعزم ، بطارية التحكم ، جامع التيار المستمر ،الخلية الوقودية ، المحرك الغير متزامن .

Table of Contents

Chapter II : Modeling of the electric vehicle system

Chapter III : Control approaches and simulation

Chapter IV : Simulation results and interpretation

General introduction

<u>Problematic</u>

The term sustainable development has become more realistic. Today, many plans had formed to achieve the goals that fall under the cover of this term the most notably one is how to face the risks of greenhouse effect ? under the rise of transportation means which is one of the largest source emitting of CO_2 gas therefore transport pollution becomes one of the biggest challenges facing developed and developing countries and since the demographic development and human activities are continuing to increase It will become more difficult to control here it gets more serious about looking for an alternative and thinking of electric vehicles as a solution.

Unlike conventional cars, electric vehicle (EV) also called electric drive vehicle do not produce any emissions nor pollutants they are differentiated by their autonomy and their CO_2 release rate.

The "Clean-vehicles" have indeed become a societal issue, due to the rise in environmental concerns and the volatility of the price of fossil fuels. The main components of an " EV " system are : the motor, controller, power supply, charger and drive train [1] , so there are several researches in each part, In order to increase effectiveness , efficiency and autonomy of it some are being done on energy management in the case of multi sources , charging and discharging of batteries and speed control ,in addition to the multiplicity of types , we can site some of topic research todays :

- ➢ Power management (multi sources)
- ➢ Traction Chain
- ➢ Source performance
- ➢ Motors
- ➢ Speed Control

One of the most subjects that was mentioned above is speed control methods, the study of vehicle's speed control is a complicated due to non-linearity, the uncertainty of this system and the difficult of measures , there are several control techniques have been developed

in order to increase the stability of the electric vehicle in the cases of accelerations and disturbance depending on their robustness , measurement uncertainty and complexity, so the problem that arises is :

How to make an effective vehicle's speed control method   by balancing between the three criteria (robustness , measurement uncertainty and complexity) ?

Our proposed system contains a fuel cell , a battery and asynchronous machine controlled with direct torque control .This work will be done under the environment MATLAB/SIMULINK$^©$ 2019 which is a mandatory and important step in this context we have simulated the complete system at the same time in order to see the effect of elements on each other.

Thesis objectives

- The main objective of this modest work is the use of DTC classic method to control the propellant motor's speed as a solution to obtain satisfactory mechanical and electrical performance.
- The secondary goal is the development of a reliable and flexible method for continuous bus adjustment in the different load profiles.

Thesis organization

The first chapter is devoted to the study and presentation of electric vehicles. At first an overview of the history is given then a description of various configurations of electric vehicles configuration from the power source until the motor and finally a justification of our chosen system configuration.

In the second chapter we are interested in modelling different system components at first we will model the PEMFC then the different converters and also the model of DC bus and the asynchronous motor , finally the model of vehicle dynamics and connecting the mechanic to electric part

The third chapter of this brief presents the different control approaches (dc/dc bus and direct torque and flow control), and the simulation in SIMULINK/MATLAB

The fourth part is devoted to the presentation of the simulation results of the overall system and the performance of the control strategies of the different parts with a discussion and interpretations.

In the end, a general conclusion summarizes the results of our investigations and our prospects for this work

Chapter I
Configuration of the electric vehicle system

Chapter I

Configuration of the electric vehicle system

I.1 Introduction

Since the appearance of air pollution problems caused by carbon dioxide emissions and linking it to the transport market as the biggest reasons. Several plans have been developed in place to reduce the impact of transportation and make it unpolluted ,the use of electric vehicle is one of them .Replacing the internal combustion engines by electric ones will reduce the system's contribution to pollution and if the first energy source is clean, we can say that the system is unpolluted anymore (CO_2 emissions).

There are many sources of clean energy, also called renewable energies ,we mention for example, solar energy, which is widely used in this field where it used to charge the vehicle's battery , we can also mention fuel cell , each one of them has its own pros and cons, which make us decide which source to use.

I.2 History

In reality the electric vehicle is not a new idea it has a past that dates back to the beginnings of the automobile where there was always competition between it and the other two types "steam and petrol" [2]. After three years from the discovery of Faraday's law in 1831 and the invention of DC motor, the electric vehicle appeared (in 1834) but it was with primary (non-rechargeable) batteries .In 1859 lead accumulator was invented by the French Gaston Planté , and in 1884, Thomas Parker seated in the first electric car in the world .

The first electric car which exceed 100 km / h is «La Jamais Contente» was built in 1899 in the United Kingdom, the car was driven by the Belgian Camille Jenatzy.
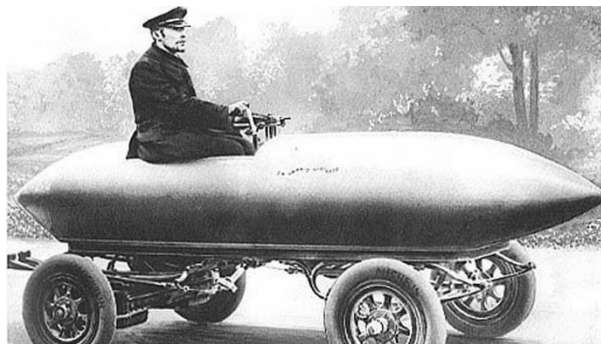
Fig I-1: La jamais contente.[4]

Electric vehicles became very popular, especially in the years 1900 and 1901, through charging stations. The battery can be charged at night and used in the day or the use of two batteries by the replacement of the empty one but after many years, specifically in 1920 electric cars faced many obstacles: its limited speed, low autonomy and the high prices have led to the decline of electric cars.

In 1972, the first hybrid car GM's Buick Skylark (General Motors) was built by Victor Wouk. After the oil shock, the American Congress breathe new life into the development of the electric vehicles by promoting the development of new technologies for batteries motors and hybrid components through « the Electric and Hybrid Vehicle Research, Development and Demonstration Act ».

The first batch of cars was marketed in 1997 by Toyota " la Prius " and from this year until 2000 many hybrid and electric models have been launched as : Honda EV Plus, G.M. EV1 Ford Ranger pickup EV, Nissan Altra EV, Chevy S-10 EV and Toyota RAV4 EV , then the market died again .

In July 2009, Mitsubishi lunched i-MiEV in Japan, and then started selling it to the Hong Kong public in May 2010 .

With the arrival of December,2010 the electric car "Nissan LEAF" has been marketed in Japan and the United States it is a car with five-seater already announced in 2009. [3-4] car manufacturers have developed several 100% electric models like Renault's model *"ZOE"* in 2013 , moreover the charging station installations are today prevalent more and more [4]

Fig I-2: Renault ZOE. [4]

I.3 Electric vehicles today

After recording strong growth over the 10 past years, the sales of electric cars are expected to fall temporary 18% in 2020 due to the coronavirus epidemic while thermal vehicles are expected to decrease by - 23%, the selling price for electric vehicles could be equivalent to that of thermals in Europe by 2022.

The transition to electric cars will face many problems in the coming years according to Colin McKerracher the head of advanced transport for the BNEF, where he warns:

"The Covid-19 pandemic is expected to cause a major slowdown in global auto sales in 2020. It raises difficult questions about the priorities of automakers and their ability to finance the transition. The long-term trajectory has not changed, but the market will be bumpy for the next three years".
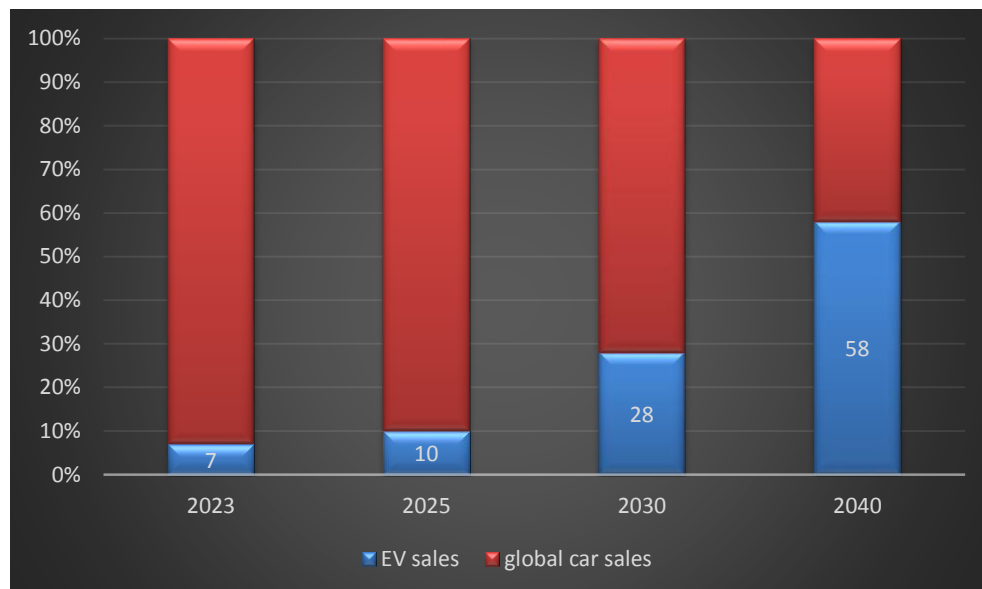
Fig I-3: Estimation of electric vehicle sales. [5]

The electric car should represent 7% of world sales by 2023, or 5.4 million units, BNEF predicts a tipping point by 2025.

In the other segments, Electricity should represent 67% of bus sales, 47% of two-wheeler sales and 24% of light utility sales.

In 2040, electric vehicles will save 17.6 million barrels of oil every day, according to BNEF's report. [5]

Electric vehicles that use batteries can develop a speed of (70 km to 200 km),the use of the fuel cell can increase the range (400 to 450 km at the moment) to arrive at values close to those of conventional vehicles . [4] On the other hand, fuel cell vehicles will be much more present in the "heavy" vehicle segment , this means it will not "encroach" on the light vehicle market , they are expected to represent less than 1% of the global passenger car. [5]

Manufacturing the power supply technologies (however batteries or fuel cell) at large scale can make the price of electric vehicles comparable to those of thermal vehicles. Indeed, the price of power source constitutes the most important part of the cost of an electric vehicle [4]

I.4 Main types of electric vehicles

Depending on how electricity is used as their energy source, there are two main types of electric vehicles:
- Fully electric vehicles.
- Hybrid electric vehicles.

I.4.1 Fully electric vehicles
I.4.1.1 Definition

Also called Pure electric vehicles, is a vehicle that only has an accumulator as an energy source [4] and driven by motor which can generate torque in low speed range without switch the reduce gears unlike traditional cars. [6] Major components of an electric vehicle include storage battery, drive motor, motor controller, power electronics converters, charge controllers and battery management system (BMS). A vehicle that has two or more energy sources and energy converters is called a hybrid vehicle. [9]

There are essentially two types of electric vehicles depending on the energy source used to power these vehicles:
- Electric cars with rechargeable batteries.
- Electric cars with fuel cell supply (alone). [4]

I.4.1.2 Electric cars with rechargeable batteries

Battery electric vehicles have become greatly viable and feasible option in automotive market for consumers. [7]

A battery is an on-board system that can store electrical energy for future use. [4] It is among the widespread and most popular option.

In order to choose the type of accumulators we should care about those parameters :

- ✓ Specific energy expressed in watt-hours per kg ; (Wh / kg) it describes the energy content and determines the vehicle range.
- ✓ Specific power or specific power expressed in watt per kg (W / kg).
- ✓ Battery Lifetime: it represents the number of charging and discharging cycles possible before it loses its ability to hold a useful charge ,it depends on the depth of discharge (DOD)
- ✓ Efficiency : is given by the energy losses that occur when charged and discharged. The amount of energy that is available to power the wheels represents the efficiency of the battery. [15]
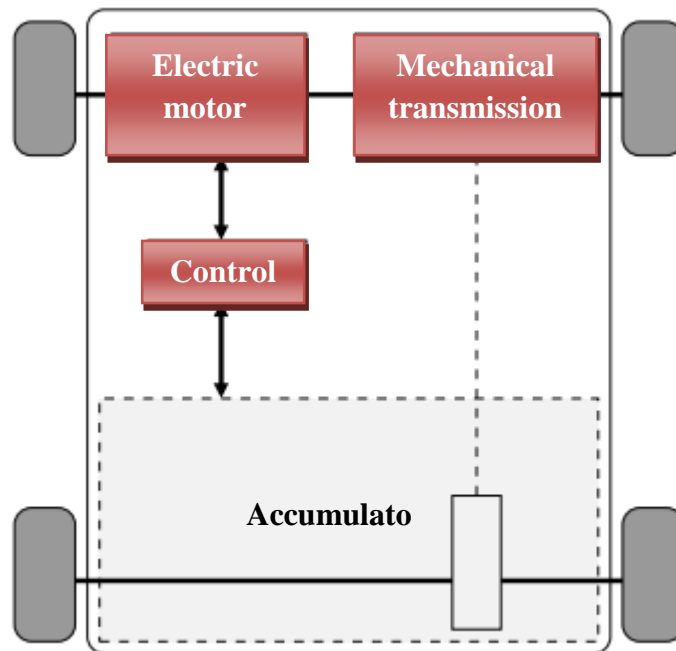
Fig I-4: Pure electric vehicles. [3]

I.4.1.3 Electric cars with FC supply

Fuel cell is electrochemical generators similar to a battery in several ways but it can directly transform the chemical energy of a fuel into electrical energy [4], there are various types of FC that work with different fuels and we will see them in the power sources's part. The application of this technology in the automotive field is fairly recent.

I.4.1.4 Comparison of engine vehicles and electric vehicles

There are many similarities between an IC engine vehicle and a battery EV. [9]

Tab I-1: Comparison of engine vehicles and electric vehicles. [9]

(ICE) Vehicles	*Electric Vehicles (EV)*
• Powertrain: IC engine.	• Powertrain: Motor (+ Engine).
• High specific energy of fuel.	• Low specific energy of battery.
• Power density: High.	• Power density: Low.
• Emits greenhouse gases.	• No tailpipe emissions.
• Travels > 300 miles / fill.	•Travels < 100 miles / charge.
• Short refilling time (< 5 min.).	• Long charging time (0.5-8 hr.).
• Fuel tank takes less space.	• Battery takes large space.
• Fuel weight is very less.	• Batteries are very heavy.
• Higher maintenance costs.	• Lesser maintenance costs.
• Braking energy not recovered	• Can recover braking energy.
• Running cost: high.	• Running cost: low.
• Engine efficiency: ~ 30%.	• Motor efficiency: ~ 80%.
• Needs complex gear system.	• Needs only one gear.
• Noisy operation.	• Quiet operation.
• Ample refilling infrastructure.	• Lacks charging infrastructure.
• Need to pick up some speed to deliver maximum torque.	• Produce maximum torque. instantly after starting of motor.
• Uses only hydrocarbons.	• Uses electricity from many resources.

I.4.1.5 The different configurations of electric vehicles

The objective of the mechanical transmission is to connect the source and the electric motor (s) to the drive wheels of the vehicle; it is a question of adapting the speed and the torque of the engine to the functional requirements of the vehicle. [3]

there are several possibilities in the associations of the elements necessary for the power transmission (clutch, gearbox, differential and the number of motors), a variety of EV configurations are possible presented in (Fig I-5) :

M: Motor , **C:** Clutch ,**VG**: Variable Gearbox , **FG:** Fixed Gearbox , **D:** Differential
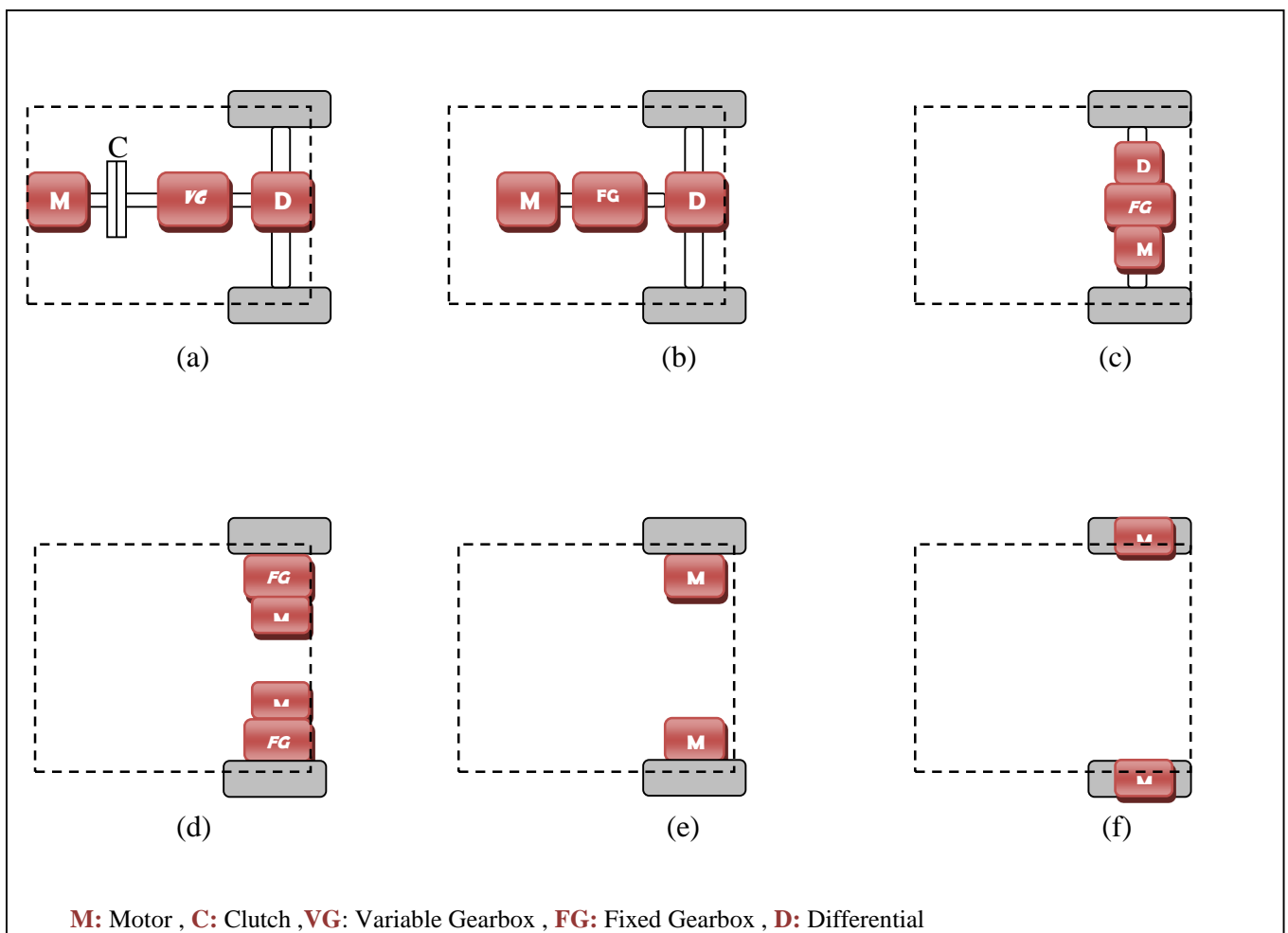
Fig I-5: Various configurations of Electric Vehicles. [9]

- **EV (a):** It is modified versions of ICE vehicles with motors in place of engines; it is consisting of clutch, a multi-speed gearbox and a differential.

- **EV (b):** Less size and weight, because it has not a clutch, it has fixed ratio gearbox and a differential.

- **EV (c):** Simplified drive train the same as (b) but the motor, fixed gearing and the differential are combined in one assembly.

- **EV(d) :** It uses the front wheels for running in a curved path, each wheel has a motor this EV has two motors in the place of the differential.

- **EV(e) :** The traction motor is placed inside the wheel, and the gear is used to enhance the drive torque.

- **EV (f) :** Similar to the drive train in (e) except that the motor is placed inside the wheel without any gear. This design is relatively less complex than in (e). [9]

For electric vehicles which have Multi-motor , there are two great architectures, one uses a double powertrain using two direct current motors which allows more reliability on the motor side the other uses an asynchronous motor and two wheel motors to increase the mechanical differential of the vehicle. [4]

I.4.2 Hybrid electric vehicles

I.4.2.1 Definition

Hybrid electric vehicles combines the advantages of internal combustion engine vehicles (the long driving range due to the high energy density) and electric vehicles (zero pollution and the high efficiency).

Generally HEVs consisting of petrol engine with a fuel tank, motor and a battery bank a high acceleration performance at low speed cannot be achieved in engine vehicles due to several mechanical constraints so the electric propulsion provides that. In addition, the power flow in traditional vehicles drive is unidirectional from engine to wheel whereas but in electric ones, power flow can be Bidirectional, from motor to wheel and from wheel to battery.
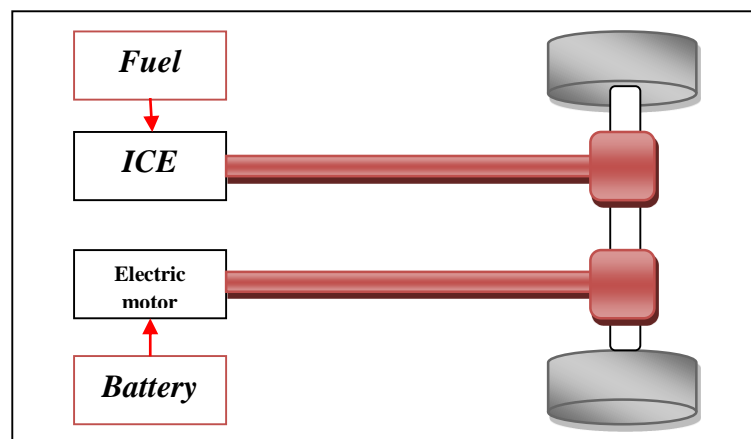
Fig I-6: Arrangement of a HEV. [9]

I.4.2.2 Classification

The hybridization factor can define as how much is the share of electric power in an HEV in comparison with the overall power:

$$HF = \frac{\text{Sum of Power of Electric Motors}}{\text{Sum of Motor Power } + \text{ Engine Power}}$$

According to this factor, we can define three classes of HEV:

a- Micro Hybrid: is the least electrified type of HEV which has an HF < 10 % like Mercedes Smart. The motor can be used to assists accessories such as power steering and air-conditioning and not for powering the vehicle

b- Mild Hybrid: which has HF from 10 % to 30 % like Honda Insight. Motor does not alone propel the vehicle but only supports starting of the engine.

c- Full Hybrid: Like Toyota Prius, it can run only with electricity. Therefore it needs a large capacity motor, Energy saving is 30%-50%.

I.4.2.3 Power train configurations

There is many powertrain configurations are possible depending on how the energy converters (i.e. ICE and electric motor) of an HEV are combined :

   i.   Series Hybrid (SHEV).

   ii.   Parallel Hybrid (PHEV).

   iii.   Series–Parallel Hybrid (SPHEV).

   iv.   Complex Hybrids (CHEV).

   v.   Fuel Cell Hybrids (FCHEV).

   vi.   Plug-in Hybrid Electric Vehicles (PHEV).

Series hybrid

Parallel hybris

Series-Parallel hybrid

Fuel cell hybrid
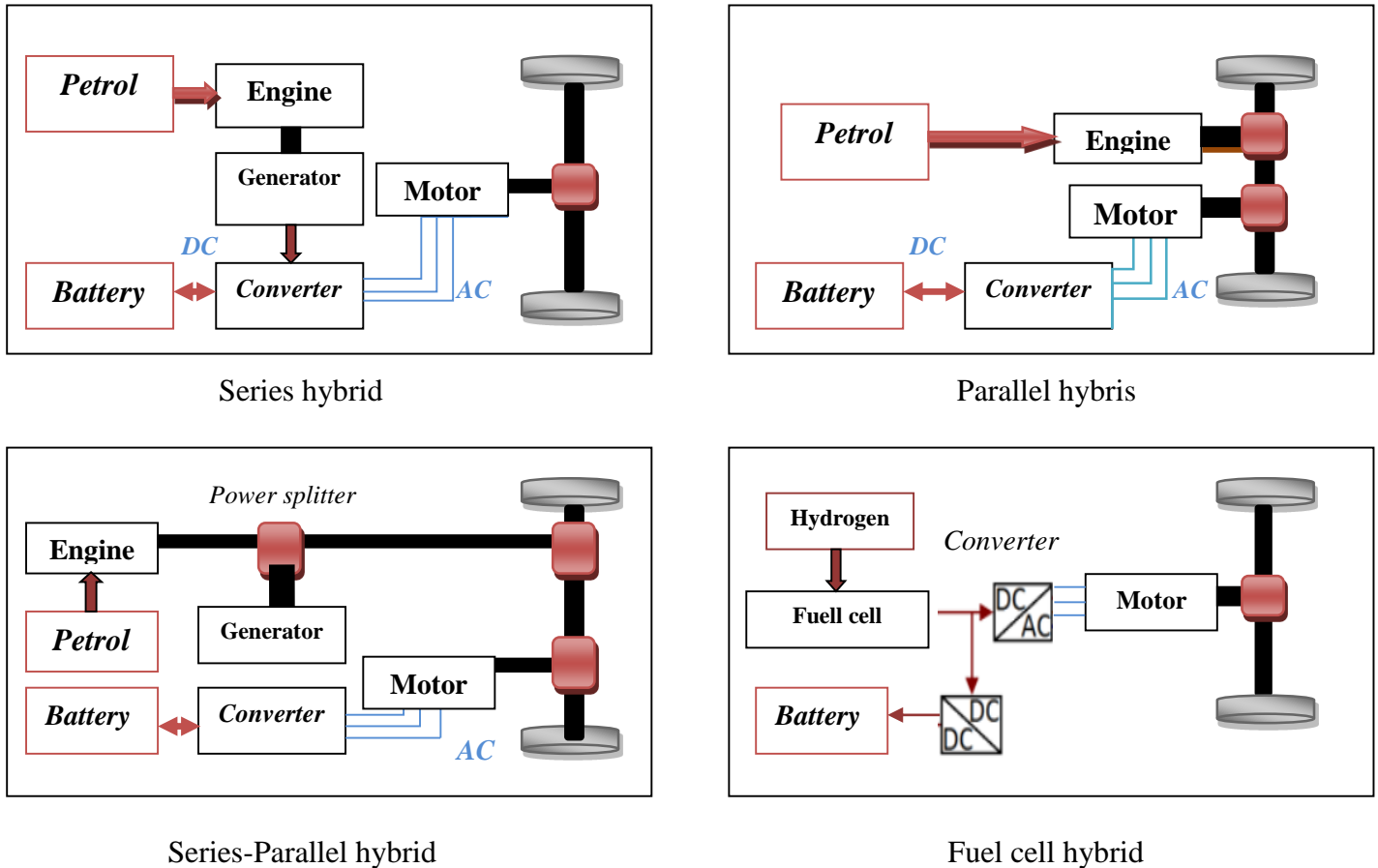
Fig I-7: Architecture of Hybrid EVs. [9]

From (Fig I-7) we can see that the simplest hybrid configuration is series drivetrain as the engine is not connected to the drive train power's traction can only get from the electric motor. The traction motor is powered by a battery or by an electric generator driven by the downsized ICE. The generator have two things to do:

a- In the case when the traction load demand is large, he powers the drive motor.

b- When the motor load demand is small, he charges the batteries.

In parallel hybrids, ICE and motor are directly connected to the drive system so they can propel the vehicle individually or jointly. In this mode, the supplied torques are added together. PHEV designs frequently contain a clutch allows to separates the inactive drive.

The need for complex mechanical systems and control algorithms is one of the downsides of this system.

Series–parallel hybrids called also power-split hybrids it needs very complex control system. SPHEV is a combination of the two past designs .The rule of the splitter is to divides

The output from the engine into mechanical and electrical transmission paths ,the motor power flow in these design is unidirectional .

The complex hybrids are similar to series-parallel hybrids just the motor power flow in these design is bi-directional .

The fuel cell design is a series hybrid configuration in which fuel cell is the energy conversion system. Usually it combined with a battery (or a super capacitor) to deliver peak acceleration power and as storage In the case of excess energy because the nature of fuel cells do not allow it to accept regenerative energy, they are true zero-emissions vehicles as they do not emit any greenhouse gases.

For plug-in Hybrid Electric Vehicles the main difference between it and standard HEV batteries of PHEVs can be recharged from any external power source unlike in standard HEVs in which batteries are recharged only by means of the engine driven generator or region-braking. [9]
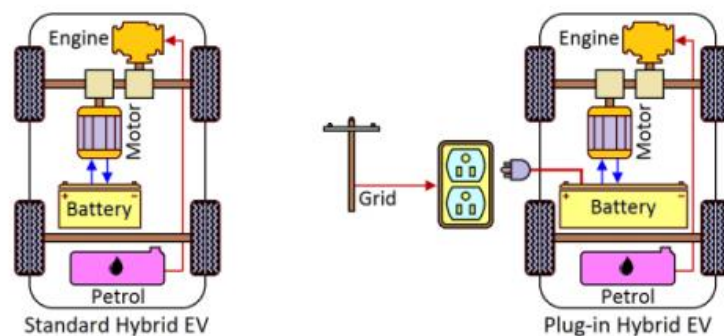
Fig I-8 : Comparison of a standard HEV and a PHEV. [9]

I.5 Advantages and Disadvantages of EV

This part shows the positive and the negative side of electric vehicles

I.5.1 Advantages

- High level of efficiency: 80% of the e-power can transfer from motor into vehicle motion. Besides, it can retrieve power when braking, [6] and it's 3 times higher than that of a heat engine. [4]

- Electric vehicles are devoid of noise pollution,[4] Because it only has low noises from air compressor, cooling fan and transmission mechanism. [6]

- Low level of environmental pollution. [6]

- With 6000 parts less than a traditional car EV has a simple technical architecture. [4]

- The electric motor does not need any draining. [4]

- Multiple energy resources available. [6]

- EVs are easy to maintain. [4]

- Electric vehicles do not consume energy in traffic jams and braking (the car recharges on its own). They are therefore very suitable for the urban environment . [4]

- Start-up is very fast, (no more start-up problems during cold winter weather). [4]

- The main advantage is independence from oil. [4]

I.5.2 Disadvantage [4]

- Battery life is not yet very important

- The price of these cars is high because it needs advanced technologies

- The recharging time of electric batteries is still important.

- Too high a mass of accumulators or a weak autonomy

Most of problems are about batteries, and to overcome this weakness of electrochemical accumulators it is interesting to realize hybrid systems to produce electricity on board of the vehicle. [3]

I.6 The different sources of electrical energy

This part is dedicated to talking about the various electrical energy sources that may be used in the EV.

I.6.1 The battery

Battery cell is made of a negative electrode and a positive electrode which are connected by an electrolyte.The chemical reaction between the electrodes and electrolyte generates electricity, so it converts the stored chemical energy into electric energy.

The battery can be recharged by reversing the current (only in rechargeable batteries because they can reverse the chemical reaction). [8]

There are several different types of batteries that have been used in electric vehicles or under development. These batteries are described here.

I.6.1.1 Lead/acid

Its chemical symbol is (Pb/A) .The active material in charged state is the lead dioxide (PbO2) which takes place in the positive electrode while the battery negative electrodes contain elementary lead (Pb) The material of electrolyte is sulphuric acid (H_2SO_4) [8] it is a mature battery technologies. These type of batteries were originally used in early electric vehicles such as General Motor's EV1, and also used in conventional vehicles, relatively inexpensive but it has a poor specific energy (34 Wh/kg). [7]

The overall reaction is :

$$Pb + PbO_2 + 2H_2SO_4 \longleftrightarrow 2PbSO_4 + 2H_2O$$
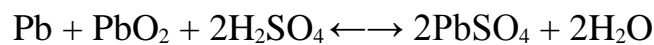
When being discharged the lead of the negative electrodes and the lead dioxide of the positive electrode reacts with the Sulphuric acid. Lead sulphate is formed on the electrodes and the electrolyte loses its dissolved Sulphuric acid and becomes water.

This type of batteries characterized by the short lifetime which is only 100 cycles for a normal SLI car battery , this cycles can boosted by the use of tubular-plate positive electrodes in that way the battery can achieve around 1500 cycles (80% DOD). [8]

I.6.1.2 Nickel Metal Hydride

Its chemical symbol is (NiMH), same as Lead/acid batteries they are mature battery technologies. These types of batteries were originally used in early electric vehicles .[7]

The nickel in positive electrode can be : a nickel iron (Ni-Fe), nickel zinc (Ni-Zn), nickel cadmium (Ni-Ca) and nickel metal hydride (Ni-MH) , The Ni-Zn and Ni-Fe batteries are not considered to be an option for EVs because of their short lifecycle [8]

NiMH batteries are considered to be superior, as they can have greater energy density and up to double specific energy (68 Wh/kg) compared with lead acid batteries. This type has some drawbacks like the low charging efficiencies and the self-discharge (up to 12.5% per day under normal room temperature conditions) [7]

The overall reaction is written as [8]:

$$MH + NiOOH \longleftrightarrow M+ Ni(OH)_2$$
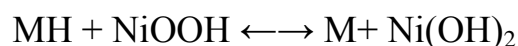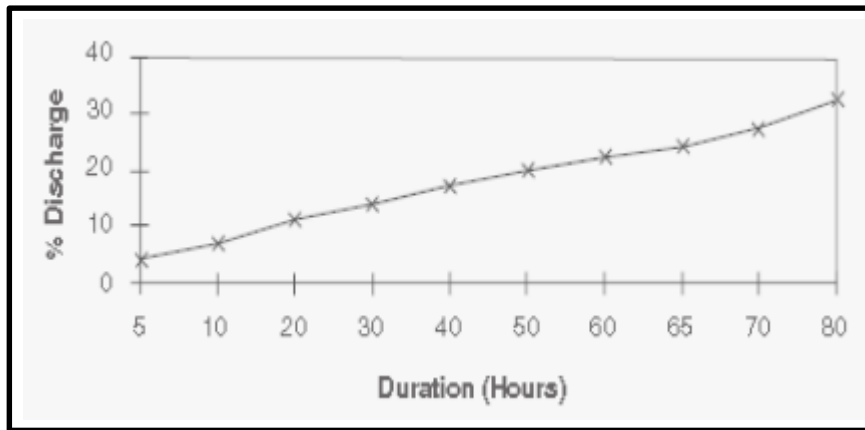
Fig I-9: Typical self-discharge for a NiMH battery. [10]

I.6.1.3 Lithium-ion

Its chemical symbol is (Li-ion), It has the characteristics that make it considered a great option for electric vehicles and It will dominate the electric car battery technology market in the next years. [8] It has excellent specific energy (140 Wh/kg) and energy density,with a self-discharge rate (5% per month) that an order of magnitude lower than NiMH batteries. Like all batteries (Li-ion) has drawbacks as well where there are also major safety concerns regarding the overcharging and overheating of these batteries. It can experience a thermal runaway, which can trigger vehicle fires or explosions. [7]

I.6.1.4 Metal air

Unlike other batteries most metal air batteries can not be recharged by only reversing the current and it happens mechanically (comparable with fuel cells).Its advantages is the weigt and that it only consists of one reactant. the other reactant is oxygen which does not have to be carried in the battery. The only metal air batteries that is commercially available is with zinc air The overall reaction is as follows: [8]

$$2Zn + O_2 \rightarrow 2ZnO$$
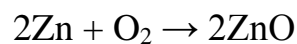
I.6.1.5 Sodium nickel chloride

Its chemical symbol is (NaNiCl2) also called zebra battery (Fig I-10), not commercialized yet the research is carried out by MES DEA company and it is the only company in the world that has this type of battery under development.

While discharging the nickel and sodium chloride are transformed into salt and nickel. The overall reaction is: [8]

$$2Na + NiCl_2 \leftarrow \rightarrow Ni + 2NaCl$$
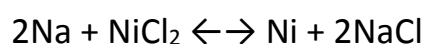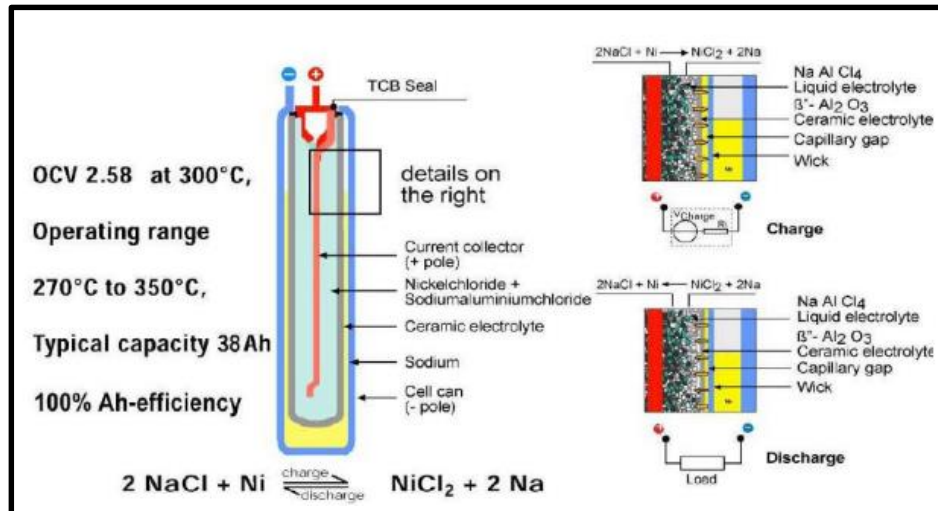
Fig I-10: The zebra battery. [8]

I.6.2 Fuel cell

Fuel cells are electrochemical devices that use hydrogen (H_2), or H_2-rich fuels, together with oxygen from air, to pro-duce electricity and heat. However there are many variants of this basic process, depending on the Fuel Cell type and the fuel used. [11]

The main difference between a fuel cell and an accumulator comes from the fact that the fuel cell works as long as it is fueled and doesn't need an electric charging. [3]

I.6.2.1 Brief history

There is great agreement about the effectiveness of fuel cell technology where many people are seeing it as a key to many of the century's problems.

Its principle of operation was discovered by German scientist C. F. Schönbein in 1838. the first fuel cell was demonstrated by Welsh scientist Sir W.R. Grove in 1839 . In 1939, British engineer F.T. Bacon successfully developed a 5 kW stationary fuel cell. In 1955, W.T. Grubb, a chemist working for the General Electric (GE) Company (USA), further modified the original fuel cell design by using a sulphonated polystyrene ion-exchange membrane as the electrolyte.

Three years later another GE chemist, L. Niedrach, devised a way of depositing platinum onto the membrane, which served as catalyst for the neces-sary hydrogen oxidation and oxygen reduction reactions. [11]

I.6.2.2 Function Structure of Fuel Cells

The basic physical structure of a single cell consists of an electrolyte layer in contact with a porous anode and cathode on either side.[11] .

The operating principle of the fuel cell (Fig I-11) is based on the production of energy by reaction between hydrogen and oxygen. This reaction actually produces electricity, water and heat [5] the following electrochemical reactions is in the case of a fuel cell with an acid electrolyte [11,12] :

Anodic reaction: $H_2 \rightarrow 2H^+ + 2e^-$

Cathodic reaction: $1/2O_2 + 2H^+ + 2e^- \rightarrow H_2O$

Overall reaction: $H2 + 1/2O_2 \rightarrow H_2O + Heat + Electricity$
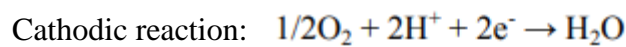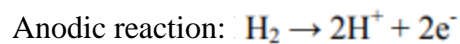
Individual fuel cells can produce only 0.7 V (theoretical) therefore usually cells are connected in series, to provide higher voltages or in parallel for high current applications at low voltage.

In general, the voltage output of a fuel cell decreases as the load current increases, due to several factors which include activation loss (a fundamental electrochemical phenomenon), internal resistance (analogous to the internal resistance of a battery) and mass transport loss due to depletion of reactants at the anode and cathode under high current conditions. [13]
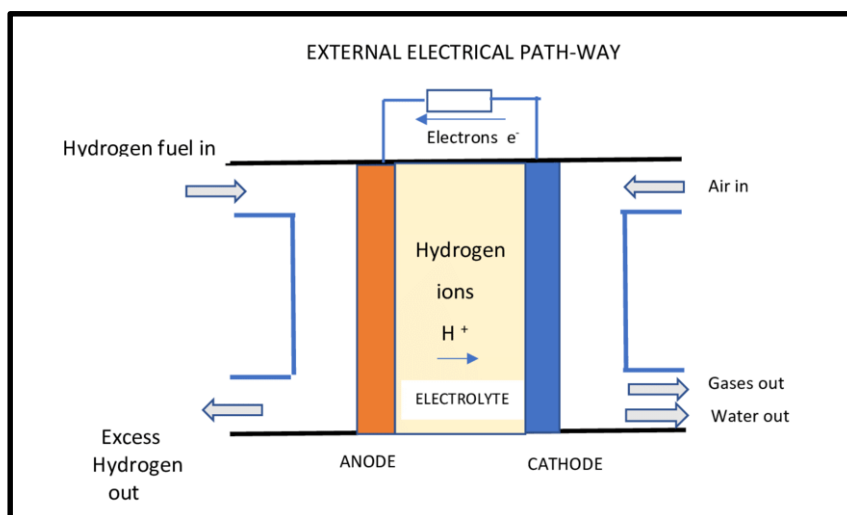
Fig I-11: Schematic diagram of hydrogen fuel cell. [13]

For oxygen, it is enough to draw it from the ambient air and about the hydrogen's problem There are two solutions for the production:

- ✓ hydrogen is stored on board the vehicle;
- ✓ the hydrogen required for the reaction is produced directly on board the vehicle, using a reformer . [12]

I.6.2.3 Fuel Cells Technologies [11]

Fuel cells can classify by their :

- ✓ operative temperature range
- ✓ the type of fuels which can be used
- ✓ the type of catalyst used by the cell
- ✓ the efficiency ratio of the energy conversion.

The main technologies available on the market are the following (Tab I-2)

- ✓ Polymeric Electrolyte Membrane Fuel Cells (PEMFC):
- ✓ Direct Methanol Fuel Cells (DMFC)
- ✓ Alkaline Fuel Cells (AFC)
- ✓ Phosphoric Acid Fuel Cell (PAFC)
- ✓ Molten Carbonate Fuel Cell (MCFC)
- ✓ Solid Oxide Fuel Cell (SOFC)

Tab I-2: The Different FCs that have been Realized and under Development. [11]

	AFC Alkaline	PEMFC Polymer Electrolyte Membrane	DMFC Direct Methanol	PAFC Phosphoric Acid	MCFC Molten Carbonate	SOFC Solid Oxide
Operating temp.(°C)	<100	60-120	60-120	160-220	600-800	800-1000 Low temperature (500-600) possible
Electrolyte	KOH	Perfluoro sulfonic acid (Nafion membrane)	Perfluoro sulfonic acid (Nafion membrane)	H_3PO_4 immobilized in SiC matrix	Li_2CO_3-K_2CO_3 eutectic mixture immobilized in γ-$LiAlO_2$	YSZ (yttria stabilized zirconia)
Charge carrier in the electrolyte	OH^-	H^+	H^+	H^+	CO_3^{2-}	O^{2-}
Anode reaction	$H_2 + 2OH^- \rightarrow 2H_2O + 2e^-$	$H_2 \rightarrow 2H^+ + 2e^-$	$CH_3OH + H_2O \rightarrow CO_2 + 6H^+ + 6e^-$	$H_2 \rightarrow 2H^+ + 2e^-$	$H_2 + CO_3^{2-} \rightarrow H_2O + CO_2 + 2e^-$	$H^2 + O^{2-} \rightarrow H_2O + 2e^-$
Cathode reaction	$\frac{1}{2}O_2 + H_2O + 2e^- \rightarrow 2OH^-$	$\frac{1}{2}O_2 + 2H^+ + 2e^- \rightarrow H_2O$	$3/2\ O_2 + 6H^+ + 6e^- \rightarrow 3H_2O$	$\frac{1}{2}O_2 + 2H^+ + 2e^- \rightarrow H_2O$	$\frac{1}{2}O_2 + CO_2 + 2e^- \rightarrow CO_3^{2-}$	$\frac{1}{2}O_2 + 2e^- \rightarrow O^{2-}$
Electrode materials	Anode: Ni Cathode : Ag	Anode: Pt, PtRu Cathode: Pt	Anode: Pt, PtRu Cathode: Pt	Anode: Pt, PtRu Cathode: Pt	Anode: Ni-5Cr Cathode: NiO(Li)	Anode: Ni-YSZ Cathode: lanthanum strontium manganite (LSM)
Applications	Transportation Space, Military Energy storage systems			Combined heat and power for decentralized stationary power systems	Combined heat and power for stationary decentralized systems and for transportation(trains, boats, …)	
Realised Power	Small plants 5-150 kW modular	Small plants 5-250 kW modular	Small plants <5 kW	Small-medium sized plants 50 kW-11 MW	Small power plants 100 kW-2 MW	Small power plants 100-250 kW
Main producers	AFC Energy (UK) UTC Power (USA) Acta Power (Italy)	Ballard (Canada) Heliocentris (Germany)	SFC Energy (Germany)	UTC Power (USA) Fuji Electric (Japan)	Fuel Cell Energy (USA)	Ceramic Fuel Cells Limited (Australia) Hexis & Vaillant (Germany) SOFC Power (Italy) Bloom Energy (USA)
*Lifetime**	Not available	2,000-3,000 h	1,000 h	>50,000 h	7,000-8,000 h	1,000 h

*Estimated values from literature data.

As we can see that there are various types of fuel cells that work with different fuels. But according to studies, the proton exchange membrane cell, considered to be the most promising for motor vehicles [4], because of its simplicity, viability, quick start-up (due to the low operative temperature) and they do not require the use of hazardous fluids, and they enjoy high power densities.[11]

The PEMFC, like all fuel cells, consists of three basic parts (Fig I-12): the anode the cathode, and the membrane.
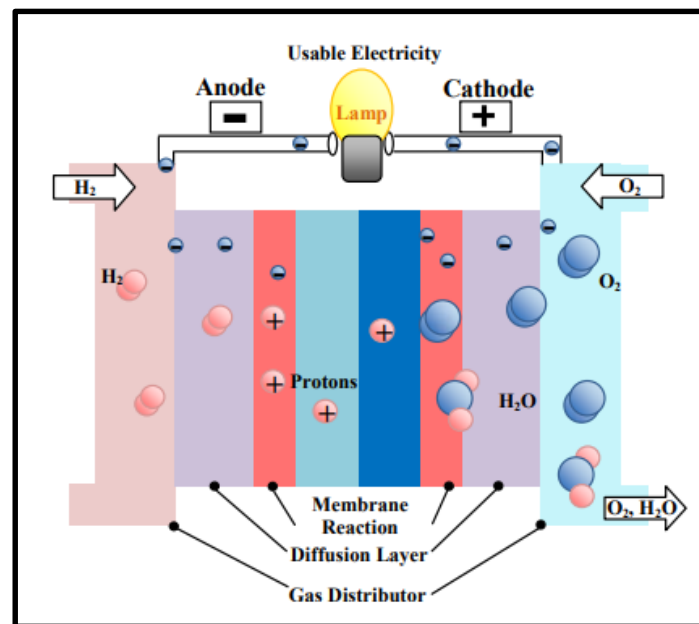
Fig I-12 PEMFC structure.[11]

Many types of membranes that being researched are: polymer-zeolite nanocomposite proton exchange membrane, sulfonated polyphosphazene based membranes and phosphoric acid-doped poly (bisbenzoxazole) high temperature ion-conducting membrane but the most common is Nafion (DuPont) , the thinner Nafion membrane allows a higher conductivity of the cell, but introduces a more problematic water management; a thicker membrane slows down the conductivity. the main characteristics of this type are :

✓ High water uptake

✓ Good proton (H+) conductor if well hydrated, but does not allow the conduction of electrons, which are constricted to follow an external path thus generating an electrical current.

✓ Does not allow the intermixing of the hydrogen and oxygen thus maintaining the two gas separated.

✓ High chemical and mechanical resistance due to the properties of Teflon backbone.

The catalyst layer is in direct contact with the membrane and the gas diffusion layer. It is also referred to as the active layer. In both the anode and cathode, The aim is to generate a gas/solid/membrane triple contact to allow to take place the electrochemical reactions.

The porous gas diffusion layer in PEM fuel cells ensures that reactants effectively diffuse to the catalyst layer. In addition, the gas diffusion layer is the electrical conductor that transports electrons to and from the catalyst layer. [11]

I.6.2.4 PEMFC advantages and disadvantages [11]:

Some advantages of the PEMFC :

✓ A very high power density of cell stack .

✓ Easy operating in pressurized system because large pressure difference between the anode and the cathode.

✓ Because of its low operating temperature many different materials can be adopted.

✓ The use of low cost carbon materials may contribute to the cost reduction of cell stack.

On the other hand, the PEMFC technology shows the disadvantages :

✓ PEMFC catalysts are susceptible to CO poisoning due to their low operating temperature. Therefore, the CO concentration has to be reduced below 10 ppm with CO removal if the reformate from hydrocarbons or alcohols is used as a fuel for the PEMFC.

✓ The temperature of recovered waste heat is lower than that of other fuel cells. As a result recovered heat can be utilized only as hot water.

✓ The water management of the membrane electrolyte is very important for the cell performance, because it secures the appropriate amount of water to show its sufficient ionic conductivity.

I.6.3 Super capacitors

The super capacitors are an energy storage systems with a low energy density but a high power density, they store energy in electrostatic form. Therefore, they are used in transient phases to provide the requested power peaks, in order to:

✓ Reduce current stresses.

✓ Decrease the size.

✓ Increase the lifespan of the main source(batteries or fuel cell).[4]

I.7 Propulsion motors

The types of electric motors can be summarized in (Fig I-13)
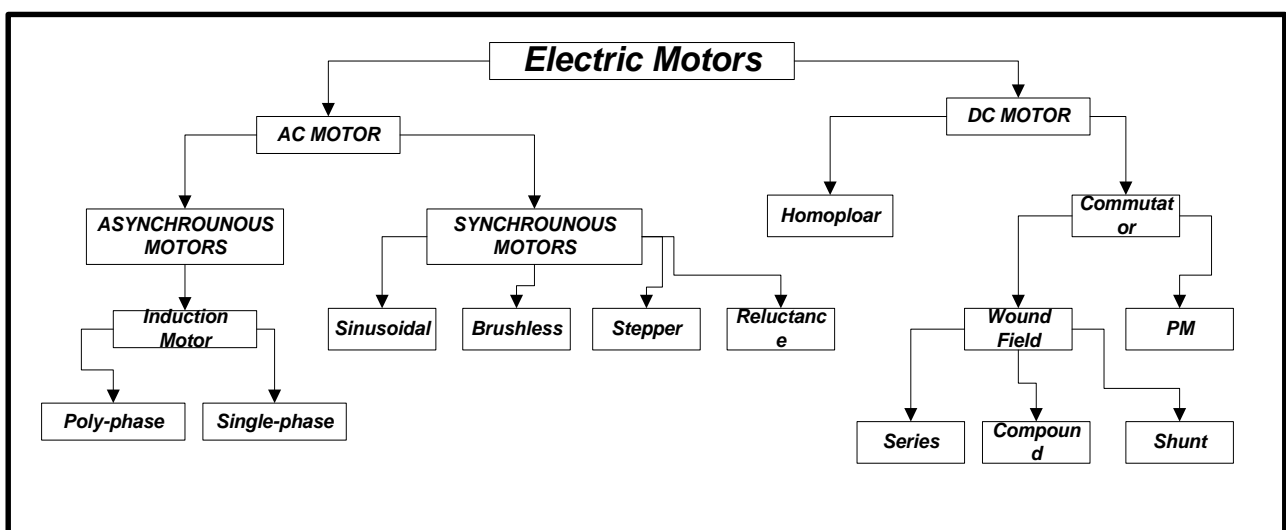
Fig I-13 Classes of Electric Motors. [14]

I.7.1 Direct current motor

I.7.1.1 Brushed DC motor

This type of motor not really attractive to use in EV applications maybe it's choice for ones where high efficiency is not a major concern .It consists of a commutator and brushes that convert a DC current in an armature coil to an AC current.

When the current flows through the armature windings, the electromagnetic field repels the nearby magnets with the same polarity, and causes the winging to turn to the attracting magnets of opposite polarity.

As the armature turns, the commutator reverses the current in the armature coil to repel the nearby magnets, thus causing the motor to continuously turn, some drawbacks of brushed DC motor are the arcing produced by the armature coils on the brush-commutator surface generating heat, wear, and electromagnetic interference .[14]

I.7.1.2 Brushless DC motor

Those motors are the most popular and widely used in control application they have simple structure , higher torque, reduced operational and mechanical noise, elimination of electromagnetic interference and offers excellent efficiency, also they can configured into single-phase, 2-phase and 3-phase. With the presence of controlled converter many desired characteristics can provided for an efficient drive system.

One of the most advantages that set it apart from the rest of the motors is the enhanced speed versus torque.[14] The BLDC do not have brushes or commutators [15]it uses a position feedback to determine when to switch the current. This motor is built with a permanent magnet rotor and wire-wound stator poles. The rotor is formed from permanent magnet and can alter from two-pole to eight-pole pairs with alternate North (N) and South (S) poles.[14]
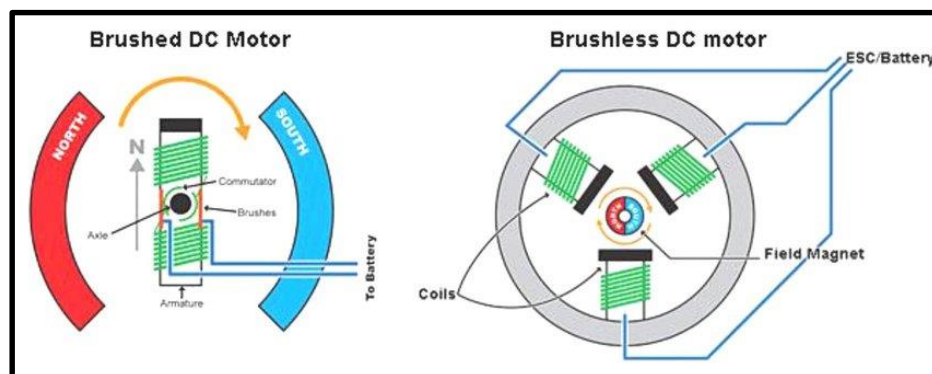
Fig I-14 Diagrams of brushed and brushless DC motors. [17]

I.7.2 Synchronous Motors

Synchronous motors are motors where the shaft of the rotor is synchronized with the frequency of the supply current. In these motors the period of the rotor is exactly same as that of the supply.[14]

This machine type includes several sub-families:

- ✓ Synchronous wound rotor machines.
- ✓ Synchronous reluctance machines.
- ✓ Permanent magnet synchronous motor.

I.7.2.1 Permanent magnet synchronous motor

The stator of Permanent Magnet Synchronous Motor is identical to that of an asynchronous machine, it consists of a stack of magnetic sheet metal which contains notches in which there are also three identical windings offset between them by 120 , rotor is generally has two types:

- ✓ Rotor having pole pieces, used for the concentration of the induction flow in which the magnets are oriented either parallel or perpendicular to the air gap, or in a more complex manner. In this type of machine, the inductor has salient poles.
- ✓ Rotor without pole pieces, therefore with constant air gap, in which the magnetization of the magnets is generally perpendicular to the air gap. [16]

Today, these motors are designed to be more powerful while also having a lower mass and lower moment of inertia. This motor can generate torque at zero speed, highly efficient and produces high power density compared to an induction motor. However, this motor requires a drive to operate. [14]

I.7.2.2 The stepper motor

When the current switches from one set of stator coil to the next coil it produces a torque in these motor, the switching currents from stator windings generates magnetic attraction between rotor and stator to rotate the rotor to the next stable position, or "step"

The stepper motor and switched reluctance motor have the same structure:

- The stator: consists of concentrated winding coils
- The rotor: made of soft iron laminates without coils

Factually this motor is unsuitable for EV application,it is ideal for precision and position control purposes.[14]

I.7.2.3 The switched reluctance motor

This type of motors does not contain coils in the rotor therefore, they cannot generate magnetic field. Torque in these motors is produced when a stator phase is energized; the stator pole pair attracts the closest rotor pole pair toward alignment of the poles. [14]

Switched reluctance motors have some advantages as high-speed drives because of their simple structure, they have no windings or permanent magnets on the rotor, which contributes to a low rotor inertia and a relatively easy cooling compared to other motor types. [15] However, because of the high torque ripple produced when the stator pole pair attraction the closest rotor pole pair toward alignment of the poles, an acoustic noise and vibration are generated.

This motor relatively produces lower torque compared with the stepper motor. Hence, its use is not popular in EV application. . [14]
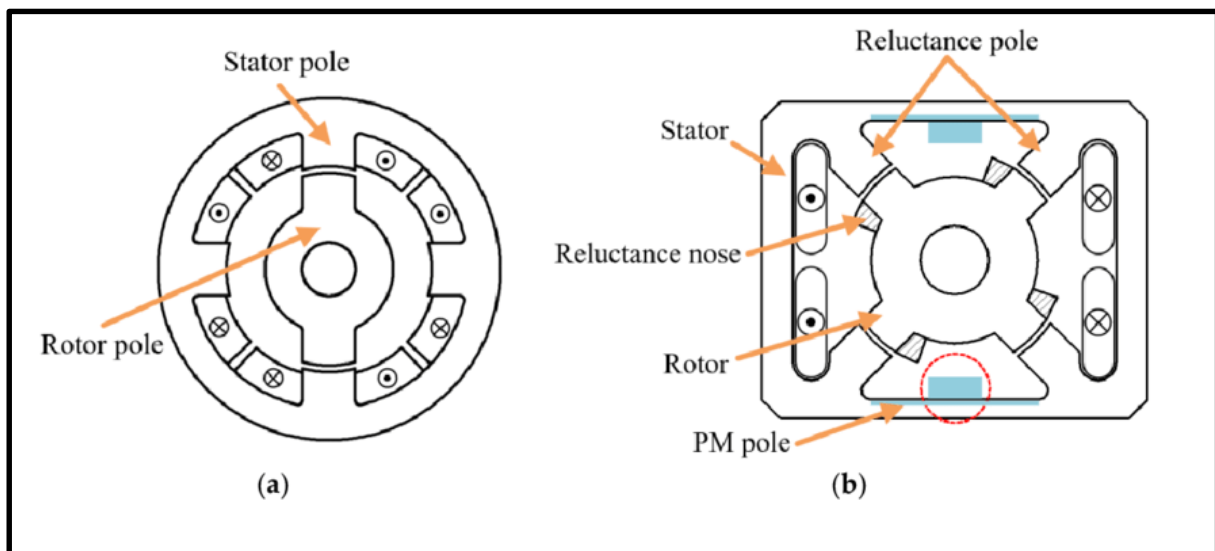
Fig I-15: Structure of conventional (a) 4/2 SRM and (b) Cyrano-type 4/4 SRM. [15]

I.7.3 Asynchrounous motor (Induction Motor)

An asynchronous machine is an alternating current machine whose rotor speed and rotating magnetic field speed are not equal. The rotor is always behind the speed of the statoric field. The asynchronous machine is called induction machine because the energy transferred from the stator to the rotor or vice versa is done by electromagnetic induction.

It has two essential parts, one fixed called stator (primary), carrying a three-phase winding housed in the notches, connected to the power source, and the other mobile or rotor (secondary) which can be either wound or cage squirrel. These two parts are coaxial and separated by an air gap. [18]

The induction motors are characterized with cheaper cost, absence of brushes, commutators and low maintenance. These features make the induction motor attractive in EVs [14]

Tab I-3: Advantages and Disadvantages of Engines Used in EVs. [3]

	DC motor	Asynchrounous	PM Synchronous	VRM
Maximum efficiency	Good	Fair	Very good	Average
Average efficiency	Average	Good	Very good	Good
Maximum speed	Fair	Good	Good	Good
Electronic power cost	Very good	Fair	Average	good
Engine cost	Fair	Good	Average	Very good
Torque-speed space	Average	Average	Very good	Good

Except that the cost criterion becomes the determining parameter so we can conclude that for a a purely electric vehicle the permanent magnet synchronous motor is the most favored in terms of better efficiency and higher mass torque. [10]

I.8 Power electronics in the electric vehicle

The aim of this section is to clarify the role of every element in an electric vehicle, not all of them are necessarily found in the vehicle

I.8.1 Rectifiers (AC / DC) [3]

Rectifiers in an electric vehicle transform alternating current, which came either from the general distribution network, or by an alternator placed on board the vehicle to direct current that can be stored in an electrochemical storage battery or in a large capacity battery.

There are different types of rectifiers:

- ✓ Rectifiers with diodes : establish a rigid relationship between the output and the input

✓ Rectifiers with thyristor: which make it possible to continuously vary the ratio between the input AC voltage and the output DC voltage by increasing the ignition angle of the thyristors.

✓ Mixed thyristor and diode rectifiers

✓ Grouping of thyristor rectifiers intended to improve perfermonces and to reduce disturbances.

✓ PWM (Pulse Width Modulation) rectifiers, which combine IGBTs (Insulated Gate Bipolar Transistors) and diodes to be slightly disruptive to alternative sources.

I.8.2 Inverters (DC-AC)

It is necessary to interpose between the DC energy source and the AC traction motor with a conversion device called an inverter, its rule is to converts electrical energy from direct current into alternating current. Which let it possible to control the motor's torque and the adjustment of the vehicle speed by different control modes as hysteresis control and PWM control (pulse width modulation). [3]

An inverter depends essentially on the nature of the generator and the receiver between which it is mounted, this leads to the existence of:

- Voltage inverters, powered by a direct voltage source,

- Current inverters, powered by a direct current source. [19]

I.8.3 The choppers

A chopper is a current converter, which makes it possible to obtain from a direct current voltage source of substantially constant value, voltages and currents that are controlled adjustable and adapted to the needs necessary to supply the various receivers (sensors, regulators, etc.).

In an electric vehicle, choppers have two essential uses:

- They are essential in the supply of propulsion motors when these are DC motors.

- They are necessary to adapt the voltage of the main battery to that of the electronic auxiliaries used (sensors, regulators, etc.).

It also makes it possible to adjust the speed and the torque of the motor therefore of the vehicle that is why the battery cannot be connected directly to the DC motor. [3]

I.9 Description and justification

In this work the design of the vehicle is fuel cell hybrid EV, which contains: battery, fuel cell two choppers DC/DC , three phases inverter DC/AC and electric motor as shown in the figure below (Fig I-16).
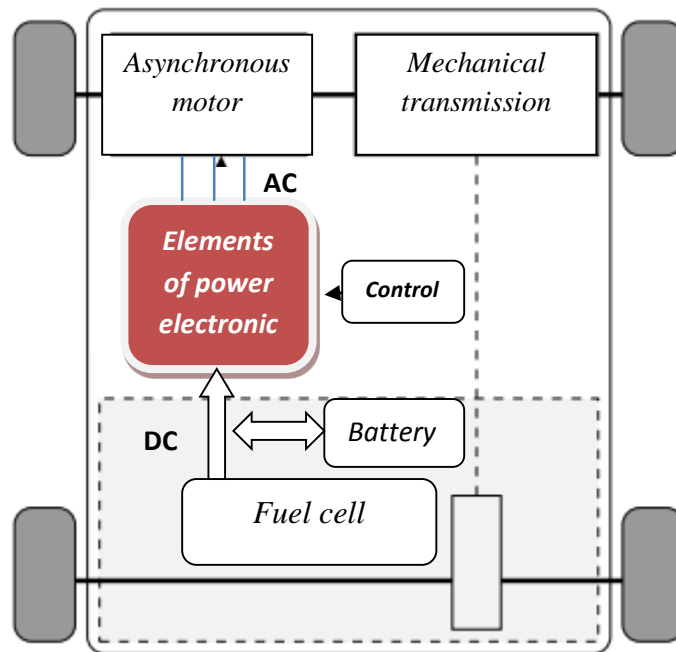
Fig I-16: Structure of our fuel cell hybrid EV.

Fuel cell's technology is proton exchange membrane cell, because it considered as the most promising for motor vehicles [4]. For the propulsion of electric vehicles asynchronous motor is seems to be the best candidate. Indeed, in a comparative study of engine topologies was made allowing, to reach this conclusion. Moreover, the asynchronous motor can operate over a wide range of speed variation with low torque ripples if combined with proper control.

Asynchronous motor drive control techniques are well covered in the literature.The best known is the vector control which is now used for electric and hybrid electric vehicle applications. In this case, torque control is applied to the transient regime and allows better dynamic performance Among these techniques, direct torque control (DTC) seems to be very suitable for electric vehicle applications.[1]

The battery that used for DC bus voltage regulation is (Li-ion), It has the characteristics that make it considered a great option for electric. [8]

I.10 Conclusion

In this chapter, we have made a general presentation of electric vehicles (EV) its History and that EV is not a new idea it has a past that dates back to the beginnings of the automobile but it continues to evolve. We saw that it is divided into two types fully electric vehicles and hybrid electric vehicles which has different configurations, moreover there are several possibilities in the associations of the elements necessary for the power transmission depending on their positions and number of motors.

In the end of the chapter, we justify the choice of the system configuration, which used an asynchronous motor for the propulsion of the vehicle and the fuel cell as principal source.

.

Chapter II
Modeling of the electric vehicle system

Chapter II

Modeling of the electric vehicle system

II.1 Introduction

This part is for modeling an electric vehicle system , at first we will model the fuel cell (PEMFC) then the power electronics converters (the chopper DC/DC , the inverter DC/AC) we will see also the model of DC bus and the asynchronous motor and finally the vehicle dynamics.

II.2 Modeling of fuel cell PEMFC

The modeling of the fuel cell plays a very important part in their development, because it help us to understand the phenomenons and explain the fundamental processes occurring in fuel cell systems. Thus, there are a large number of fuel cell models, which generally each one have their own specificities and uses, depending on the phenomena studied. Mathematical models provide a notable and indispensable tool for approving the design and performance of fuel cells. [20] There are two main modeling approaches presented in the literature. The first approach includes structural models, which aim to simulate heat transfer, mass transport and electrochemical phenomena produced in fuel cells, some of these models focus on modeling specific elements such as the anode, cathode and membrane, while others aim to present a full simulation of the fuel cell. The second approach includes models based on empirical or semi-empirical equations without examining in detail the physical and electrochemical phenomena we applied them in order to predict the effect of different operating parameters on the current-voltage characteristics of the fuel cell.

II.2.1 Static model of PEMFC

In this part, we will use the electrochemical model (Amphlett et al.) because it is the most used in the literature which describes the voltage curve of a PEMFC and predicts their polarizations. [21] This model is described using the combination of elementary laws and empirical models. In the development of elementary models, Maxwell's equations are used in the matter transport,thermodynamic equilibrium potentials are defined using the Nernst equation. Activation potentials are calculated by the Tafel equations.

Internal resistance is determined by the Nernst-Planck equations. Using Ohm's Law, we can express cell voltage as:

$$V_{FC} = E_{nernst} - Vact - Vohm - Vcon \tag{II-1}$$

- V_{FC} : Fuel cell voltage.

- E_{nernst} : Nernst voltage.

- Vact: Activation polarization loss.

- Vohm: Ohmic polarization loss.

- Vcon: Concentration polarization loss.

II.2.1.1 Nernst voltage

Called reversible voltage is the thermodynamic equilibrium potential defined using the Nernst equation :

$$E_{nerst} = \frac{\Delta G}{2.F}. - \frac{\Delta S}{2.F}\left(T - T_{ref}\right) + \frac{R.T}{2.F}[\ln(PH_2) + \frac{1}{2}\ln(PO_2)] \tag{II-2}$$

Or :

- **ΔG :** Is change of free energy (J / k.mol).

- **F:** is the faraday constant (96.487 C / K mol).

- **ΔS:** is the change in entropy (J / k.mol).

- **R:** is the universal gas constant (8.314 J / K.mol).

- **PH_2, PO_2:** are respectively the partial pressures of hydrogen and oxygen (atm).

- **T:** indicates the fuel cell operating temperature (K).

- **T_{ref} :** is the reference temperature (K).

Using standard values of temperature and pressure, the expression of the Nernst equation arranged with a numerical calculation will be: [22]

$$E_{nerst} = 1.229 - 0.85 \times 10^{-3}(T - 298.15) + 4.31 \times 10^{-5}.T[\ln(PH_2) + \frac{1}{2}\ln(PO_2)] \tag{II-3}$$

We notice that reversible voltage depends on operating pressures and temperature, for 1.229 it's in the case that liquid water is the product but when we get the water production in the form of steam 1.229 should be replaced by 1.18V. [23]

II.2.1.2 Activation polarization loss :

The activation overvoltage are due to the start of chemical reactions at the anode and the cathode. Some of the available energy is used to break and reform chemical bonds at the electrodes. While the oxidation of hydrogen at the anode is much faster than the reduction of oxygen at the cathode, activation losses are mainly due to cathodic reactions. [21]

To calculate activation overvoltage Tafel equation given below is used : [22]

$$V_{act} = -[\xi_1 + \xi_2.T + \xi_3.T.\ln([CO_2]) + \xi_4 \ln(I_{stack})] \qquad \text{(II-4)}$$

While :

I_{stack} : is the cell load current in [A]

$[CO_2]$: the concentration of oxygen in the cathode catalyst interface estimated on the basis of the oxygen partial pressure and cell temperature by the law of Henry [22,23]:

$$[Co_2] = \frac{PO_2}{5.08 \times 10^6 \times e^{(-\frac{498}{\tau})}} \qquad \text{(II-5)}$$

ξ [1-4] : represent the parametric coefficients defined on the basis of kinetic, thermodynamic   and electrochemical phenomena ($\xi_1$theoretical = -0.949 V , ξ_2 = 0.02866 , ξ_3 =7.6×10^{-5} ξ_4 =1.93×10^{-4}. [30]

II.2.1.3 Ohmic polarization loss

Ohmic polarization loss are derived from membrane resistance to transfer protons and from electrical resistance of the electrodes to transfer electrons .At a later stage, as current density rises, ohmic losses prevail. [23]

We can express ohmic losses by the following equation:

$$V_{ohm} = I_{stack} \times (R_m + R_c) \qquad \text{(II-6)}$$

Where

R_c : is the proton resistance considered as constant.

I_{stack} **:** is the function current of the fuel cell.

R_m : is the equivalent resistance of the electron flow.

$$R_m = \frac{\rho_M \cdot l}{A} \tag{II-7}$$

Where

- ρ_M : is the specific resistivity of the membrane for the electron flow (Ω.cm).

- A : is the active area of the cell in (cm^2).

- l :is the width of the membrane in (cm). [22]

For Nafion membrane :

$$\rho_M = \frac{181,6.[1+0,03.\left(\frac{I_{stack}}{A}\right)+0,062\left(\frac{T}{303}\right)^2.\left(\frac{I_{stack}}{A}\right).\left(\frac{I_{stack}}{A}\right)^{2.5}]}{\left[\Psi-0,643-3.\left(\frac{I_{stack}}{A}\right)\right].exp[4,18\left(\frac{T-303}{T}\right)]} \tag{II-8}$$

- Ψ: Fraction of the open area of a perforated plate [22] it is adjustable parameter with a possible maximum value of 23 , the exponential term in the denominator is the temperature factor correction if the cell is not at 30°C and the terms $\frac{181.6}{[\Psi-0.634]}$ is the specific resistance (Ω.cm) at no current and at 30°C [23].

II.2.1.4 Concentration polarization loss

When the oxygen and nitrogen inside the cell cannot be delivered by constant pressure due to flow resistance (This pressure reduction depends on the current delivered and the characteristics of the gas circuits),concentration voltage loss is generated.[23,21]

The concentration polarization is given by the following relation:

$$V_{con} = -B.\ln(1 - \frac{J}{J_{max}}) \tag{II-9}$$

- J: current density (A / cm^2)

- J$_{max}$: the maximum current density (A / cm^2)

- B: Designates the electrochemical constant (V) and given by the following relation :

$$B = \frac{R.T}{n.F}$$ (II-10)

- R: is the universal gas constant (8.314J / K.mol)0

- T: is the temperature (K).

- n: Number of elementary cells of the cell.

- F: Faraday's constant (96.487 C / K.mol). [29]

The Previous laws was obtained by applying the assumption that parameters for individual cells can be lumped together to represent a fuel-cell stack Therefore they can be calculated for individual cell and multiply them n the end by the number of cells , and the output voltage of the fuel-cell stack become :

$$V_{stack} = \text{NN}_{cell}(\text{E}_{nernst} - \text{Vact} - \text{Vohm} - \text{Vcon})$$ (II-11)

- N$_{cell}$ is the number of cells in the stack

The instantaneous electrical power supplied by the cell to the load can be determined by the equation: [23]

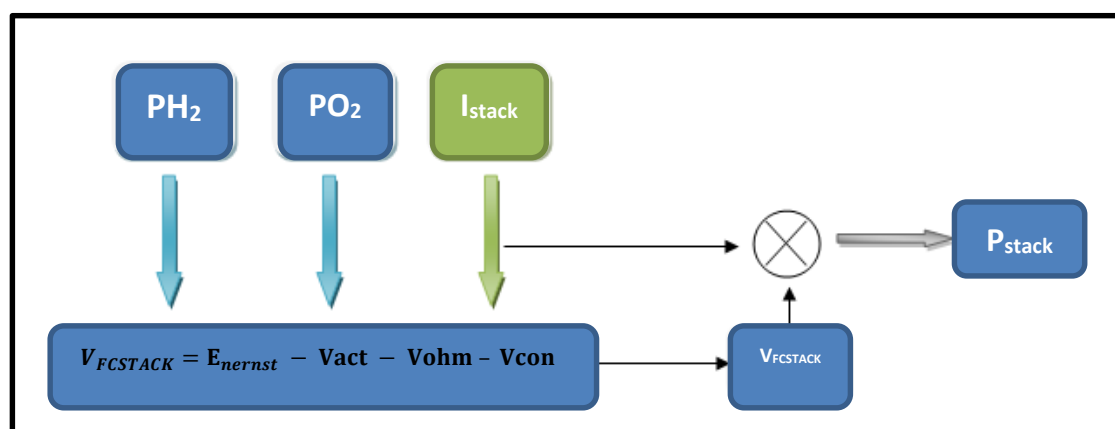$$\text{P}_{stack} = \text{V}_{stack} \times \text{I}_{stack}$$ (II-12)

Fig II-1 : Static Model of PEMFC. [23]

Previous laws is used to describe the voltage / current density characteristic curve of a PEMFC fuel cell (The characteristics of a fuel cell considered are illustrated in Tab (II-1):

Tab II-1: Technical characteristics of the fuel cell. [20]

| Model parameters	
Ideal gas constant	8.314 J/molK
Faraday's constant	96487 Coulombs
Temperature	80 C
Hydrogen pressure	$P\_H2 = 3$ atm
Air pressure	$P\_air = 3$ atm
Area of cell	100
Number of Cells	90
Internal Resistance	0.19 Ohm-cm^2
Transfer coefficient	0.5
Amplification constant	0.085
Exchange Current Density	10^-6.912 A/cm^2
Limiting current density	1.4 A/cm2
Gibbs function in liquid form	-228170 J/mol
Constant k used in mass transport	1.1
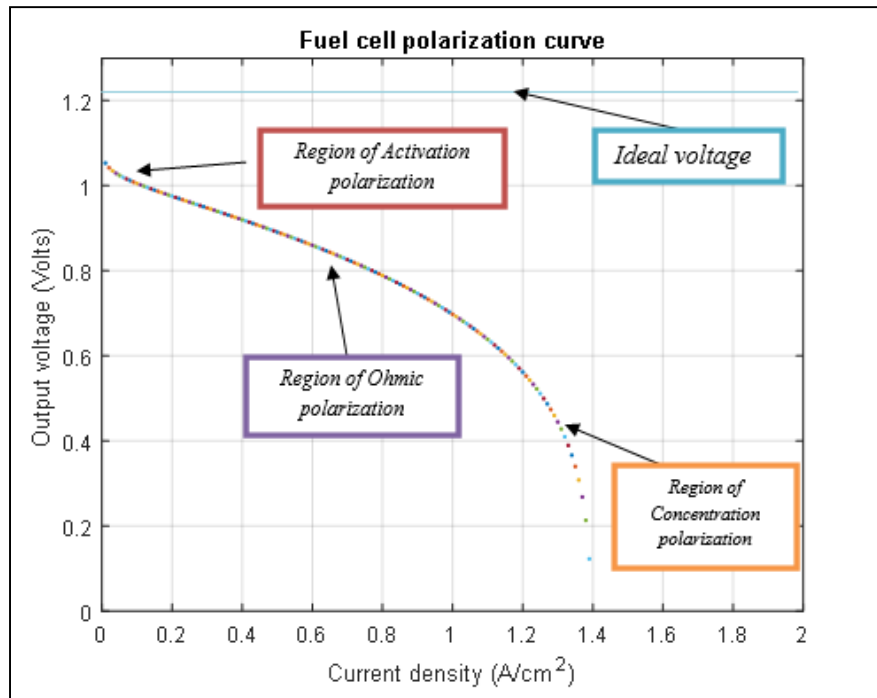
Fig II-2: PEMFC polarization curve.

- This curve obtained using MATLAB algorithm it contains three predominant zones as a function of the value of the current density.

The first zone is more important for low current densities, it represents region of activation polarization.

- The second is the linear zone, it represents the region of ohmic polarization,because of the linearization make it the most used area.

- The third zone related to the concentration polarization, we could observe a rapid drop in potential.

II.2.2 Dynamic model of PEMFC [23]

The membrane in a PEM fuel cell allows only the H^+ ions to pass, at the same time the electrons at the anode pass through the external load and until the surface of the cathode and the protons of hydrogen will be attracted. Thus, two charged layers of opposite polarity are formed across the boundary between the porous cathode and the membrane. These two layer separated by the membrane act as double charged layer, which can store electrical energy, due to this property this can be treated as a capacitor.
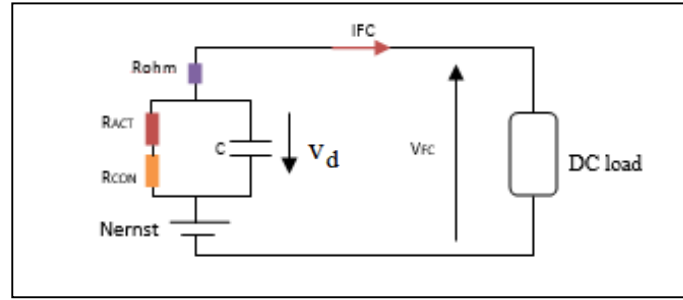
Fig II-3 Equivalent electrical circuit of PEM fuel cell [23]

Equation that described This model of fuel cell is :

$$\frac{d\,v_d}{d\,t} = \frac{1}{C} \times I - \frac{1}{\tau_f} \times v_d \qquad\qquad (II\text{-}13)$$

- V_d : the dynamical voltage across the equivalent capacitor.

- **C:** is the equivalent electrical capacitance.

- **τf:** is the fuel cell electrical time constant dependent of the cell temperature given by the

equation V_d

$$\tau_f = (RACT + RCON)C \qquad\qquad (II\text{-}14)$$

Then FC voltage can be defined :

$$VFC = Nernst - Vd - I \times Rohm \qquad\qquad (II\text{-}15)$$

Where

- Rohm, RACT, RCON are respectively the representation for the ohmic, the activation and the concentration resistance.

Using (II-12) , (II-13) and Laplace transformations, transfer function (II-14) was obtained, in which s represents Laplace operator:

$$VFC = Nernst - [\,\frac{RACT+RCON}{sC(RACT+RCON)+1} + Rohm\,]I \qquad\qquad (II\text{-}16)$$

II.2.3 Fuel cell efficiency [20]

II.2.3.1 Matter efficiency

A material efficiency is the ratio between the quantity of hydrogen consumed by the cell and the quantity produced by the hydrogen reformer as it shown bellow :

$$\eta m = \frac{M°H2}{m°H2} \tag{II-17}$$

In a fuel cell, each "membrane-electrode" assembly must be supplied in an identical manner, which assumes the same flow rate and identical partial pressures. These assemblies being in series, any defect for one of them has repercussions on the others. We define a gas utilization coefficient that is typically estimated at 95%.

II.2.3.2 Thermodynamic efficiency:

It is the comparison of the electrical energy created with the heat energy of the electrochemical reaction :

$$\eta_{thermo} = \frac{\Delta G°(T)}{\Delta H°(T)} \tag{II-18}$$

For the reaction of water formation, when it is produced in the liquid state at 25° and under a pressure of 1 bar, these quantities are :
- Standard free enthalpy variation: $\Delta G° = -237$ kJ / mol.
- Standard enthalpy change: $\Delta H° = -265.8$ kJ / mol.

The thermodynamic efficiency is then worth: 83%

II.2.3.3 Voltaic efficiency

It is calculated by the ratio between the output voltage of the fuel cell (V fc) and the voltage E0(1.23 v) at the temperature concerned :

$$\eta vol = \frac{V fc}{1.23} \tag{II-19}$$

II.2.3.4 Overall efficiency

This is to take into account all previous values :

$$\eta ov = \eta vol \times \eta m \times \eta_{thermo} \tag{II-20}$$

In practice, the operating voltage of a PEM cell is around 0.7V. We can then calculate an approximate overall efficiency: 0.43

II.3 Modeling of power electronics converters

II.3.1 Chopper DC/DC

II.3.1.1 Mathematical model of the boost converter [24]

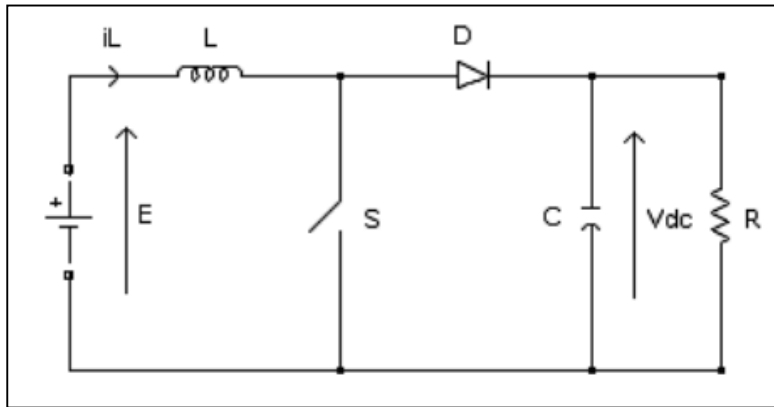By applying Kirchhoff's laws to the basic chopper scheme,we can obtain a mathematical model. [24]

Fig II-4: Electrical scheme of boost chopper. [24]

$$\begin{cases} L\dfrac{di_L}{dt} = E - V_{dc}(1-u) \\ \\ C\dfrac{dV_{dc}}{dt} = i_L(1-u) - \dfrac{Vdc}{R} \end{cases} \qquad \text{(II-21)}$$

While I_L is the current in the coil, E is the input voltage, Vdc is the output voltage and u is the control signal.

Derivation of the dynamic equations is in continuous conduction regime. In switch-on mode, u is equal to 1, the diode is blocked and the equations in this case is :

$$\begin{cases} L\dfrac{di_L}{dt} = E \\ \\ C\dfrac{dV_{dc}}{dt} = -\dfrac{Vdc}{R} \end{cases} \qquad \text{(II-22)}$$

And in the second state ($u = 0$) :

$$L\frac{di_L}{dt} = E - V_{dc} \quad , \quad C\frac{dV_{dc}}{dt} = I_L - \frac{V_{dc}}{R} \tag{II-23}$$

By putting $X_1 = I_L$ and $X_2 = V_{dc}$ then the equations of state become :

$$\begin{cases} \dot{x}_1 = \dfrac{E}{L} - \dfrac{x_2(1-u)}{L} \\[2mm] \dot{x}_2 = \dfrac{x_1(1-u)}{C} - \dfrac{x_2}{RC} \end{cases} \tag{II-24}$$

Then, the classical representation in state space $x' = Ax + Bu$ of (II-22) transforms into:

$$\begin{bmatrix} \dot{x}_1 \\ \dot{x}_2 \end{bmatrix} = \begin{bmatrix} 0 & -\dfrac{1-u}{L} \\[2mm] \dfrac{1-u}{C} & -\dfrac{1}{RC} \end{bmatrix} \begin{bmatrix} x_1 \\ x_2 \end{bmatrix} + \begin{bmatrix} \dfrac{1}{L} \\ 0 \end{bmatrix} E \tag{II-25}$$

It is Mean model of the boost converter The parameters of the system are: the inductance of the coil L in [H], the capacity C in [F] and the resistance of the load R in [Ω]. The state variables are the current in the coil and the voltage across the capacitor. The control signal u is included in the discrete domain of {0; 1} and it indicates the state of the switch S.
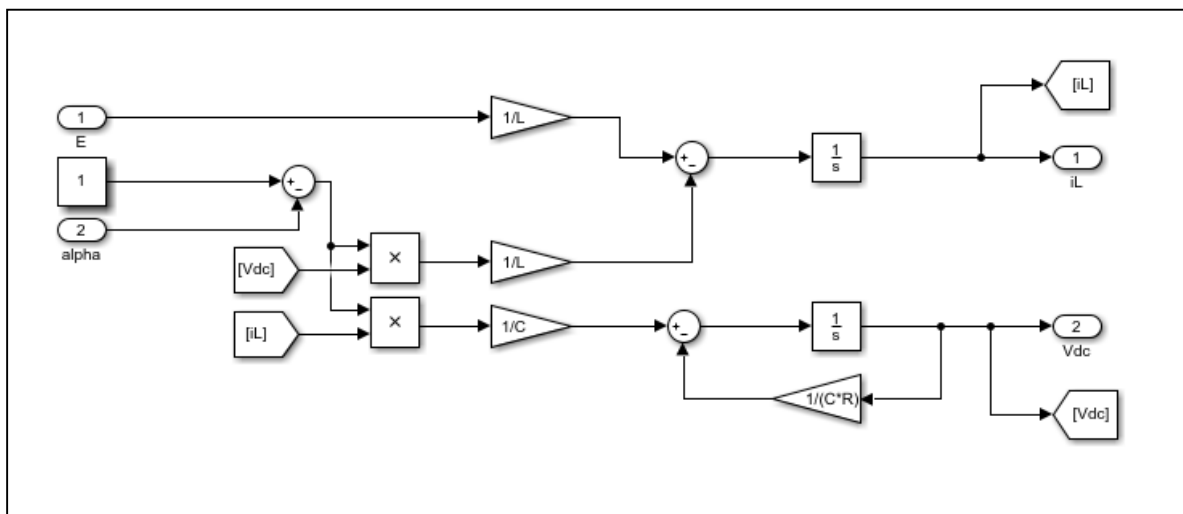

Fig II-5: Mathematical model of Boost converter using Simulink®.

II.3.1.2 Sizing of the Boost converter [25]

ΔI_L is the ripple of the current in the inductor :

For the first period $(0 < t \leq \alpha T)$:

$$\Delta I_L = I_{Lmax} - I_{Lmin} = \frac{E}{L}\,\alpha T \tag{II-26}$$

For the other period $(\alpha T \leq t < T)$:

$$\Delta I_L = I_{Lmax} - I_{Lmin} = \frac{V_{dc} - E}{L}\,(1 - \alpha)T \tag{II-27}$$

By combining these two relations, we can write :

$$V_{out} = V_{dc} = \frac{E}{1 - a} \tag{II-28}$$

From the past equations and at $t = \alpha T$:

$$I_{Lmax} = I_{Lmin} + \frac{E}{L}\,\alpha T \tag{II-29}$$

$$\text{And} \quad \Delta I_L = \frac{\alpha E}{L\,F} \tag{II-30}$$

The expression (II-29) shows us that the ripple of current decreases when the switching frequency F or the inductance value L increases. And from (II-27) we can write :

$$\Delta I_L = \frac{\alpha(1 - \alpha)V_{dc}}{L\,F} \tag{II-31}$$

by solving $\frac{\Delta I_L}{d\alpha} = 0$ we find that the current ripple is maximum for $\alpha = \frac{1}{2}$ and so :

$$L \geq \frac{V_{dc}}{4\,F\Delta I_{Lmax}} \tag{II-32}$$

From the expression of the voltage ripple shown bellow and we assume that the output current is perfectly constant we can find the value of capacitor C

$$\Delta V_{dc} = \frac{\alpha\,V_{dc}}{R.C.F} \tag{II-33}$$

This expression shows us that the voltage ripple decreases when the switching frequency or the value of the capacitor C increases , and so :

$$C \geq \frac{\alpha_{max}V_{dc}}{R\,F\Delta V_{dc}} \tag{II-34}$$

In our case input voltage V_{fc} is variable so :

$$\alpha_{max} = 1 - \frac{V_{fc\,min}}{V_{dc}} \qquad \text{(II-35)}$$

II.3.2 Three-phase inverter DC/AC [19]

Called two-level inverter , A three-phase inverter can be produced by grouping together, in parallel, three single-phase inverters (in bridge or half-bridge) and control the switches of each to obtain three phases at the output offset by 120 °. In fact, by grouping three single-phase half bridges, we obtain a three-phase bridge inverter with six switches shown in Fig II-6

We must distinguish the simple voltage V_{an} , V_{bn} and V_{cn} measured between the branch and neutral on the alternative side (engine) and on the other hand, there are the compound voltages V_{ab}, V_{bc} and V_{ca} measured between two phases.
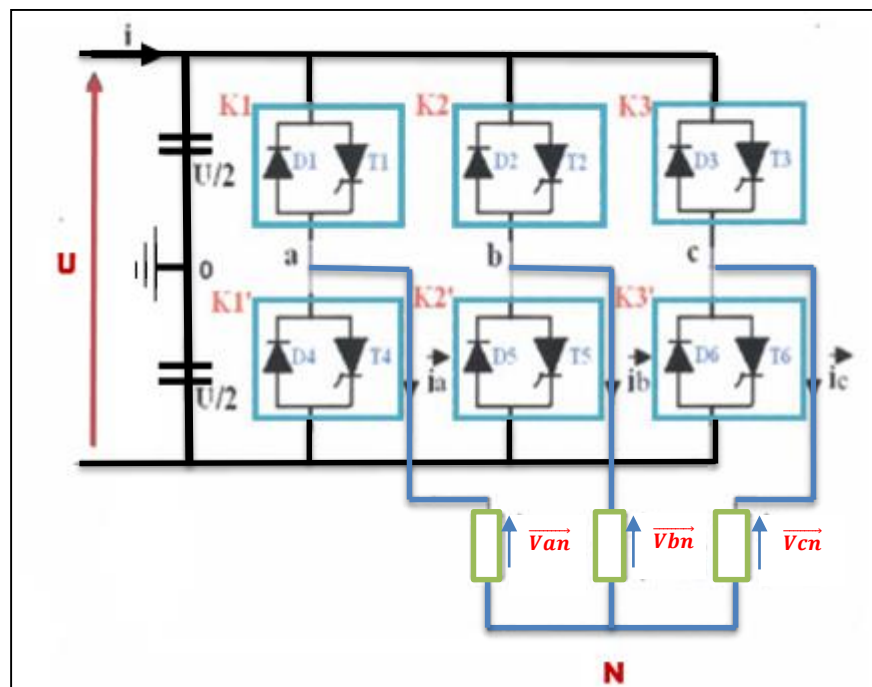

Fig II-6: Power circuit of a three-phase voltage inverter.

Switches of the same arm of the inverter must be complementary so that the direct voltage U is never short circuited and so that the circuits of the currents i_a, i_b and i_c are never open.

In this part, we will assume that:
- The voltage at the terminals of the switches is negligible.
- The load is balanced and star-coupled.

The sum of the line currents is zero, which implies that the sum of the phase-to-neutral voltages is equal to zero, therefore

$$V_{an} + V_{bn} + V_{cn} = 0 \tag{II-36}$$

And we have from Fig II-6 :

$$\begin{cases} V_{ao} = V_{aN} + V_{No} \\ V_{bo} = V_{bN} + V_{No} \\ V_{co} = V_{cN} + V_{No} \end{cases} \tag{II-37}$$

From the previous equations (II-35) and (II-36), we can determine the phase-to-neutral voltages:

$$V_{No} = \frac{1}{3}[V_{ao} + V_{bo} + V_{co}] \tag{II-38}$$

By substitution of (II-37) in (II-36) :

$$\begin{cases} V_{aN} = \dfrac{1}{3}[2V_{ao} - V_{bo} - V_{co}] \\[2mm] V_{bN} = \dfrac{1}{3}[-V_{ao} + 2V_{bo} - V_{co}] \\[2mm] V_{cN} = \dfrac{1}{3}[-V_{ao} - V_{bo} + 2V_{co}] \end{cases} \tag{II-39}$$

The compound voltages V_{ab}, V_{bc} and V_{ca} :

$$\begin{cases} V_{ab} = V_{ao} + V_{bo} \\ V_{bc} = V_{bo} + V_{co} \\ V_{ca} = V_{co} + V_{ao} \end{cases} \tag{II-40}$$

II.3.3 DC bus

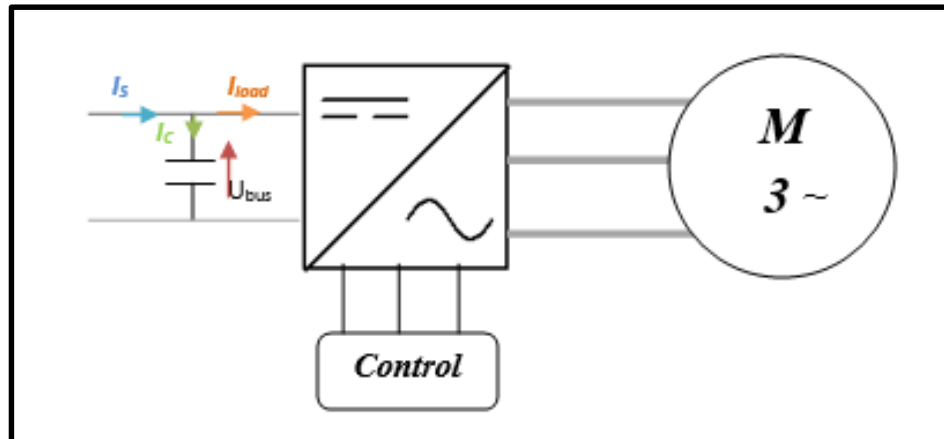The DC bus is a capacitor C for the purpose of smoothing the voltage and three currents.

Fig II-7: DC bus scheme.

From (Fig II-7) :

$$I_C = I_S - I_{load} \tag{II-41}$$

$$\frac{dU_{bus}(t)}{dt} = \frac{1}{c} \, I_c(t) \tag{II-42}$$

$$U_{bus} = \int \frac{dU_{bus}}{dt} + U_{bus}(t_0) \tag{II-43}$$

.

II.3.4 Asynchronous motor [26]

In order to model the motor we will rely on a number of simplifying hypotheses:

1- We assume that we are working in an unsaturated regime.

2- We neglect the saturation of the magnetic circuit, the phenomenon of hysteresis, eddy currents and the skin effect.

3- Sinusoidal spatial distribution of magnetomotive air gap forces. This amounts to considering the sinusoidal variation of the mutual inductances between stator and rotor windings as a function of the angle of their magnetic axes.

There are some important consequences of these hypotheses as the flow additivity the constancy of the own inductances.

II.3.4.1 The equations in the frame of reference (A, B, C)

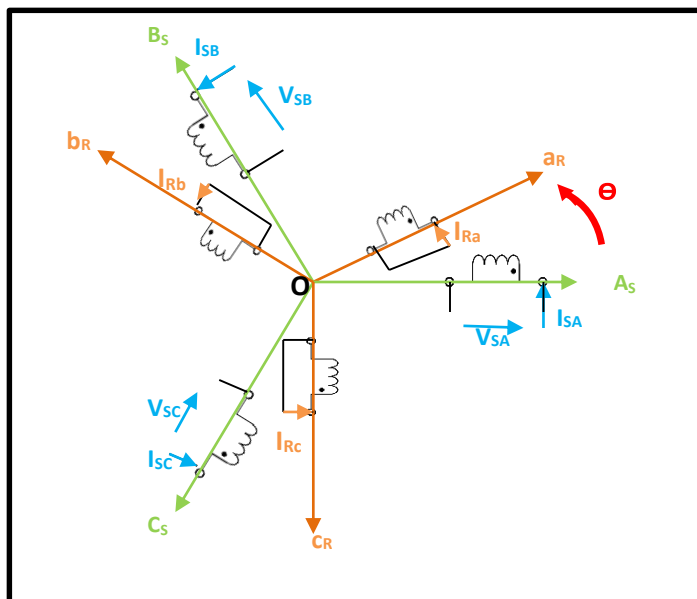The main structure of the three-phase asynchronous machine is as shown in Fig II-8

Fig II-8: Spatial representation of the ASM windings.

The electrical voltage equations of the three-stator phases and of the three rotor phases are presented in the following form:

$$\begin{cases} [V_{SABC}] = [R_S].[i_{SABC}] + \dfrac{d}{dt}[\phi_{SABC}] \\ [V_{rabc}] = [R_r].[i_{rabc}] + \dfrac{d}{dt}[\phi_{rabc}] \end{cases} \tag{II-44}$$

Where:

$[V_{SABC}] = [V_{SA}\, V_{SB}\, V_{SC}]^T$: Stator voltage vector

$[V_{rabc}] = [V_{ra}\, V_{rb}\, V_{rc}]^T$: Rotor voltage vector

$[i_{SABC}] = [i_{SA}\, i_{SB}\, i_{SC}]^T$: Stator current vector.

$[i_{rabc}] = [i_{ra}\, i_{rb}\, i_{rc}]^T$: Rotor current vector.

$[\phi_{SABC}] = [\phi_{SA}\, \phi_{SB}\, \phi_{SC}]^T$: Stator flux vector.

$[\phi_{rabc}] = [\phi_{ra}\, \phi_{rb}\, \phi_{rc}]^T$: Rotor flux vector.

R_S, R_r : The stator and rotor resistances per phase such as:

$$[R_s] = \begin{bmatrix} R_S & 0 & 0 \\ 0 & R_S & 0 \\ 0 & 0 & R_S \end{bmatrix} \quad , \quad [R_R] = \begin{bmatrix} R_r & 0 & 0 \\ 0 & R_r & 0 \\ 0 & 0 & R_r \end{bmatrix}$$

The magnetic equations representing the stator and rotor fluxes are given by:

$$\begin{cases} [\emptyset_{SABC}] = [L_{SS}].\,[i_{SABC}] + [M_{Sr}].\,[i_{rabc}] \\[2mm] [\emptyset_{rabc}] = [L_{rr}].\,[i_{rabc}] + [M_{rS}].\,[i_{sabc}] \end{cases} \tag{II-45}$$

Such as:

$$[M_{Sr}] = [M_{rs}]^T = m_{sr}.\begin{bmatrix} \cos(\theta) & \cos(\theta + \frac{2\pi}{3}) & \cos(\theta - \frac{2\pi}{3}) \\ \cos(\theta - \frac{2\pi}{3}) & \cos(\theta) & \cos(\theta + \frac{2\pi}{3}) \\ \cos(\theta + \frac{2\pi}{3}) & \cos(\theta - \frac{2\pi}{3}) & \cos(\theta) \end{bmatrix}$$

$$[L_{SS}] = \begin{bmatrix} L_s & m_s & m_s \\ m_s & L_s & m_s \\ m_s & m_s & L_s \end{bmatrix}, \qquad [L_{rr}] = \begin{bmatrix} L_r & m_s & m_s \\ m_s & L_r & m_s \\ m_s & m_s & L_r \end{bmatrix}$$

With :

[L$_{SS}$]: Matrix of stator inductance coefficients.

[L$_{rr}$]: Matrix of rotor inductance coefficients.

[L$_S$]: Self-inductance coefficient of a stator phase.

[m$_s$]: Coefficient of mutual inductance between two stator phases.

[L$_r$]: Coefficient of inductance specific to a rotor phase.

[m$_r$]: Mutual inductance coefficient between two rotor phases.

[M$_{Sr}$]: Matrix of mutual inductance coefficients of the rotor on the stator.

[M$_{rS}$]: Matrix of mutual inductance coefficients of the stator on the rotor.

By replacing relations (II-43) in (II-44) we obtain

$$
\begin{cases}
[V_{SABC}] = [R_S].\,[i_{SABC}] + [L_{SS}].\dfrac{d}{dt}[i_{SABC}] + \dfrac{d}{dt}.(M_{Sr}[i_{rabc}]) \\[2mm]
[V_{rabc}] = [R_r].\,[i_{rabc}] + [L_{rr}].\dfrac{d}{dt}[i_{rabc}] + \dfrac{d}{dt}.(M_{Sr}[i_{SABC}]) = [0]
\end{cases}
\qquad \text{(II-46)}
$$

The M_{Sr} coefficient represents the maximum value of the mutual inductance coefficients between rotor and stator phase.

II.3.4.2 Equations in the frame of reference (d, q)

The solution of the system obtained in the previous part is very difficult because of the high order and some non-fixed coefficient so Park transformation is a good solution to solve them.

$$
\begin{cases}
V_{Sd} = R_S.\,i_{Sd} + \dfrac{d\varnothing_{Sd}}{dt} - \dfrac{d\theta_S}{dt}.\varnothing_{Sq} \\[2mm]
V_{Sq} = R_S.\,i_{Sq} + \dfrac{d\varnothing_{Sq}}{dt} - \dfrac{d\theta_S}{dt}.\varnothing_{Sd} \\[2mm]
V_{rd} = R_r.\,i_{rd} + \dfrac{d\varnothing_{rd}}{dt} - \dfrac{d\theta_r}{dt}.\varnothing_{rq} = 0 \\[2mm]
V_{rq} = R_r.\,i_{rq} + \dfrac{d\varnothing_{rq}}{dt} - \dfrac{d\theta_r}{dt}.\varnothing_{rd} = 0
\end{cases}
\qquad \text{(II-47)}
$$

The magnetic equations can be expressed as :

$$
\begin{cases}
\varnothing_{Sd} = M_{Sr}.\,i_{rd} + L_{SS}.\,i_{Sd} \\[1mm]
\varnothing_{Sq} = M_{Sr}.\,i_{rq} + L_{SS}.\,i_{Sq} \\[1mm]
\varnothing_{rd} = M_{Sr}.\,i_{Sd} + L_{rr}.\,i_{rd} \\[1mm]
\varnothing_{rq} = M_{Sr}.\,i_{Sq} + L_{rr}.\,i_{rq}
\end{cases}
\qquad \text{(II-48)}
$$

$L_{SS} = L_S - m_S$: The cyclic stator inductance.

$L_{rr} = L_r - m_r$: The cyclic rotor inductance.

$M_{Sr} = \dfrac{3}{2}m_{Sr}$: The cyclic mutual inductance between stator and rotor.

The expressions of electromagnetic couple can be established according to the chosen variables:

$$
T_{em} = \frac{3}{2}.\,p.\,(\varnothing_{Sd}.\,i_{Sq} - \varnothing_{Sq}.\,i_{Sd})
\qquad \text{(II-49)}
$$

$$
T_{em} = \frac{3}{2}.\,p.\,(\varnothing_{rq}.\,i_{rd} - \varnothing_{rd}.\,i_{rq})
\qquad \text{(II-50)}
$$

$$T_{em} = \frac{3}{2} \cdot p \cdot M_{Sr} \cdot (i_{Sq} \cdot i_{rd} - i_{Sd} \cdot i_{rq}) \tag{II-51}$$

$$T_{em} = \frac{3}{2} \cdot p \cdot \frac{M_{Sr}}{L_S} \cdot (\emptyset_{Sq} \cdot i_{rd} - \emptyset_{Sd} \cdot i_{rq}) \tag{II-52}$$

$$T_{em} = \frac{3}{2} \cdot p \cdot \frac{M_{Sr}}{L_S} \cdot (\emptyset_{Sd} \cdot i_{Sq} - \emptyset_{rq} \cdot i_{Sd}) \tag{II-53}$$

$$T_{em} = J \cdot \frac{d\Omega}{dt} + f_v \cdot \Omega + C_r \tag{II-54}$$

There are different possibilities for choosing the orientation of the d, q axis coordinate system which generally depends on the objectives of the application.

Frame of reference fixed regarding to the stator :

$$\begin{cases} \dfrac{d\theta_S}{dt} = 0 \\ \dfrac{d\theta_r}{dt} = \omega_r = -\omega \end{cases} \tag{II-55}$$

Frame of reference fixed regarding to the rotor:

$$\begin{cases} \dfrac{d\theta_S}{dt} = \omega_S = \omega \\ \dfrac{d\theta_r}{dt} = 0 \end{cases} \tag{II-56}$$

Frame of reference fixed regarding to rotating field

$$\begin{cases} \dfrac{d\theta_S}{dt} = \omega_S \\ \dfrac{d\theta_r}{dt} = \omega_r \\ \dfrac{d\theta}{dt} = \omega_S - \omega_r \end{cases} \tag{II-57}$$

This reference adapts perfectly to vector control, and the electrical equations become:

$$\begin{cases} V_{Sd} = R_S \cdot i_{Sd} + \dfrac{d\emptyset_{Sd}}{dt} - \omega_S \cdot \emptyset_{Sq} \\ V_{Sq} = R_S \cdot i_{Sq} + \dfrac{d\emptyset_{Sq}}{dt} - \omega_S \cdot \emptyset_{Sd} \\ V_{rd} = R_r \cdot i_{rd} + \dfrac{d\emptyset_{rd}}{dt} - \omega_r \cdot \emptyset_{rq} = 0 \\ V_{rq} = R_r \cdot i_{rq} + \dfrac{d\emptyset_{rq}}{dt} - \omega_r \cdot \emptyset_{rd} = 0 \end{cases} \tag{II-58}$$

While The electromagnetic equations become :

$$\begin{cases} V_{Sd} = \left(R_S + L_S.\dfrac{di_{Sd}}{dt}\right) + M_{Sr}.\dfrac{di_{rd}}{dt} - L_S.\omega_S.i_{Sq} - M_{Sr}.\omega_S.i_{rq} \\[2mm] V_{Sq} = \left(R_S + L_S.\dfrac{di_{Sq}}{dt}\right) + M_{Sr}.\dfrac{di_{rq}}{dt} - L_S.\omega_S.i_{Sd} - M_{Sr}.\omega_S.i_{rd} \\[2mm] V_{rd} = \left(R_S + L_S.\dfrac{di_{rd}}{dt}\right) + M_{Sr}.\dfrac{di_{Sd}}{dt} - L_S.\omega_S.i_{rq} - M_{Sr}.\omega_S.i_{Sq} = 0 \\[2mm] V_{rq} = \left(R_S + L_S.\dfrac{di_{rq}}{dt}\right) + M_{Sr}.\dfrac{di_{Sq}}{dt} - L_S.\omega_S.i_{rd} - M_{Sr}.\omega_S.i_{Sd} = 0 \end{cases} \qquad \text{(II-59)}$$

II.4 Modeling of the vehicle

The vehicle model is a set of mechanical and aerodynamic equations ,which represents the different forces exerted on the vehicle during a driving cycle.
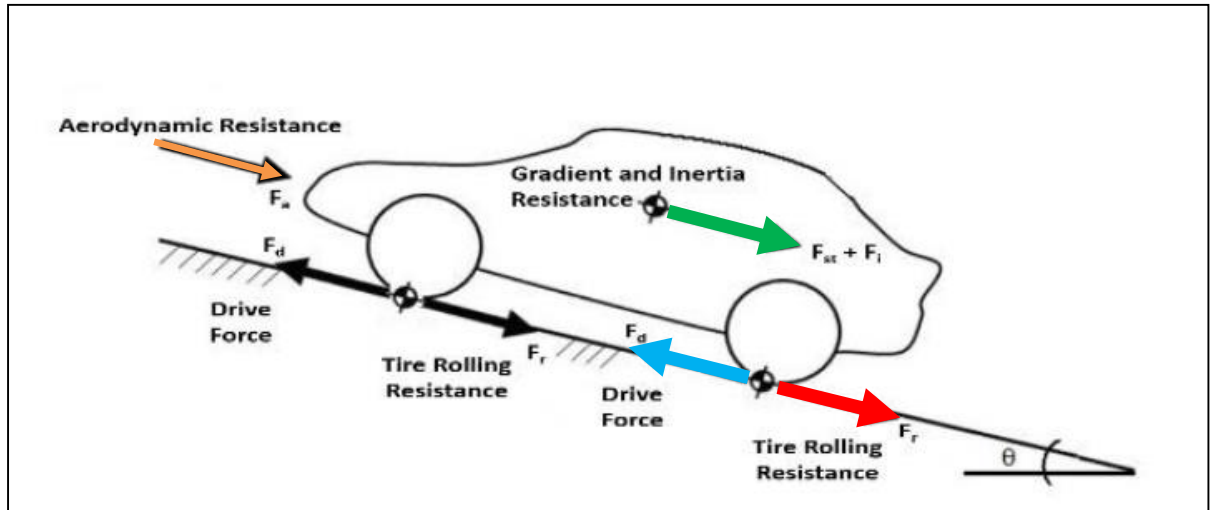
Fig II-9: Vehicle resistance forces.[27]

II.4.1 Aerodynamic resistance [27]

Called aerodynamic drag resistance, it is the force facing the vehicle while moving in air opposite to their motions

$$F_a = 0.5\rho. C_d. A_f (V + V_0)^2 \qquad \text{(II-60)}$$

- ρ :Density

- A_f : Reference area.

- V: velocity.

- C_d: aerodynamic resistance coefficient is determined experimentally according to vehicle shape

Tab II-2: Vehicle type and C_D.

Vehicle type	C_D
Cabriole	0.5-0.7
Car	0.3-0.4
Bus	0.6-0.7
Truck	0.8-1.5
Optimal design	0.2-0.3

II.4.2 Tire rolling resistance [27]

It is a resistance force against the rotational movement of the tire.

$$F_r = mgC_r \cos \alpha \qquad \text{(II-61)}$$

C_r: Tire rolling resistance coefficient varies according to the road surface

Tab II-3: Road surface and C_r

Road surface	C_r
Concrete or Asphalt	0.013
Small gravel ground	0.02
Macadamized road	0.025
Soil road	0.1-0.35

II.4.3 Gradient resistance [27]

When a vehicle is moving on a slope. A resistance arises due to the component of gravity.

$$F_{st} = mg \sin \alpha \qquad \text{(II-62)}$$

- α: the gradient of the path in degrees.

II.4.4 Inertia resistance [27]

It generated during positive and negative acceleration of the vehicle.

$$F_i = m.a \qquad \text{(II-63)}$$

Total resistance force :

$$F_{Load} = F_i + F_a + F_r + F_{st} \qquad \text{(II-64)}$$

II.4.5 Driving cycle :

A driving cycle represents a set of vehicle speed points in a function of time. It is used to assess a vehicle's fuel consumption and pollutant emissions in a standardized way, so the different vehicles can be compared with each other, like NEDC (New European Driving Cycle) and WLTP (Worldwide Harmonized Light Vehicles Test Procedure) cycles are used.
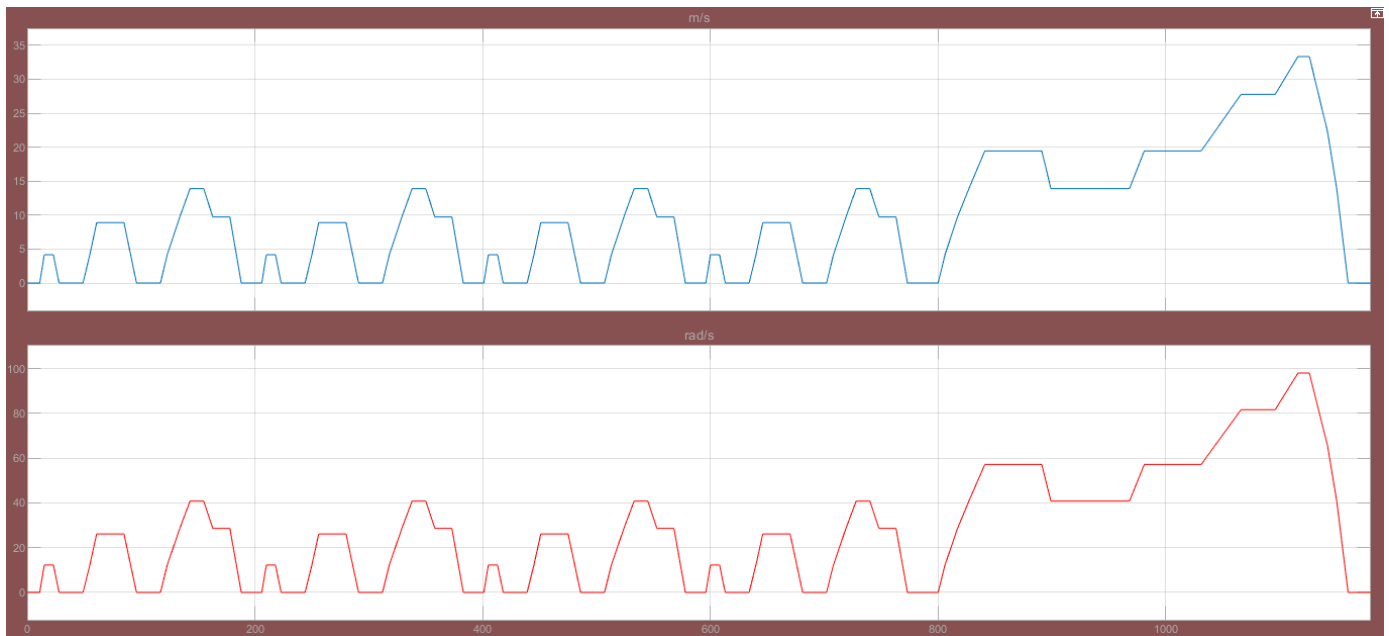
Fig II-10: NEDC Cycle (m/s and rad/s).

We can see from (Fig II-10) four similar shapes in the beginning then a surge in speed the Maximum Speed is 120 (km/h) and the time range is [0-1180] (S). All this can be summarized in (Fig II-11).the conversion from (rad/s) to (m/s) can be found using the equation

$$V(\frac{rad}{s}) = \frac{V(\frac{m}{s})}{r} \qquad \text{(II-65)}$$
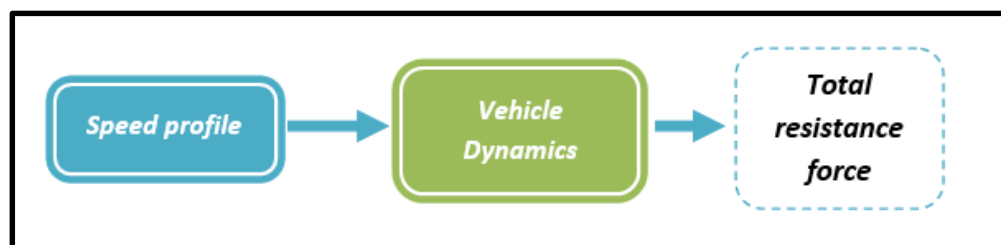
Fig II-11: General diagram of vehicle dynamics

II.5 Coupling between two mechanical and electrical models [28]

The electric motor is coupled to the dynamic part of the vehicle through a reduction gear, and this involves modeling the environment of the vehicle through the resistive torque applied to the electric motor.

$$T_{rr} = [F_i + F_a + F_r + F_{st}]r \tag{II-66}$$

In the case of a lossless reduction gear, the resistance torque applied to the machine is deduced from the above expression

$$T_r = \frac{T_{rr}}{G} \tag{II-67}$$

$$T_r = [m.g\sin\alpha + m.a + m.g.C_r\cos\alpha + 0.5\rho.C_d.A_f\left(\frac{\omega_r.r}{G}\right)^2] \times \frac{r}{G} \tag{II-68}$$

Another way to express the force to overcome a slope is using percentage in which slope of 100% corresponds to an inclination angle of 90 ° (infinite slope)

:

$$m.g.\sin\alpha = m.g.p\% \tag{II-69}$$

II.6 Conclusion

In this chapter, we have seen the operation and the modeling of our electric vehicle powered by a fuel cell as main energy source and a battery for the bus voltage regulation.We saw fuel cell inverter model and the sizing of the chopper by deducing the performance indices.

We saw also the coupling between the mechanical part and the electrical part the importance of this modeling is to simulate the whole vehicle at the same time or each part alone to see the system behavior and the influence of each parameter on the system. The model can also be used to determine the performance of electric vehicle such as the starting process or running with constant speed or in other case as we will show in the simulation chapter.

In the next chapter we will talk about the control system applied to the different system components in order to satisfy our goals

Chapter III

Control approaches and simulation

Chapter III

Control approaches and simulation

III.1 Introduction

In this chapter, we will present in an explicit way the control approaches used to control the three static converters introduced,then a simulation will be done using Matlab simulink 2019a. The proposed control device consists mainly of three control blocks as it shown in :

- A control block for the DC / DC boost converter associated with the fuel cell.
- A control block for the DC / DC buck-boost converter associated with the battery.
- A control block for the DC / AC converter on the load's side.

The first control block proposed in this chapter is for the purpose of generate impulses in order to increase the input voltage of fuel cell to the desired voltage 550 v , and the same about the 2nd control block but it is for the DC bus voltage regulation if there is a disturbance in the voltage generated by the chopper of fuel cell , finally the main goal of the last control block is to generate impulses for the DC / AC converter in order to control the speed of the asynchronous motor.
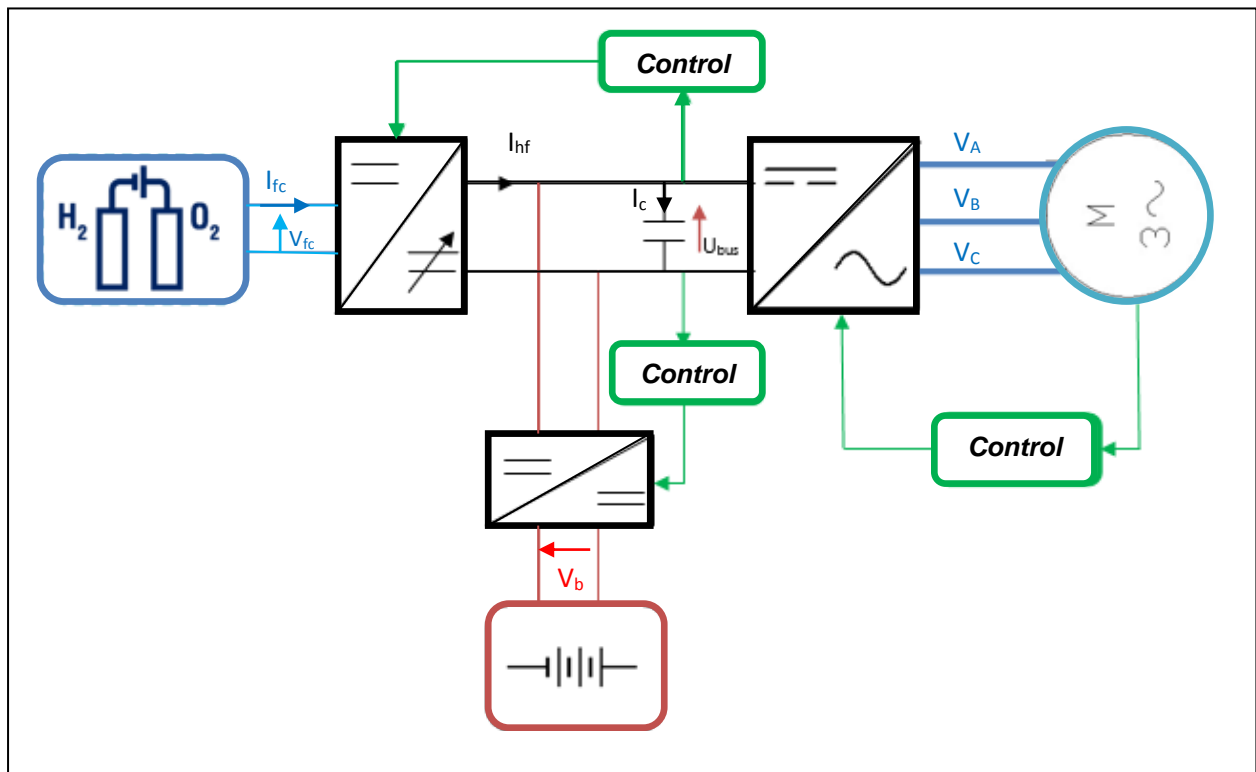
Fig III-1: Synoptic of the proposed system.

III.2 The DC part

This part contains of the main source (fuel cell) ,the battery a boost chopper and a buck-boost chopper.
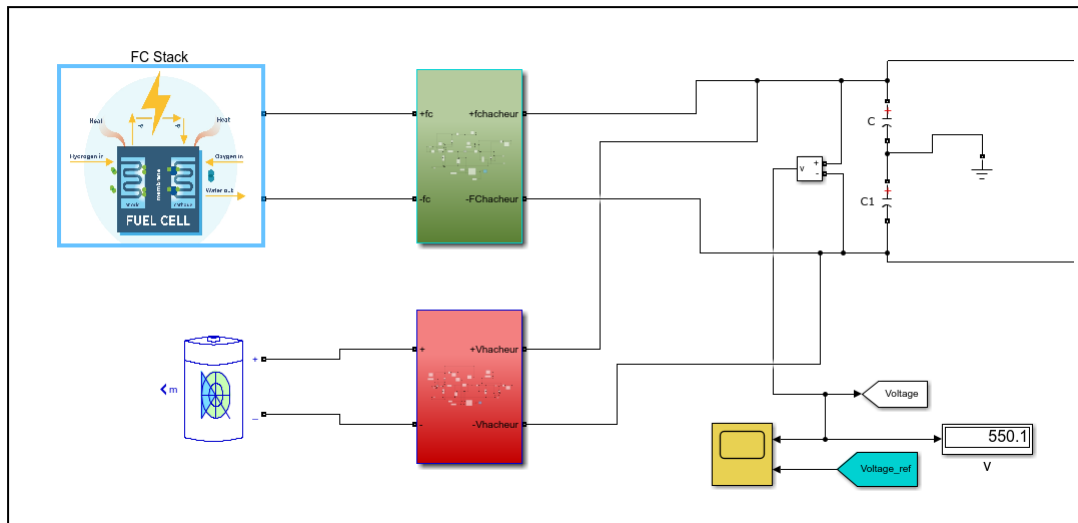
Fig III-2: MATLAB/SIMULINK® model of the DC part.

III.2.1 The control structure of DC/DC converters

A vital part of controlling a power interface is the regulation of certain intermediate quantities such as, the DC bus voltage or the output current of the fuel cell , under fairly strict constraints .The chosen structure is the one illustrated by Fig IV-1, the battery is connected to the DC bus by a reversible current chopper which will be described later, the function of these batteries is to keep the DC bus voltage constant. [32]

There several levels of control each has a specific function and specific specifications. However, communication and coordination between these levels are essential to ensure proper functioning :Close control, Energy management and the intermediate control (Regulators) [29] which we are going to focus mainly on it.

Currently, the most representative regulators for the control of continuous quantities are the proportional (P) and the proportional Integral (PI) [29]. Their roles is to modify the transfer function in order to respect the different constraints.

The proportional regulator has the advantage to obtain a fairly low position error while ensuring sufficient robustness by choosing the highest possible value of this gain but an inevitable disadvantage for the regulator to eliminate errors in permanent mode, after a change of set point or a variation of load. However, it is much easier to use a corrector with integral action which automatically allows the output to be brought back to the desired set-point,the main role of the integral action is to eliminate static error. However, the integral action is a phase lag element, so increasing the integral action (i.e. decreased T_i) produces instability

as it shifts the Nyquist locus to the left [30]. using this digital corrector the chopper can be well controlled via its current or the DC bus voltage but this one will have to respond to sudden stresses from the load, which is not recommended when the dynamics are important [29].in this work we are going to use it but with adding a battery which will have to compensate for the high dynamics and which will also be able to regulate the DC bus voltage.

Therefore the PI makes it possible to eliminate the regulation error which persisted with a proportional regulator alone. So to get a faster and more precise response, we use a proportional-integral corrector.
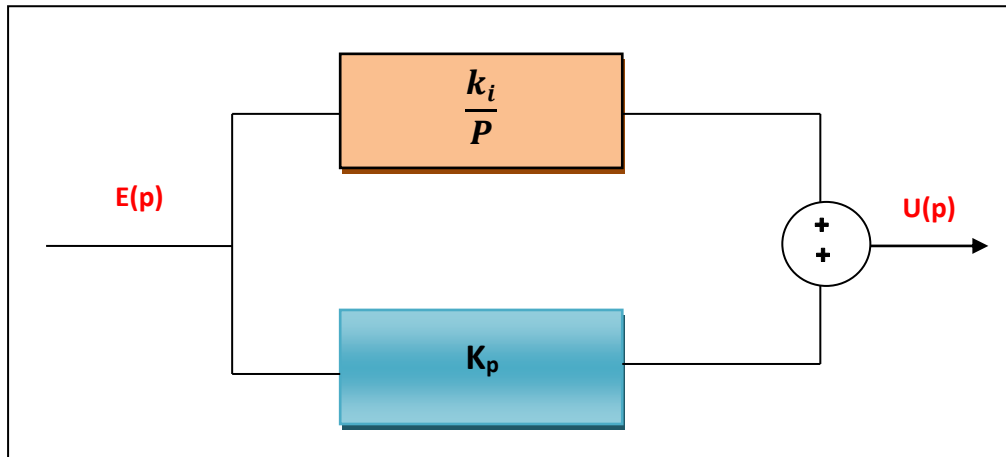
Fig III-3: Integral proportional corrector block diagram.[30]

From (Fig III-3)we can define the output of this regulator as:

$$U(t) = K_p \left(e(t) + \frac{1}{K_i} \int_0^t e(\tau)d\tau \right)$$ (III -1)

Using the Laplace transform the function transfer of the regulator PI is as follows :

$$C(p) = \frac{U(p)}{E(p)} = K_p \left(1 + \frac{1}{k_i\, p} \right) = K_p \left(\frac{1+k_i p}{k_i p} \right)$$ (III -2)

K_p , K_i and τ are respectively the gain and the time constant of the regulator. .[30]

Because both choppers are for the purpose of maintaining a desired fixed voltage (DC bus voltage) so we have to deduce their transfer function
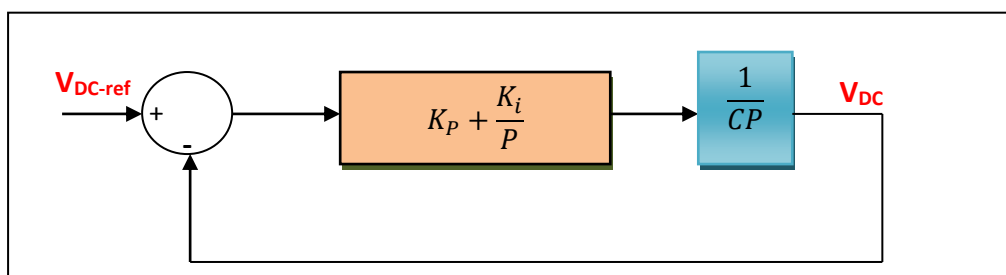
Fig III-4: DC bus regulation by a classic PI. [37]

The transfer function will be : [31]

$$F(P) = \frac{CK_pP + \frac{K_i}{C}}{P^2 + K_pP + \frac{K_i}{C}}$$ (III -3)

By choosing a desired characteristic equation of double pole type :

$$F_{des}(P) = (P + \lambda)^2$$ (III -4)

by the equalization of the equations (III -3) and (III -4) we can deducted K_P and K_i

$$K_p = \frac{4}{\tau} \quad , \quad K_i = \frac{4C}{\tau^2}$$

We note that : $\lambda = \frac{2}{\tau}$.

III.2.2 Simulation

The simulation was performed under the following conditions :

➢ Fuel cell

The characteristics of fuel cell used in this simulation is shown in the figure bellow :
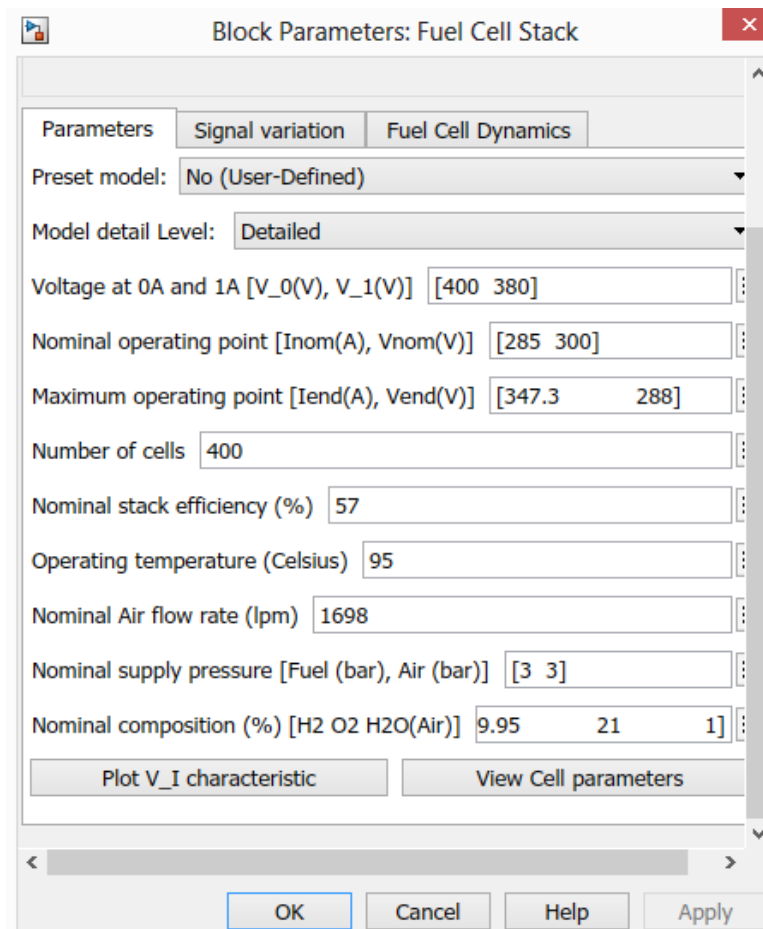
Fig III-5: Fuel cell stack parameters in MATLAB/SIMULINK®

➢ The battery

The characteristics of the battery used in this simulation is shown in the figure bellow :
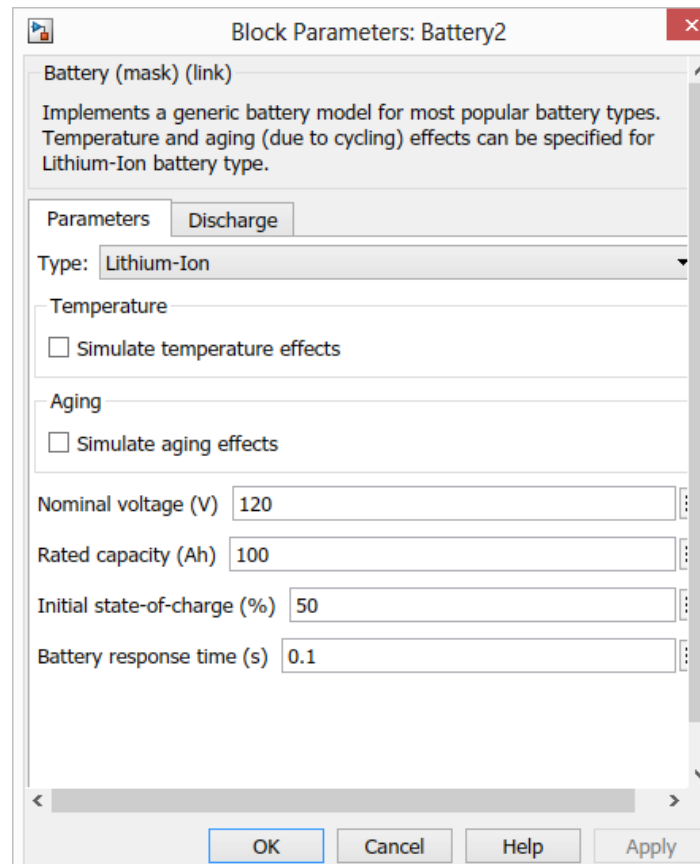
Fig III-6: Battery block parameters in MATLAB/SIMULINK®

In another hand the modeling of the DC bus using its transfert function under MATLAB/SIMULINK is:
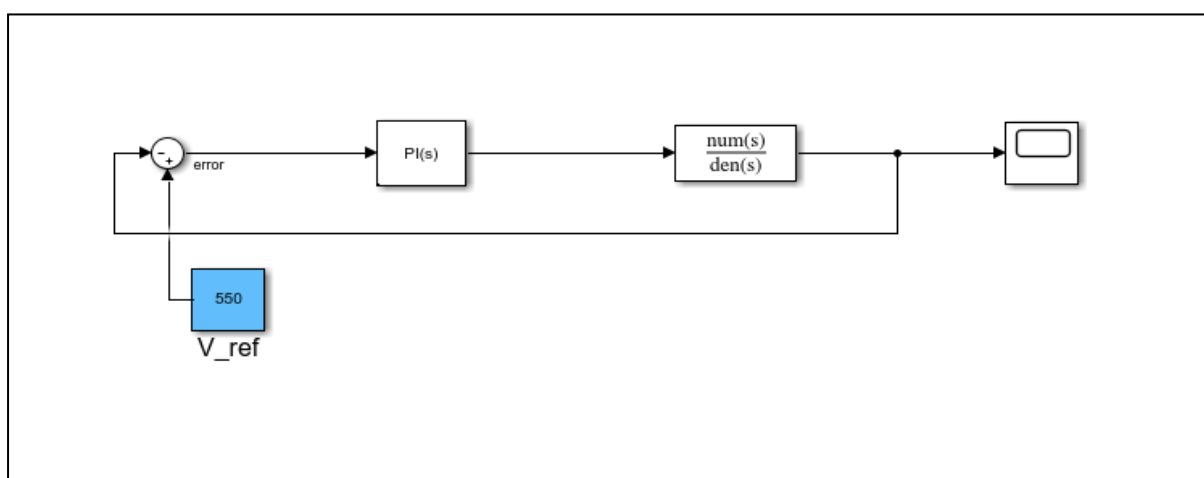
Fig III -7: MATLAB/SIMULINK® model of DC bus.

Another method we can use to deduct K_P and K_i parameters is by using the tuner in Matlab simulink exactly in PID block parameters , it is a easy process of finding the values of proportional and integral gains of a PI controller to achieve a desired performance
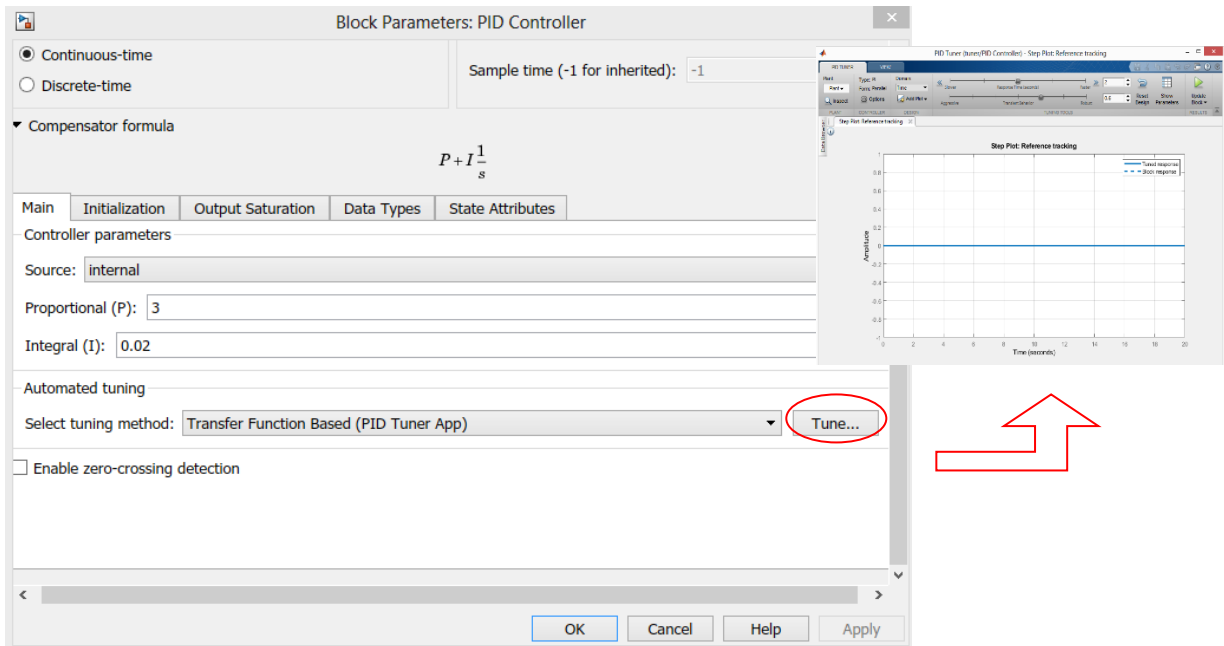
Fig III-8: Block parameters of PI controller MATLAB/SIMULINK®

Using tuner's method :

$$k_p = 0.02 \; ; \;\; k_i = 2$$

Then the model in MATLAB/SIMULINK® can be :
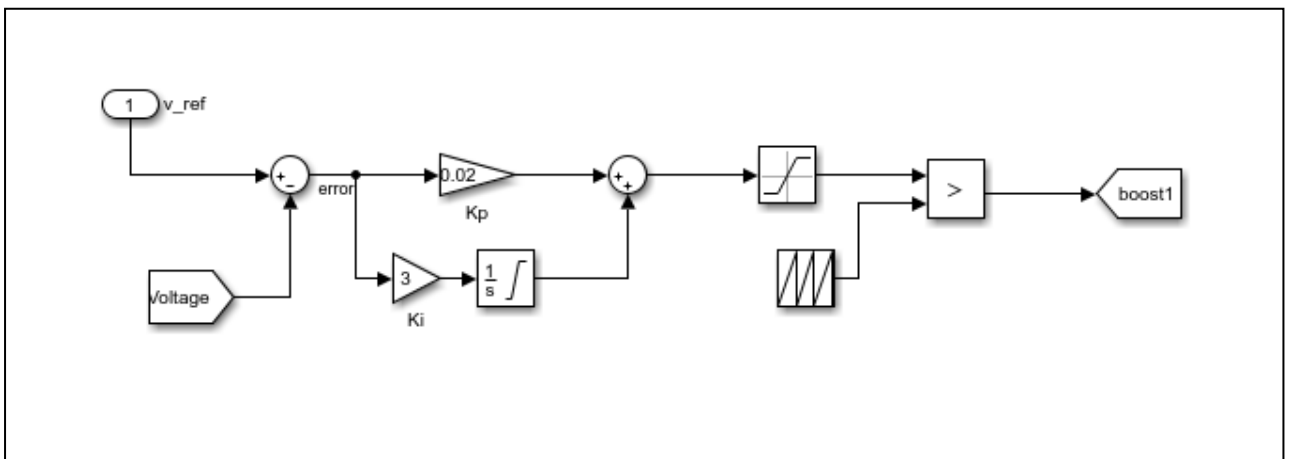
Fig III-9: MATLAB/SIMULINK® model of PI controller for boost converter.
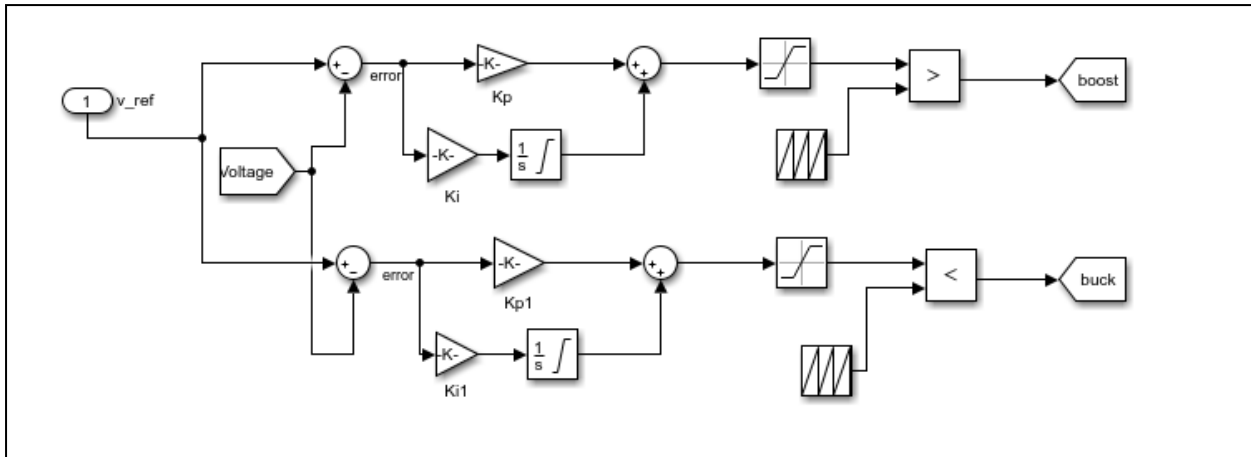
Fig III-10: MATLAB/SIMULINK® model of PI controller for buck-boost converter.

In the same time the system (buck-boost converter/ battery) should controlled in the way that the battery just works only in the case when the the DC bus voltage exceeds the permissible voltage drop value ΔU , this value can be selected by recognized standards or define it according to what we want the response to be.

The control process in MATLAB/SIMULINK® is shown in the (Fig III-11) below.
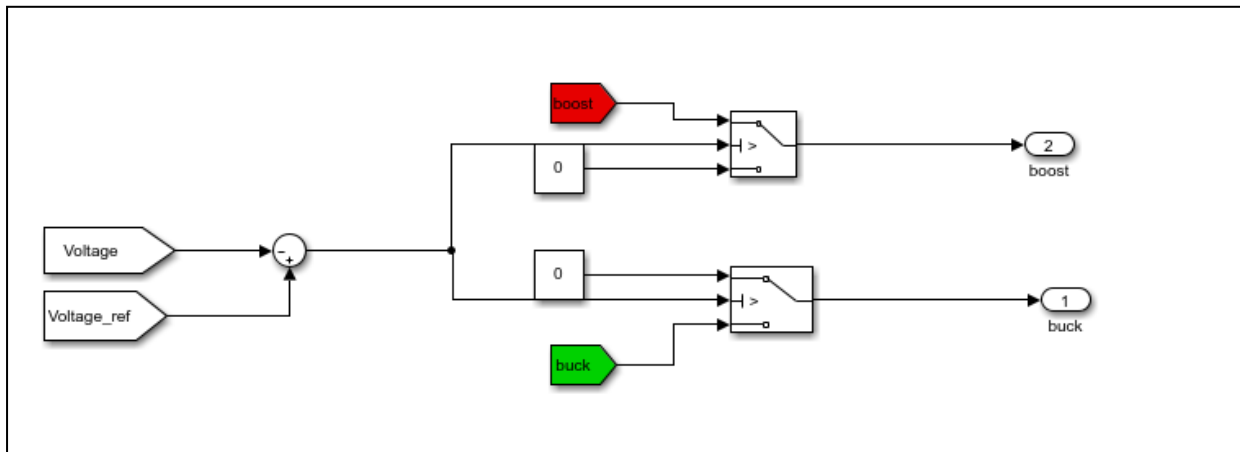
Fig III-11: Control process of the system battery-converter.

The switch is controlled by the second input which came from the difference between voltage and reference voltage (error), then it will be compared to a fixed value ΔU :

- If the relation is true ➔ first input will pass.

- If the relation is false ➔ second input will pass.

III.3 The AC part

This part contains the DC/AC inverter, the asynchronous machine and the block of direct torque control.

III.3.1 The technique of direct torque control

III.3.1.1 Principle of classic DTC

The technique of direct torque control (DTC) was introduced in 1985 by Takahashi. Several works have allowed a rigorous modeling of this approach.This technique consists to control directly the closing or opening of inverter's switches from the pre-calculated (estimated) values of the stator flux and the torque. [33] So the state of the switches is directly linked to the evolution of the electromagnetic state of the asynchronous motor .In this technique, we no longer need the position of the rotor to choose the voltage vector, this particularity defines the DTC as a method well suited for the control without mechanical sensor of AC machines. [34] therefore the controlled variables are: The stator flux and the electromagnetic torque which are usually controlled by hysteresis regulators. [33] When the torque or stator flux modulus reaches the upper or lower limit of the hysteresis, an appropriate voltage vector is applied to decrease the magnitude within its hysteresis band and it is better to work with a high calculation frequency in order to decrease the vibrations of the torque caused by the hysteresis controllers. [35]

The general characteristics of a direct torque control are: [35]

- Direct torque and flux control, based on the choice of optimal inverter switching vectors.
- Indirect control currents and voltages of stator's machine..
- Obtaining stator fluxes and currents close to sinusoidal shapes.
- Very fast dynamic machine response.
- The existence of torque oscillations which depends, among other things, on the factors of the bandwidth of the hysteresis regulators.
- The switching frequency of the inverter depends on the amplitude of the hysteresis bands.

The figure III-9 represents the block diagram of an asynchronous machine control based on the direct torque control strategy. The control of the inverter is instantaneous, so it is requiring a very low sampling period. [35]
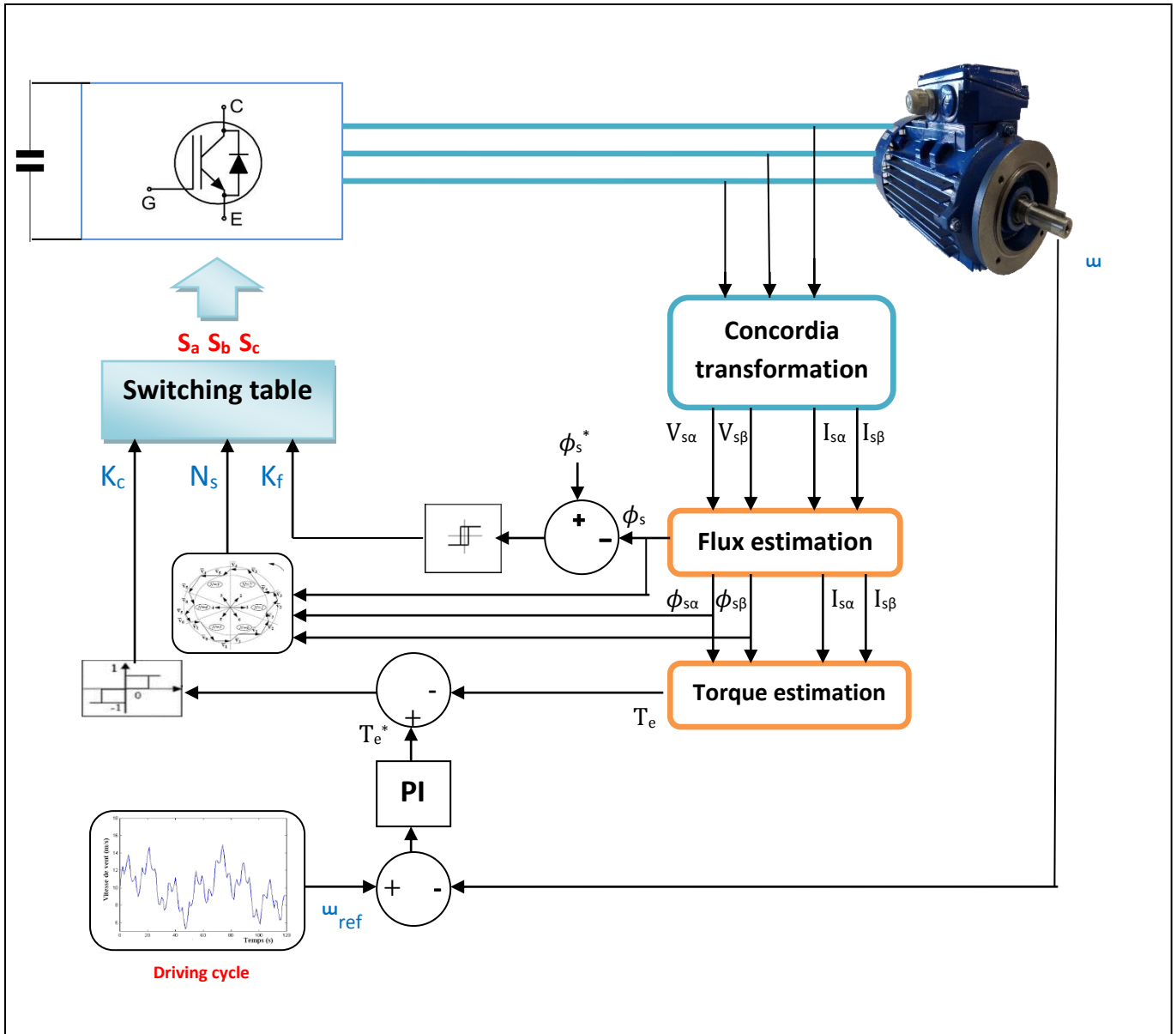

Fig III-12: General structure of direct torque control.

III.3.1.2 Estimation of stator flux and torque

The flux can be estimated from measurements of the stator current and voltage of the machine from the equation [33]:

$$V_s = R_s i_s + \frac{d\emptyset_s}{dt} \tag{III-5}$$

$$\vec{\emptyset}_s = \int_0^t (\vec{V_s} - R_s \vec{i_s}) dt \tag{III-6}$$

And we get the components α and β of the vector $\emptyset_s$

$$\begin{cases} \emptyset_{s\alpha} = \int_0^t (V_{s\alpha} - R_s i_{s\alpha}) dt \\ \emptyset_{s\beta} = \int_0^t (V_{s\beta} - R_s i_{s\beta}) dt \end{cases} \tag{III-7}$$

With :

$$\overline{\emptyset_s} = \emptyset_{s\alpha} + j\emptyset_{s\beta} \tag{III-8}$$

The zone N_s in which the vector $\emptyset_s$ is located is determined from the components $\emptyset_\alpha$ and $\emptyset_\beta$. The angle θ_s between the frame of reference and the vector $\emptyset_s$, is equal to [35] :

$$\theta_s = arctg\left(\frac{\emptyset_{\beta s}}{\emptyset_{\alpha s}}\right) \tag{III-9}$$

The components α and β of the stator current vector Iα and Iβ are obtained by applying the Concordia transformation to the measured currents [34]

Once the two components of the flux are obtained, the electromagnetic torque can be estimated from its formula :

$$T_{em} = \frac{3}{2} p \left[\emptyset_{\alpha s} i_{\beta s} - \emptyset_{\beta s} i_{\alpha s}\right] \tag{III-10}$$

III.3.1.2 Flux and torque corrector

The flux corrector has the role to maintain the end of the stator flux vector $\vec{\emptyset}_s$ in a circular band as indicated (Fig III-9), the output which indicate the evolution's direction of the module $\vec{\emptyset}_s$ is injected into the two-level hysteresis controller which generates the Boolean variable K_f at its output with the following rules[33] :

$$\begin{cases} \text{If } K_f = 1 \rightarrow \text{ the amplitude of the flux must be increased} \\ \text{If } K_f = 0 \rightarrow \text{ the amplitude of the flux must be decreased} \end{cases}$$

So as to maintain:

$$\left|(\emptyset_s)_{ref} - \emptyset_s\right| \leq \Delta\emptyset_s$$

With : $(\emptyset_s)_{ref}$ is the flow setpoint and $\Delta\emptyset_s$ is the corrector hysteresis width.
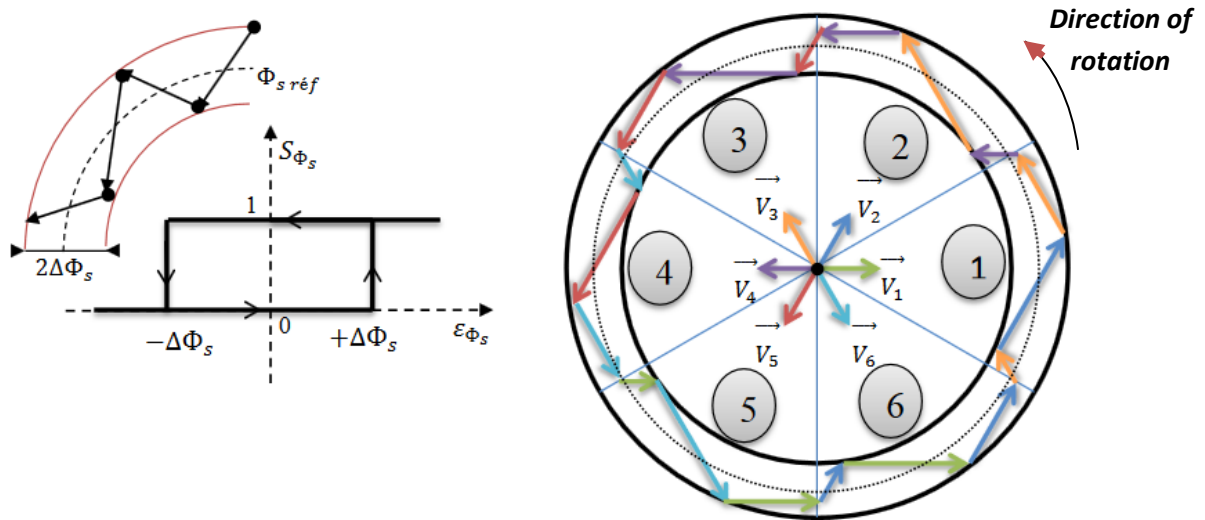
Fig III-13: Hysteresis flux corrector and selection of the corresponding voltage vectors[36]

For the torque corrector is identical to the one used for flux control ,the only difference is that the electromagnetic torque can be positive or negative depending on the direction of rotation of the machine . The goal of this corrector is to keep the torque within limits :

$$\left|(T_{em})_{ref} - T_{em}\right| \leq \Delta T_{em}$$

With

$(T_{em})_{ref}$: is the reference torque and ΔT_{em} corrector hysteresis band.

Two solutions can be proposed (two-level or three-level corrector):

➢ Two-level corrector

This corrector only allows to control the torque in one direction of rotation , noted that for each sector , there will be an arm of the inverter which never switches, this makes it possible to reduce the average switching frequency of the inverter, thus reducing the losses linked to the switching of the static converter.

This type of corrector is easy to implement, however, it is necessary to cross two phases of the machine to reverse the direction of rotation.

➢ Three-level corrector

It allows the motor to be controlled in both directions of rotation, either for positive or negative torque. The output of the corrector, represented by the Boolean variable K_c indicates directly whether the amplitude of the torque must be :

- Increased in absolute value (K_c =1 for a positive setpoint / K_c = - 1 for a negative setpoint).

- Decreased when K_c =0 . [34]
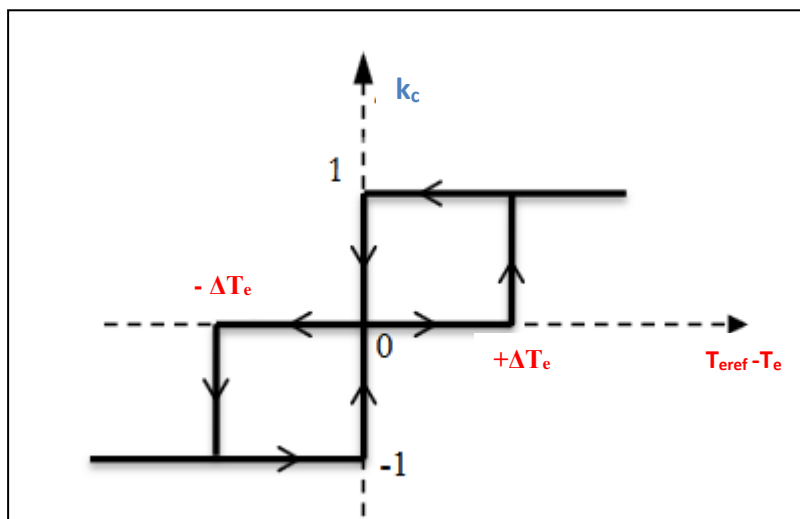
Fig III-14: Three-levels torque corrector[36]

III.3.1.3 Building the switching table

There are two types of switching table:

- Switching table with null sequences: In this case, all sequences are used , when the null vectors V_0 or V_7 is selected the rotation is stopped, resulting in a decrease in torque while the torque modulus remains unchanged.

- Switching table without null sequences: In this case, only the active sequences are used. This strategy is simpler to implement and makes it possible to avoid randomness when the machine is operating in generator mode

In our work we will use the first type ,the choice of the stator voltage vector Vs depends on the position of the stator flux vector in the complex plane αβ, the variation desired for the modulus of the flux, the variation desired for the torque, and the direction of rotation of the flux. [34]

Tab III-1: Switching table (ST) for DTC with null vectors. [33]

	N	1	2	3	4	5	6	Corrector		
$K_F = 1$	$K_C = 1$	$\vec{V_2}$	$\vec{V_3}$	$\vec{V_4}$	$\vec{V_5}$	$\vec{V_6}$	$\vec{V_1}$	*Two levels*		
	$K_C = 0$	$\vec{V_7}$	$\vec{V_0}$	$\vec{V_7}$	$\vec{V_0}$	$\vec{V_7}$	$\vec{V_0}$			
	$K_C = -1$	$\vec{V_6}$	$\vec{V_1}$	$\vec{V_2}$	$\vec{V_3}$	$\vec{V_4}$	$\vec{V_5}$	Three levels		
$K_F = 0$	$K_C = 1$	$\vec{V_3}$	$\vec{V_4}$	$\vec{V_5}$	$\vec{V_6}$	$\vec{V_1}$	$\vec{V_2}$	*Two levels*		
	$K_C = 0$	$\vec{V_0}$	$\vec{V_7}$	$\vec{V_0}$	$\vec{V_7}$	$\vec{V_0}$	$\vec{V_7}$			
	$K_C = -1$	$\vec{V_5}$	$\vec{V_6}$	$\vec{V_1}$	$\vec{V_2}$	$\vec{V_3}$	$\vec{V_4}$	Three levels		

K_f =1 for Increasing the flux , K_f =0 for decreasing

K_c =1 for Increasing the torque , K_c =0 for decreasing the torque and K_c =-1 for its maintenance.
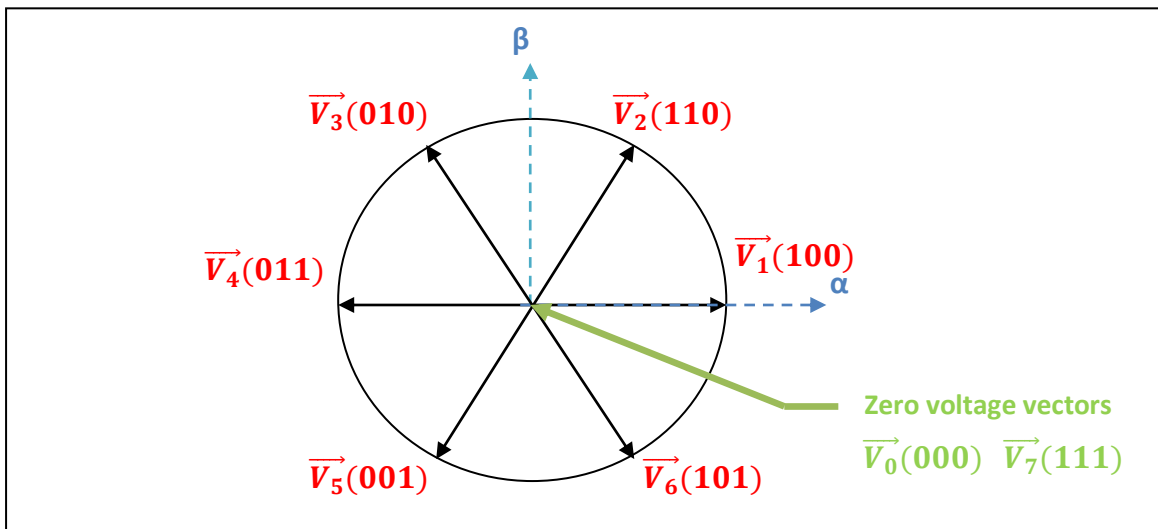
Fig III-15: Representation of voltage vectors.

III.3.1.4 Speed regulation [37]

The PI regulator has been applied for the control of asynchronous machines due to its various advantages. Indeed, it allows high performance to be obtained (low overshoot, zero static deviation,…) ,the speed regulation loop with the use of an PI type regulator is shown in (Fig III-16).
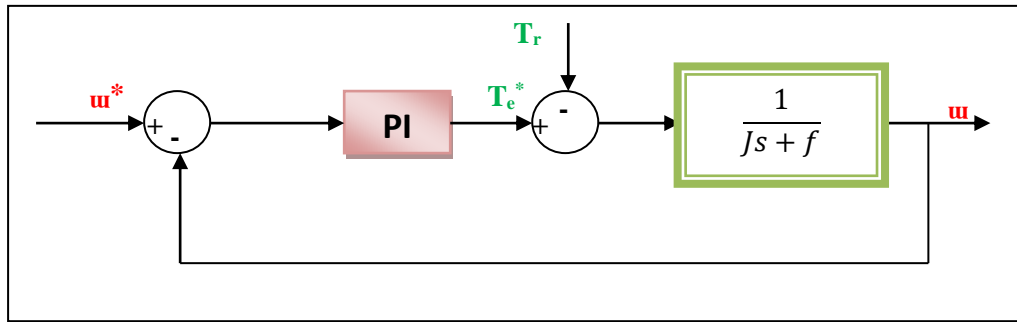
Fig III-16: Speed regulation loop with PI regulator.

The integral action reacts slowly to variations in the error and ensures a progressive catching up of the reference.

The proportional action depends in K_p value, If K_p is big the correction is quick but the risk of overshoot and oscillation increases and if K_p is small, the correction is slow but there is less risk of oscillations.

The mechanical equation that governs our system is

$$\frac{d\omega}{dt} = \frac{1}{J}\left[T_{em} - T_r - \frac{f}{p}\omega\right] \qquad (\text{III-11})$$

Then the closed loop transfer function will be

$$\frac{1+\tau S}{1+\left(\tau+\frac{f}{k_i}\right)S+\frac{J}{k_p S^2}} \qquad (\text{III-12})$$

For the system to behave like a first-order system :

$$H(S) = \frac{1}{1+\tau S} \qquad (\text{III-13})$$

It is necessary that :

$$k_p = \frac{J}{\tau} \quad ; \quad k_p = \frac{f}{\tau}$$

The regulator time constant is chosen according to the stator time constant which characterizes the torque dynamics

$$\tau = \frac{l_s}{R_s}$$

III.3.1.5 Advantages and disadvantages : [33]

The DTC has the following advantages :
- Not to require calculations in the rotor reference mark (d, q).
- There is no PWM voltage modulation calculation block.
- It is not necessary to decoupling the currents from the control voltages, as in the case of vector control.
- It has only one regulator, that of the external speed loop.
- It is not necessary to know the rotor position angle with great precision, because only information on the sector in which the stator flux vector is located is necessary.
- The dynamic response is very fast.

And for disadvantages:
- The existence of low speed problems;
- The need to have stator flux and torque estimates;
- The existence of torque oscillations
- The switching frequency is not constant (use of hysteresis regulators). This leads to rich harmonic content increasing losses, acoustic noises and torque oscillations which can excite mechanical resonances.

III.3.2 Simulation

The general structure of direct torque control using MATLAB/SIMULINK® is shown in (Fig III-17) below :
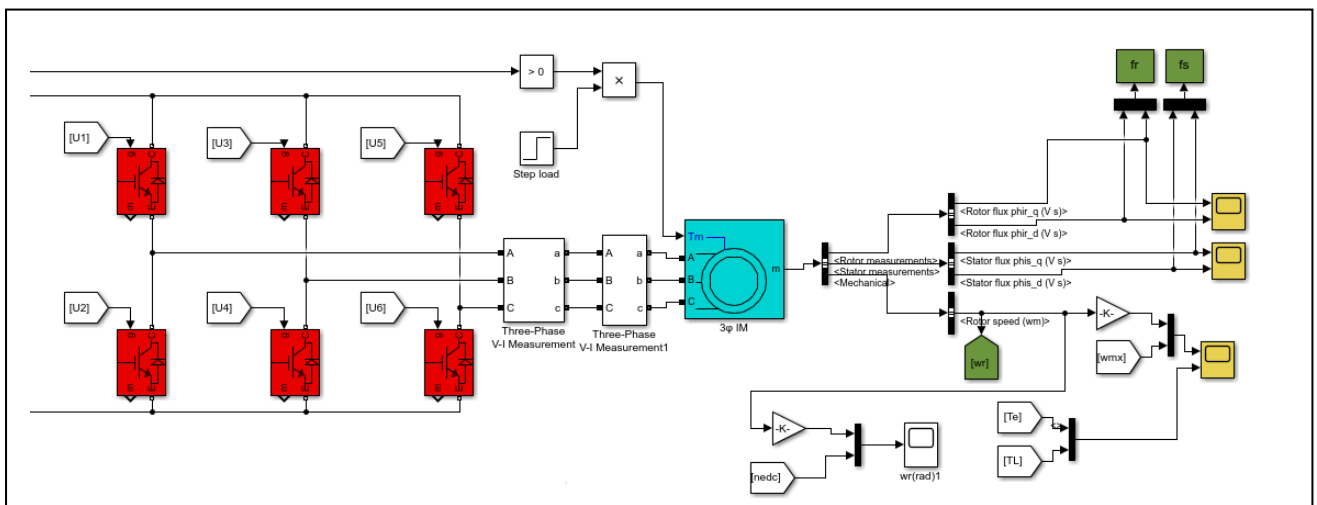
Fig III-17: MATLAB/SIMULINK® model of AC part.
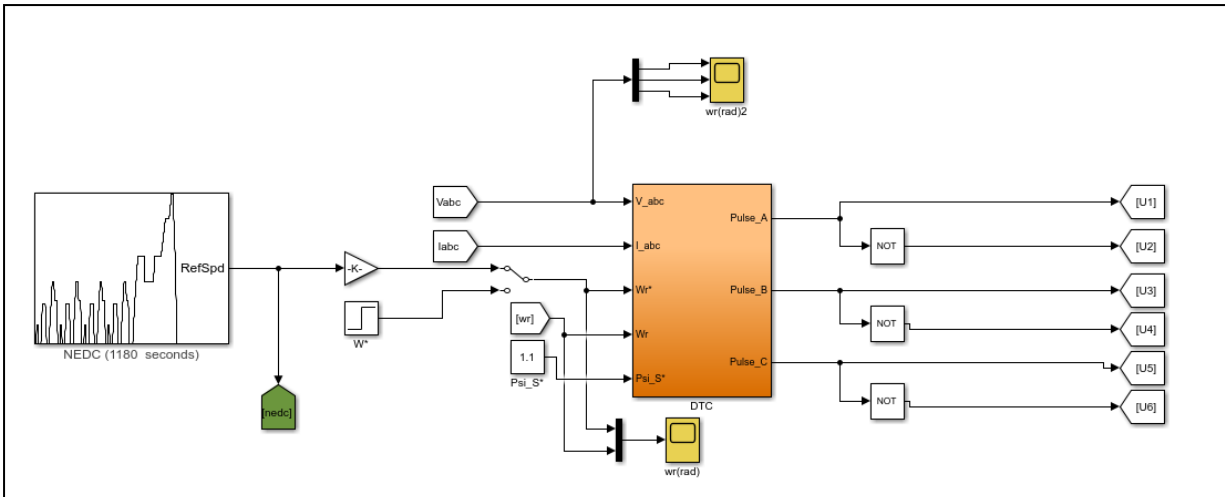
Fig III-18: MATLAB/SIMULINK® block of DTC

The block has :

- Inputs : measured speed, flux reference, measured currents/voltages and speed reference , two cases : step as motor's speed reference directly injected to the DTC block and NEDC driving cycle m/s acting as vehicle speed reference so the idea is to transform it to rad/s and to what corresponds to motor's speed using a gain.

- Inverter's pulses as output.
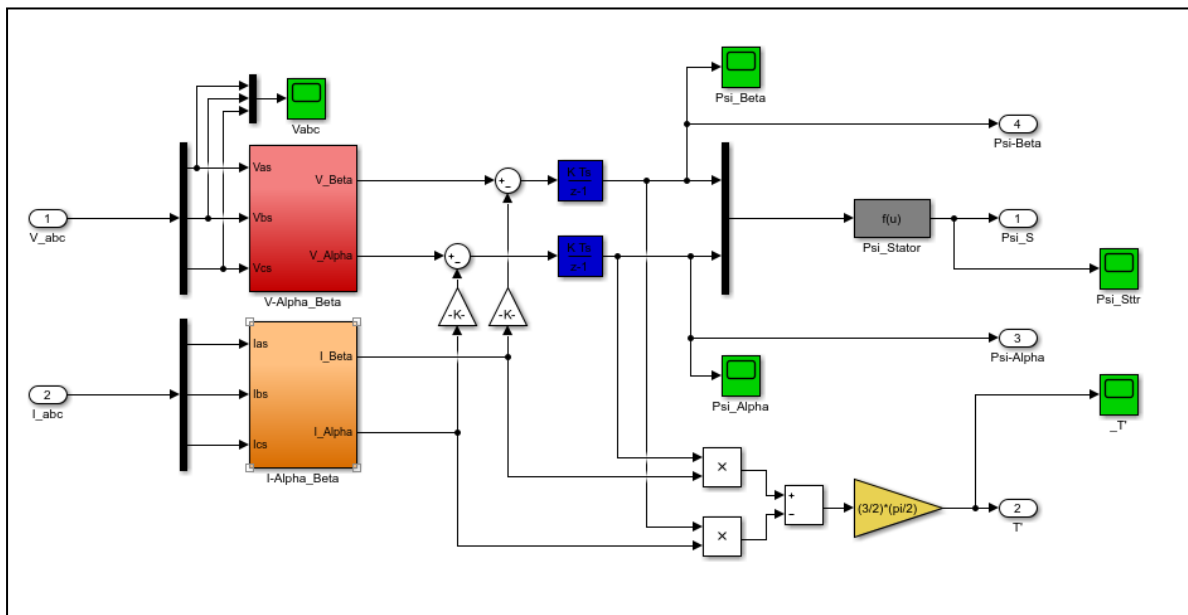
Fig III-19: MATLAB/SIMULINK® model of flux and torque estimation.

The simulation was performed under the following conditions:

➢ The asynchronous motor
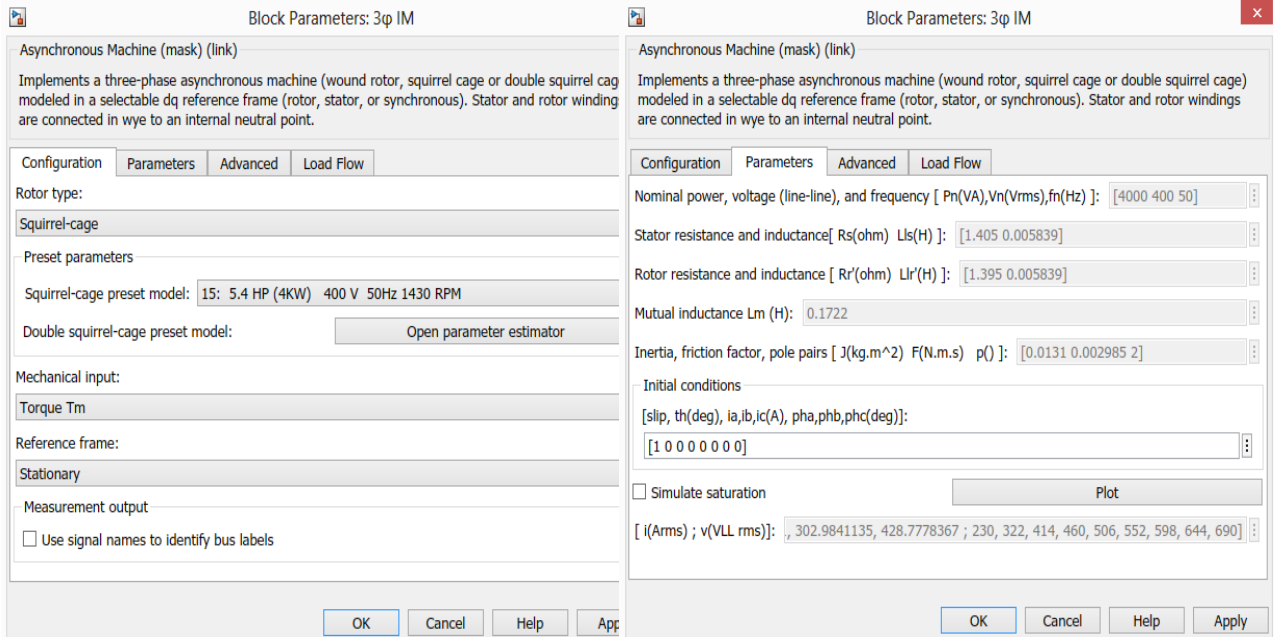
Fig III-20: MATLAB/SIMULINK® motor's block parameters.
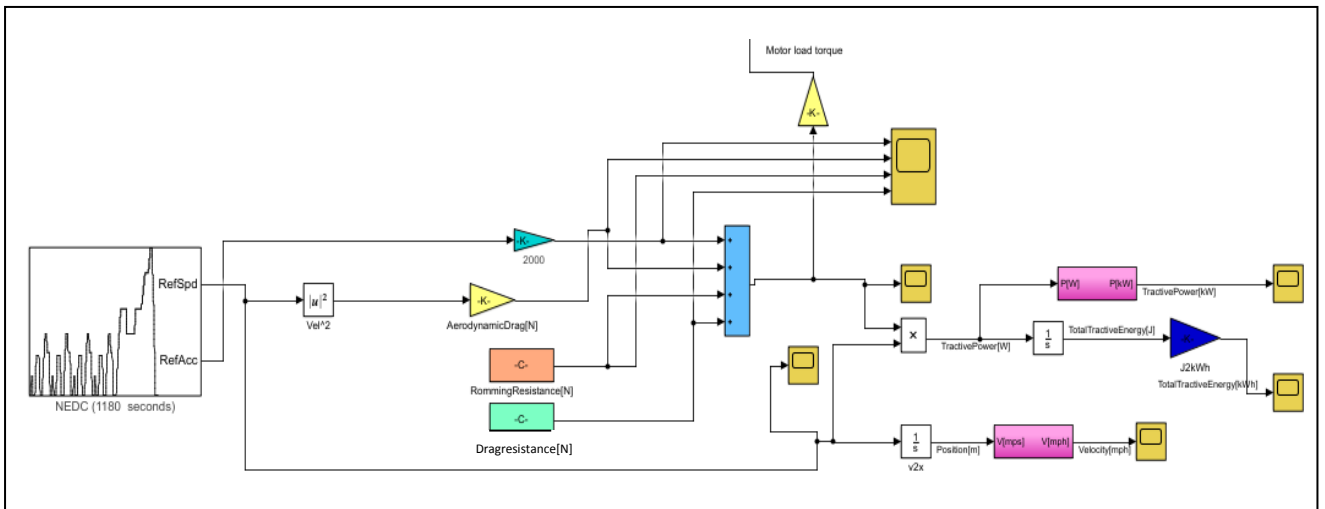
Fig III-21: MATLAB/SIMULINK® model of vehicle dynamic.

It is necessary to reset the negative forces. For this reason, by adding the "Compare to Zero" block, no resistance forces are generated when the vehicle is stationary [27].The same case for the motor's load.

III.4 Conclusion

This chapter included a very detailed overview of different approaches that can control the proposed system (battery, fuel cell and asynchronous motor). At first we presented "with storage" architecture, in which the DC bus voltage is regulated using battery associated with chopper controlled by PI regulator.

The AC part of proposed system was controlled using direct torque control for the improvement of the autonomy and the driving efficiency of the vehicle, thus has the advantages of not requiring a mechanical sensor and it gives a promising solution to the problems of robustness, so this chapter included a very detailed overview of the direct torque control and how to choose the two regulators of flux and torque and the setting of the switching table.

A simulation it's done using MATLAB/SIMULINK °2019 in order to see the system's responses which will present in the next chapter.

Chapter IV

Simulation results and interpretations

Chapter IV

Simulation results and interpretation

IV.1 Introduction

In this chapter, we will present the different results of simulation ,at first we will show power source's characteristics (fuel cell and battery) then results of DC and AC part through different robustness tests and also the simulation results for a given speed reference and finally we will present the system's answer after linking mechanic and electric part.

IV.2 Characteristics of energy sources

➢ Fuel cell

We suppose there is no change in temperature (T=368 k).

- Fuel supply pressure is : 3 bar.

- Air supply pressure is : 3 bar.

- Nerst voltage of one cell : 1.1729 v
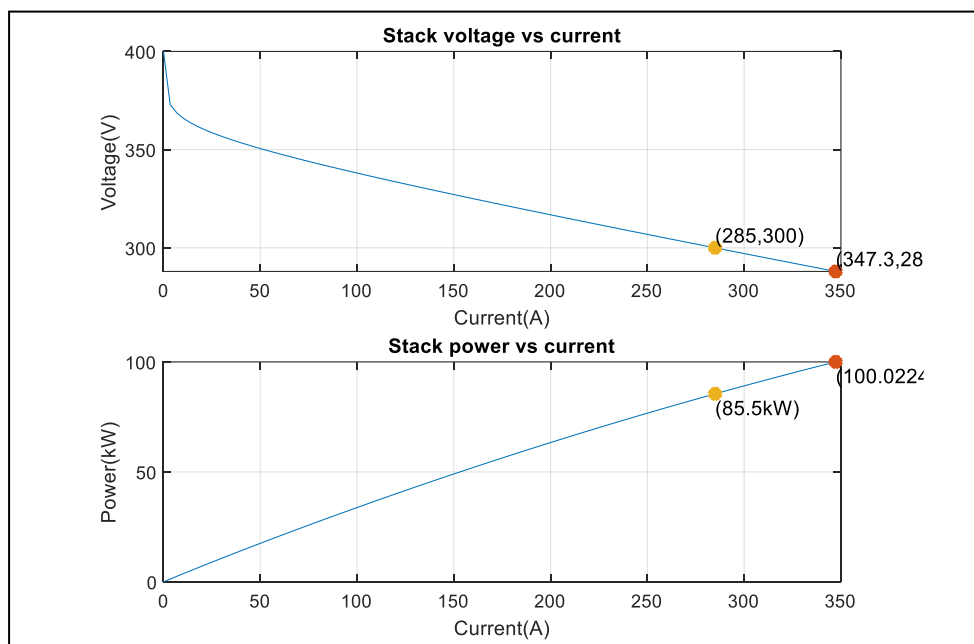
Fig IV-1: P-I and V-I curves of fuel cell stack.

From the curves we can determine :

- Nominal stack current :285.3 A

- Short-circuit current 347.3 A

- Nominal stack voltage : 300 v

- Nominal stack power : 85,5 kw

- Maximal stack power : 100.0224 KW

The reason for using a fuel cell with high power is to make this work a start for another study cases like vehicles with 2 or 4 traction motors , be sure that the power requested by the load is ensured in the case of temperature and pressure are variable.

> ➢ The battery

The discharge curve is interesting because it will make it possible to determine the Max / Min voltage range delivered by the battery.
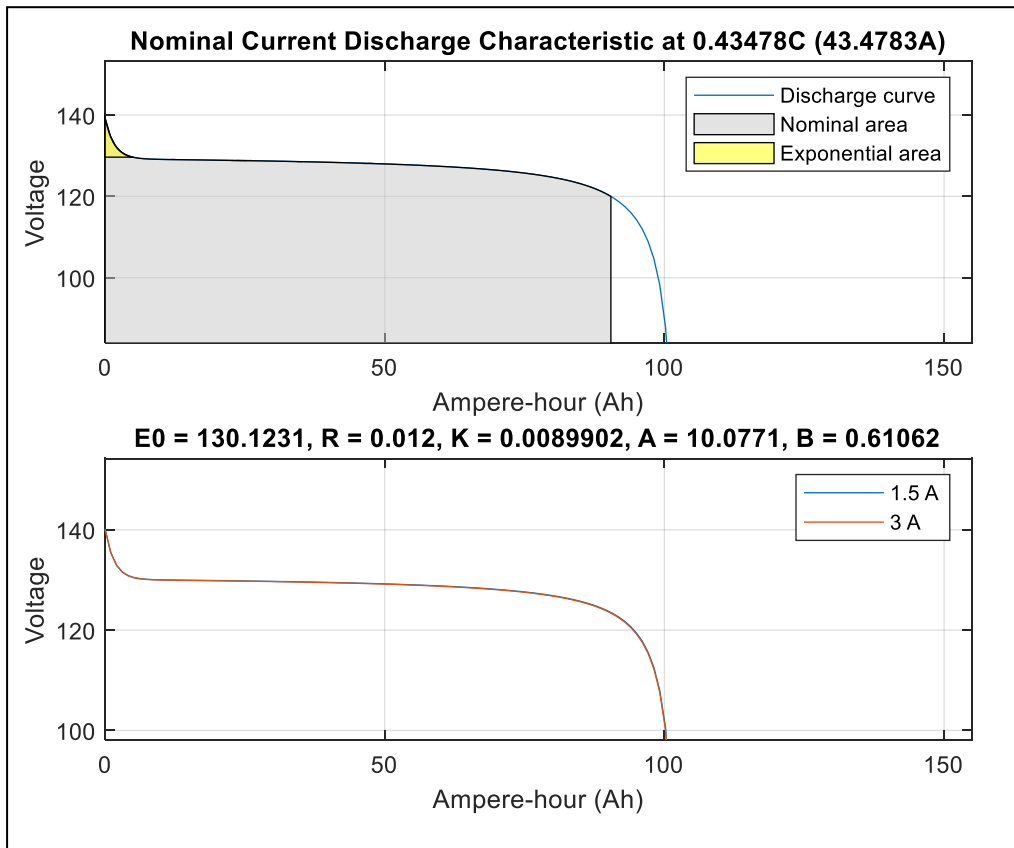
Fig IV-2: Discharge depending on capacity curve.

Fig IV-2 presents the relationship between battery capacity and discharge current at specific C-rated. The curve display the overall and the exponential area of Lithium-ion battery's discharge curve at 0.43C .As shown in Fig IV-2 the nominal discharge current is 43.478% of the rated battery capacity which is 43.47 A. It means that the 99.98 Ah Lithium-ion battery provides 43.47 A for 2.3 hours if discharged at the mentioned C rate.

Based on the exponential area, the battery voltage decreases from 139.3 V to 129.6 V. Meanwhile, the nominal area has revealed that the total capacity that can be extracted from the Lithium-ion battery is 90.43 Ah before the discharge process stops,when the tension drops off.

IV.3 Results of DC part

In order to see the robustness of the DC part we will make some tests

IV.3.1 No-load start followed by load disturbances

Fig IV-3 below present the simulation results over 2s the it illustrates the responses of the DC bus for a no-load start at 0.05 s followed by the application of a nominal load of 12 (N.m) at time '0.6s'
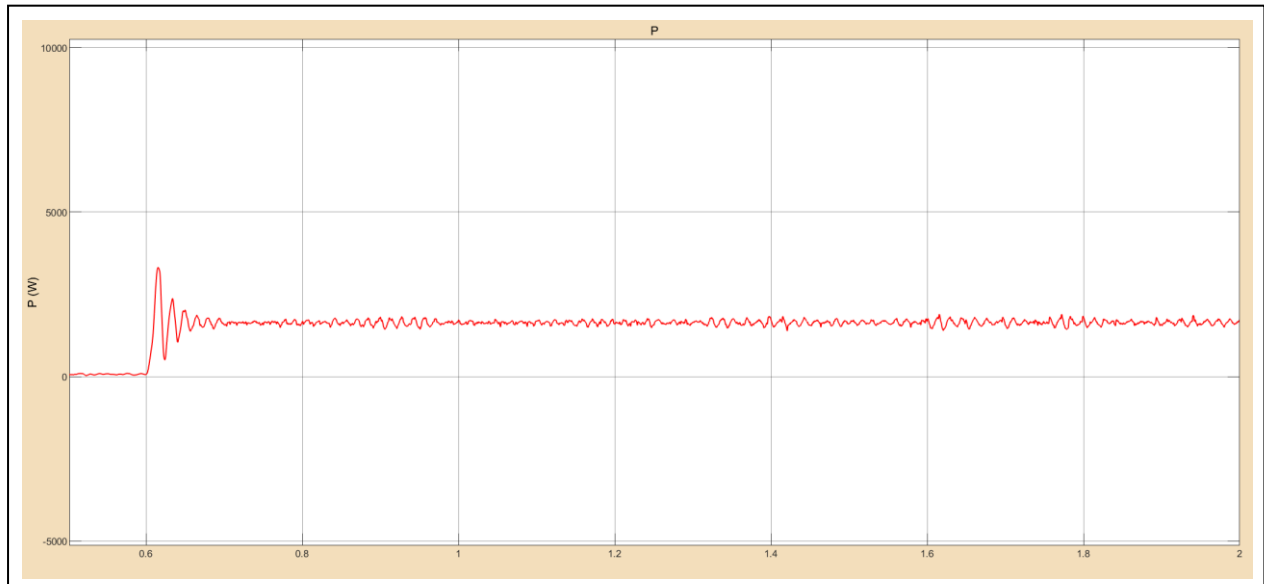
Fig IV-3: Fuel cell power with applying load at 0.6s

Fig IV-3 shows that there is a power peak when the load is connected equal to 3000 w
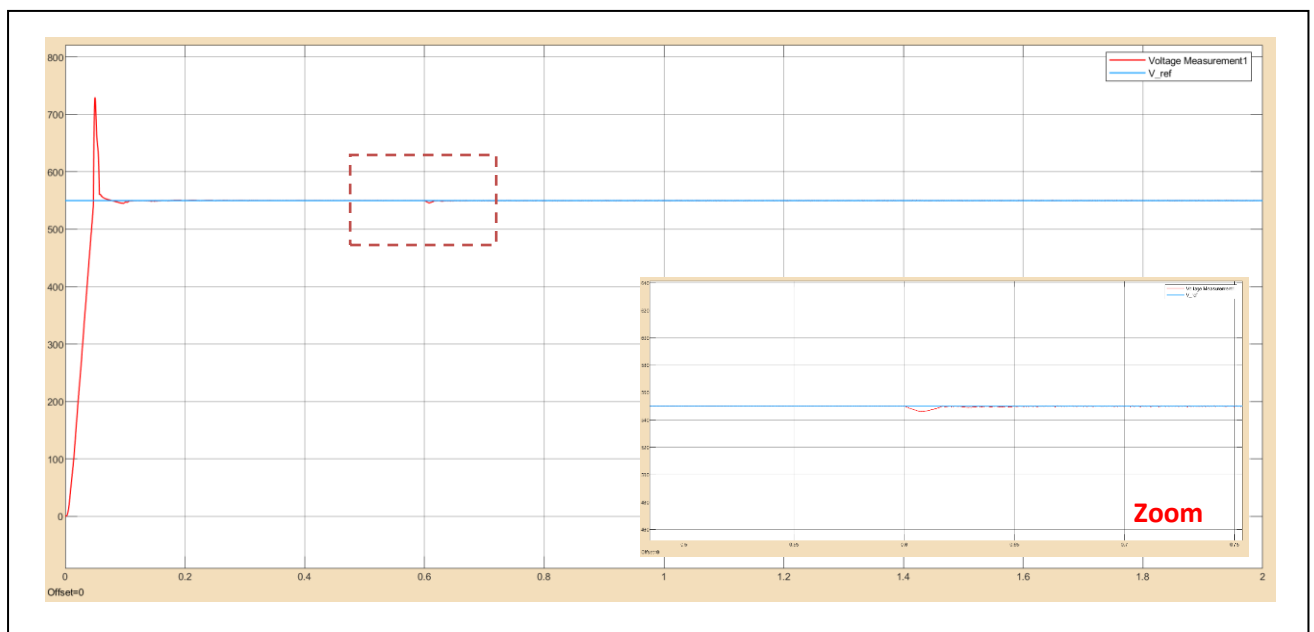
Fig IV-4: DC bus and reference voltage with applying load at 0.6s.

Fig IV-4 shows that there is an exceedance at 0.05 (s) equal to 175 v this value is not small but In order to accelerate system stability it has been worked on also we can see that the voltage increase in a linear way in another hand there is a 4 v drop in voltage when the load is connected.

IV.3.2 Load-start

The figures below show the simulation results over 2s for a resistant torque of 12N.m
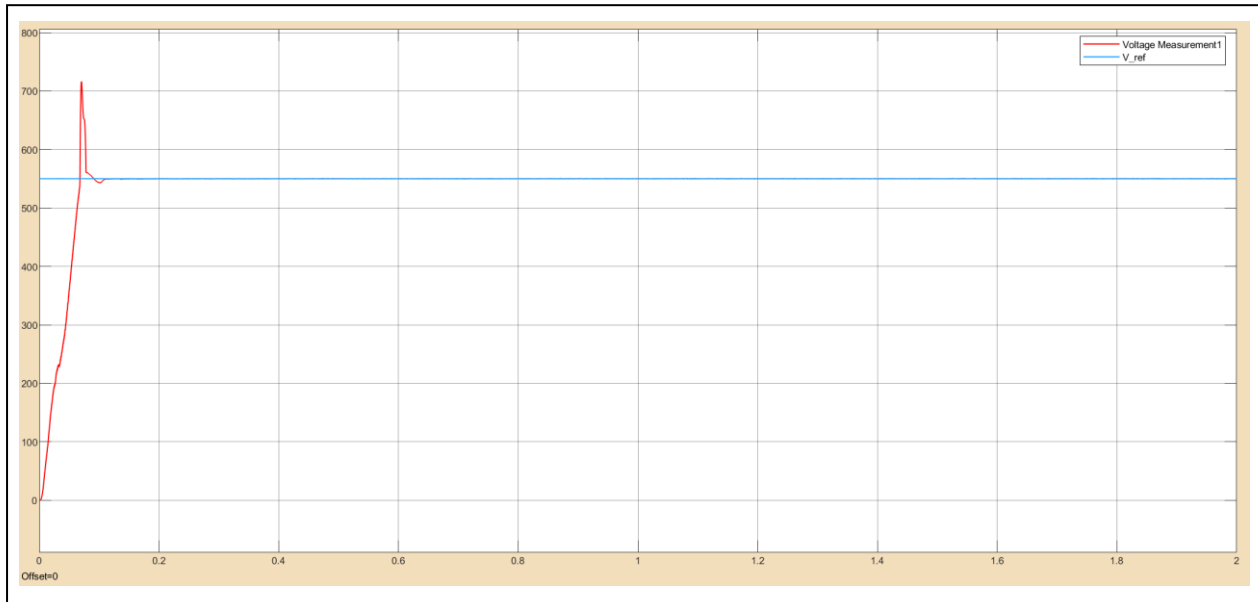
Fig IV-5: DC bus and reference voltage curves with load-start

The voltage increase in a linear way because it includes some perturbation, also there is an exceedance but Less than the previous case.

IV.3.3 Reversing the direction of rotation

➢ **Battery switch Δu =11**
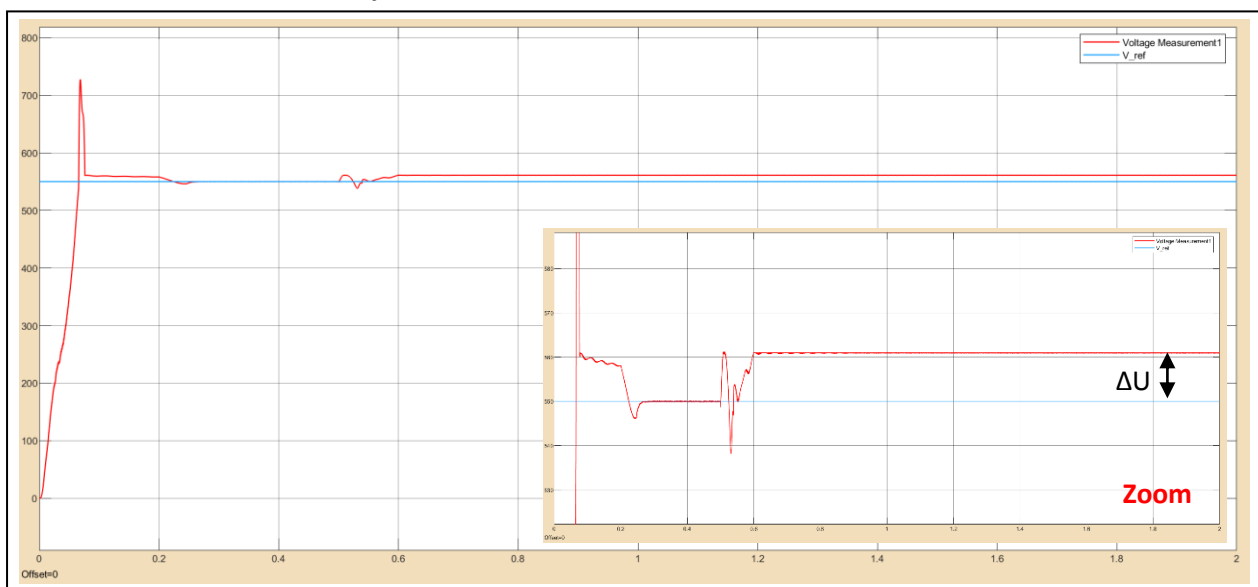
Fig IV-6: DC bus and reference voltage curves " Reversing the direction/ Δu =11"

➢ **Battery switch ∆U =0.5**
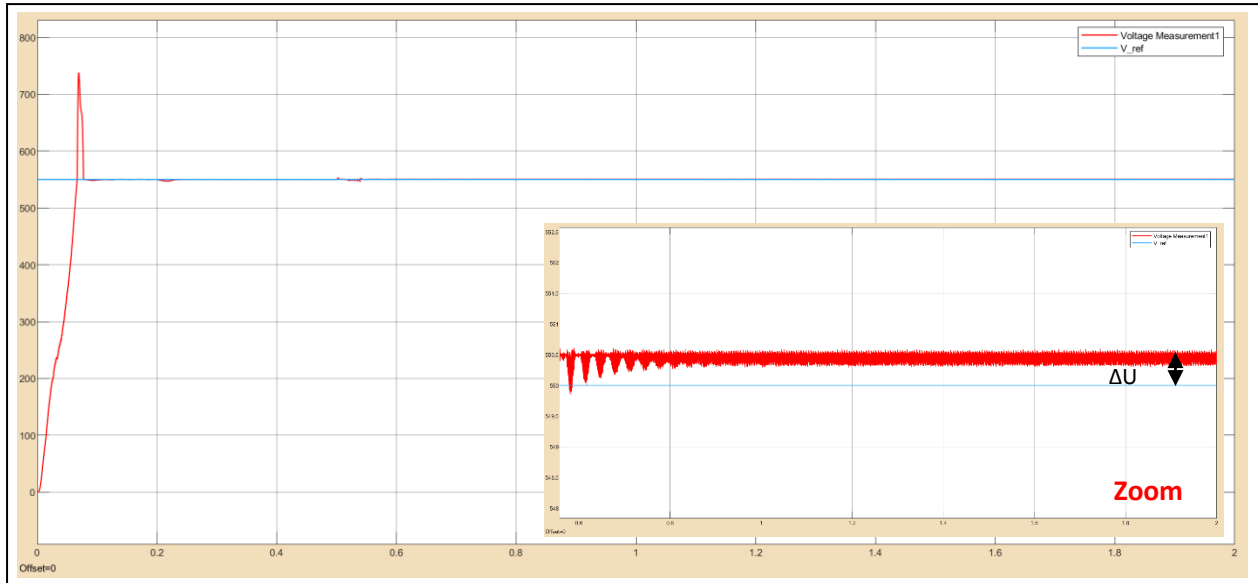
Fig IV-7: DC bus and reference voltage curves" Reversing the direction/ ∆u =0.5"

The figures Fig IV-6 and Fig IV-7 show the simulation results of DC bus response over 2s with reversing of speed direction at 0.5 s with load torque.

➢ **Battery switch ∆U =0.1**

The figures Fig V-8 shows the simulation results of Dc bus response over 2s with reversing of speed direction at 1 s with applying a resistant torque during all the test.
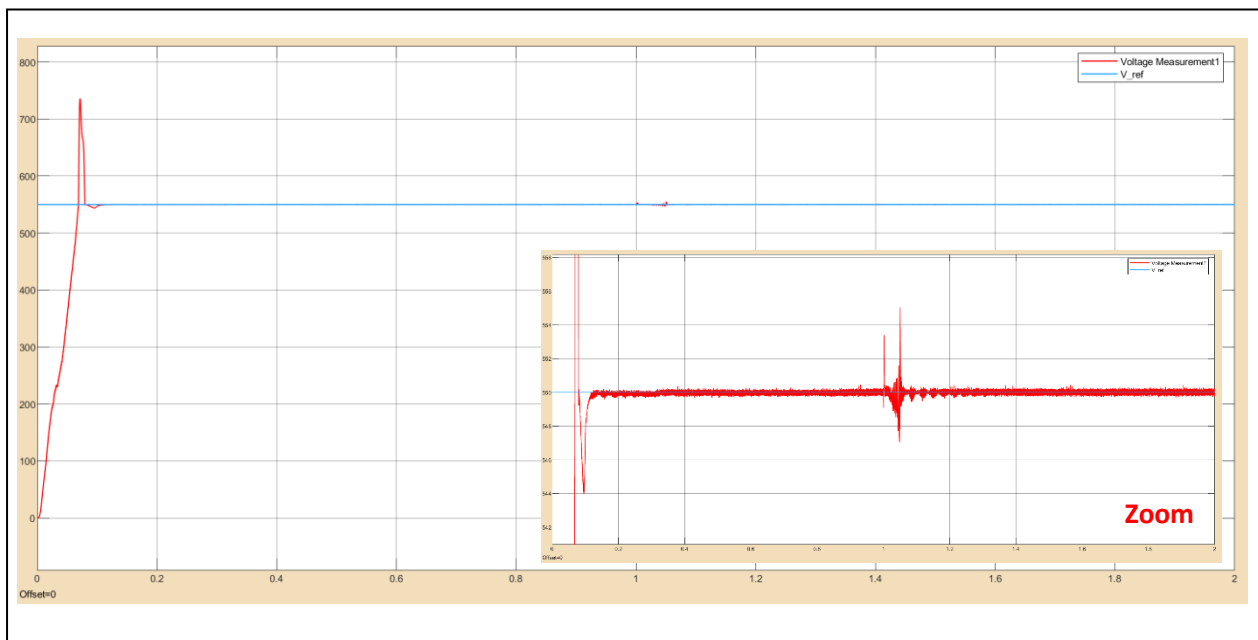
Fig IV-8: DC bus and reference voltage with T_r and reversing the direction

From Fig IV-6 , Fig IV-7 and Fig V-8 we can see that there is perturbation when changing the direction , and the error between voltage reference and measured voltage really depends in battery's switching value.
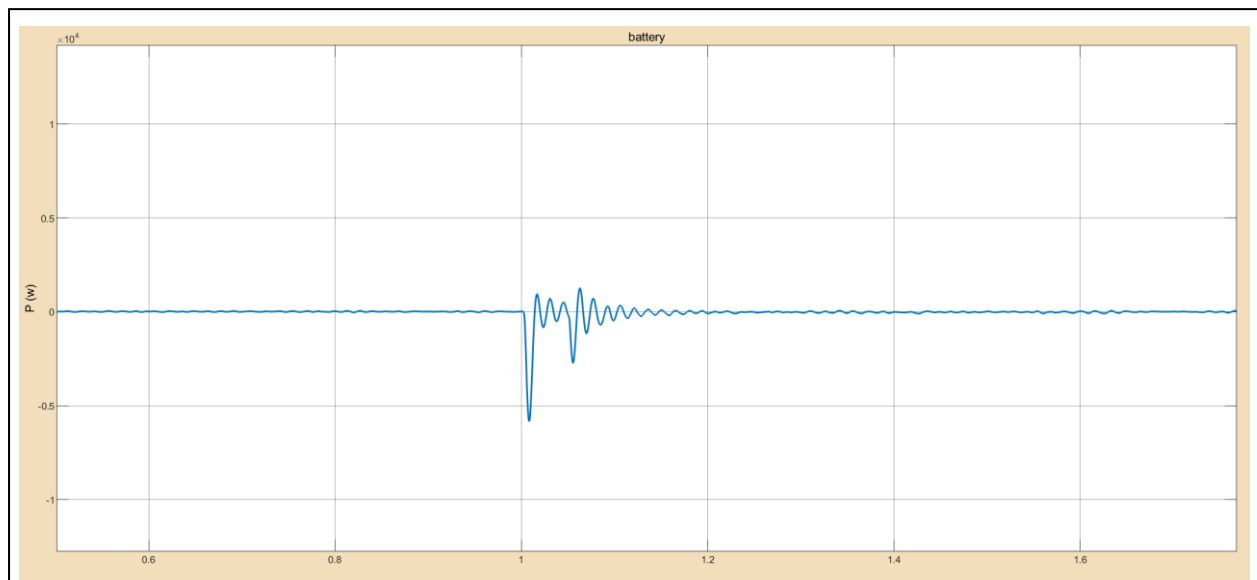
Fig IV-9: Battery response at speed's reversing time.
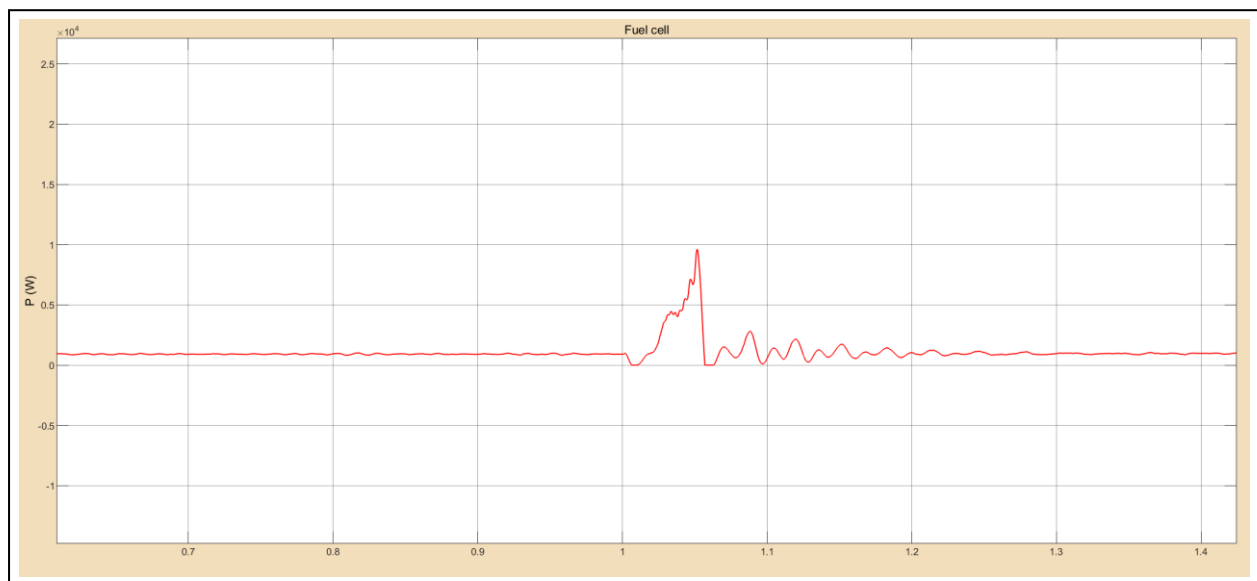
Fig IV-10: Fuel cell response at speed's reversing time.

Fig IV-9 shows that the battery working as receiver (power < 0) so it charges when the speed decreases in order to change direction until it reaches the zero rad/s. Then when starting again in the opposite direction the battery turned off.

Fig IV-10 shows that fuel cell reached the zero when the battery worked (braking case) then there is a start's peak.

Fig IV-11 shows the result of DC bus voltage without load and with with reversing of speed direction at 0.5 (s).
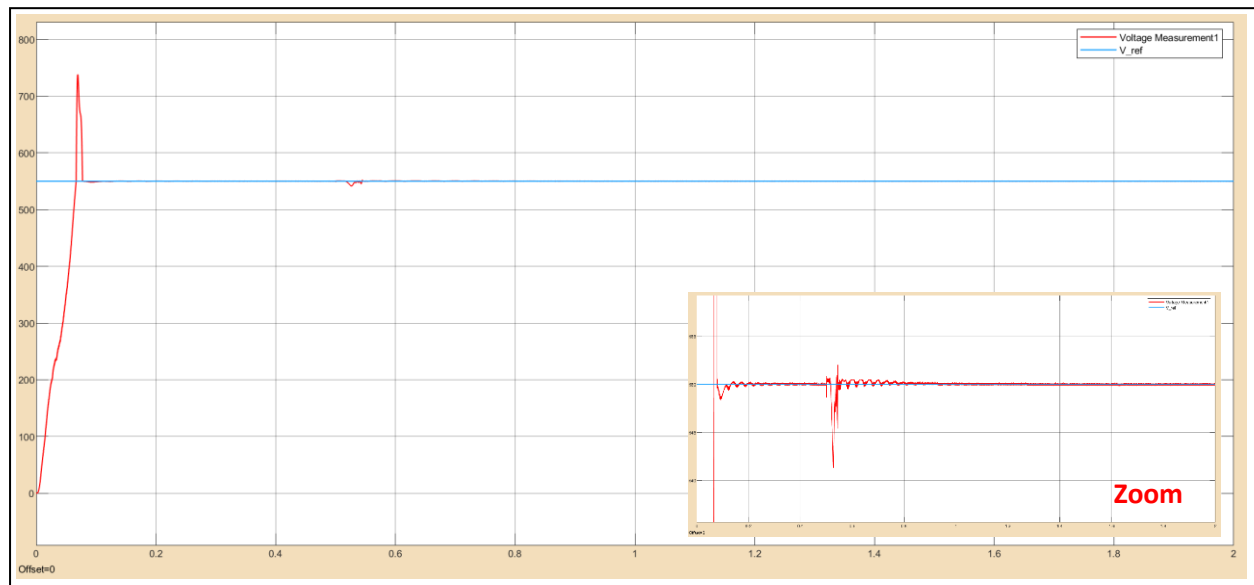
Fig IV-11: DC bus and reference voltage without load and with reversing of direction.

IV.3.4 Low speed test

Fig IV-12 shows the simulation results over 1s for a resistant torque of 12N.m and speed reference 12 rad/s
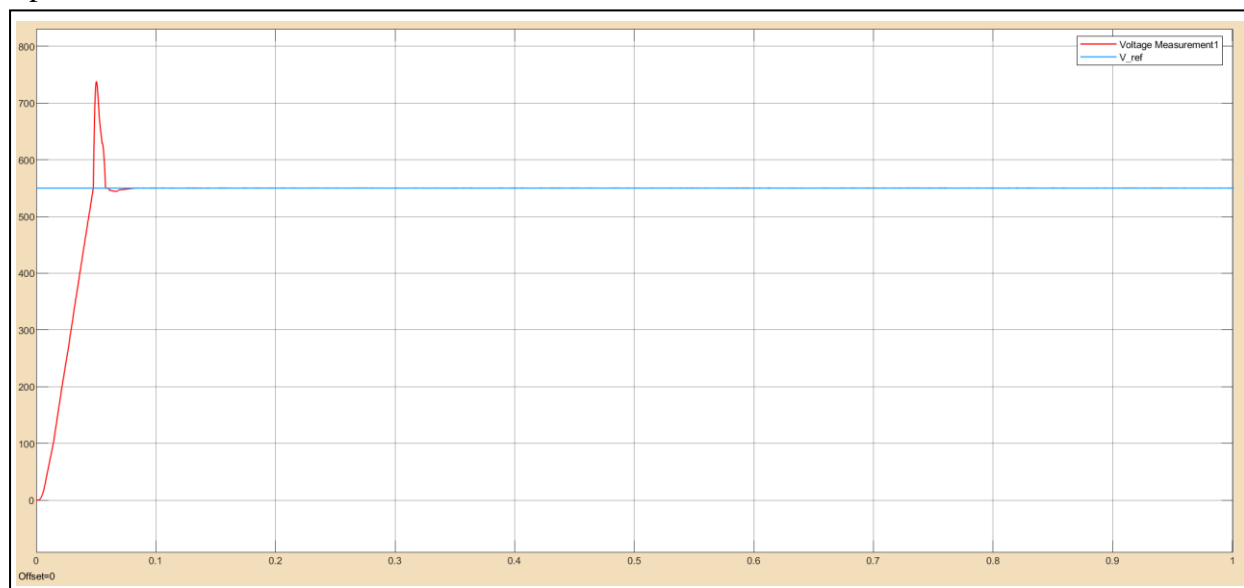
Fig IV-12: DC bus voltage response and reference voltage curves" Low speed"

IV.4 Results of AC part

IV.4.1 No-load start followed by load disturbances

The figures below present the simulation results over 2s for No-load start followed by load disturbances 12N.m at 0.6 s and a reference flow at 1.1 Wb. The width of the hysteresis

band of the torque comparator is in this case fixed at ± 0.2N.m and that of the flux comparator at ± 0.02 Wb with a reference speed of 120 rad /s.
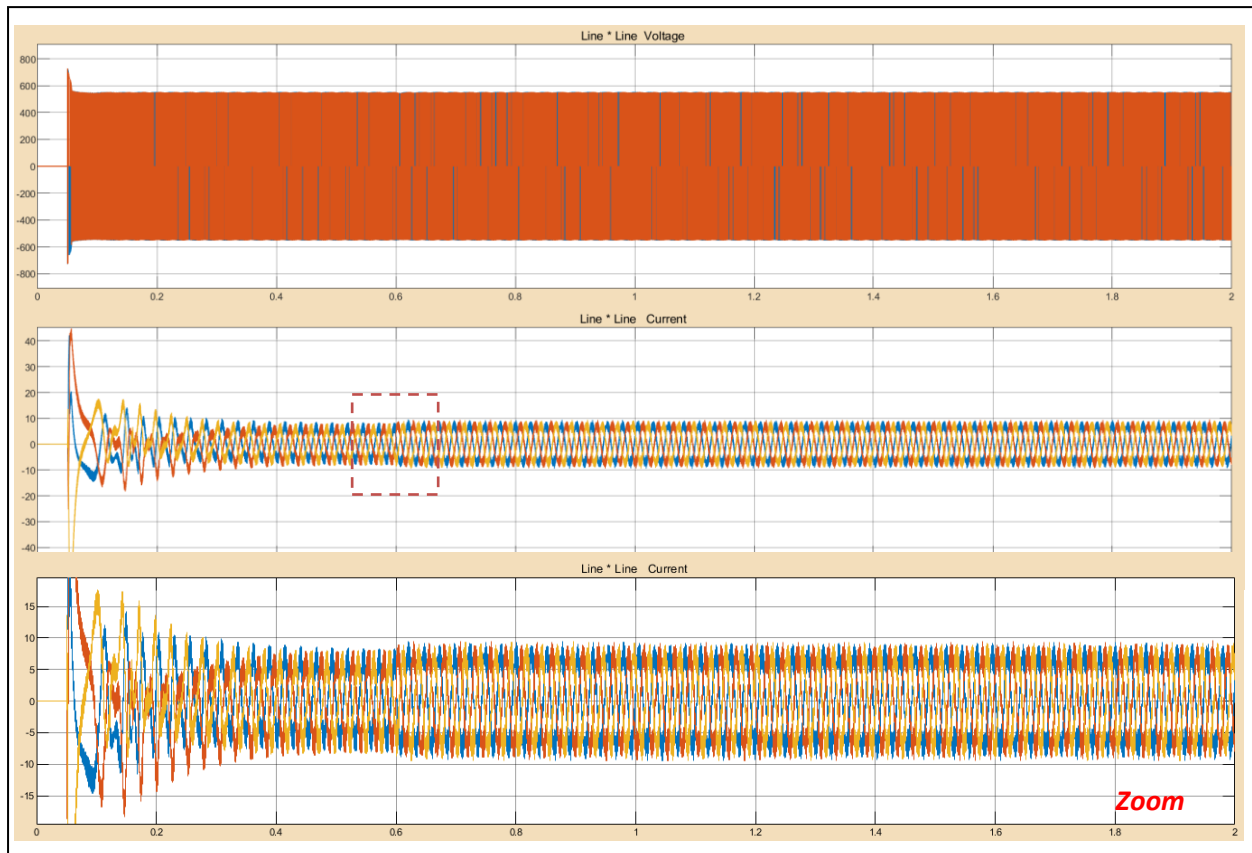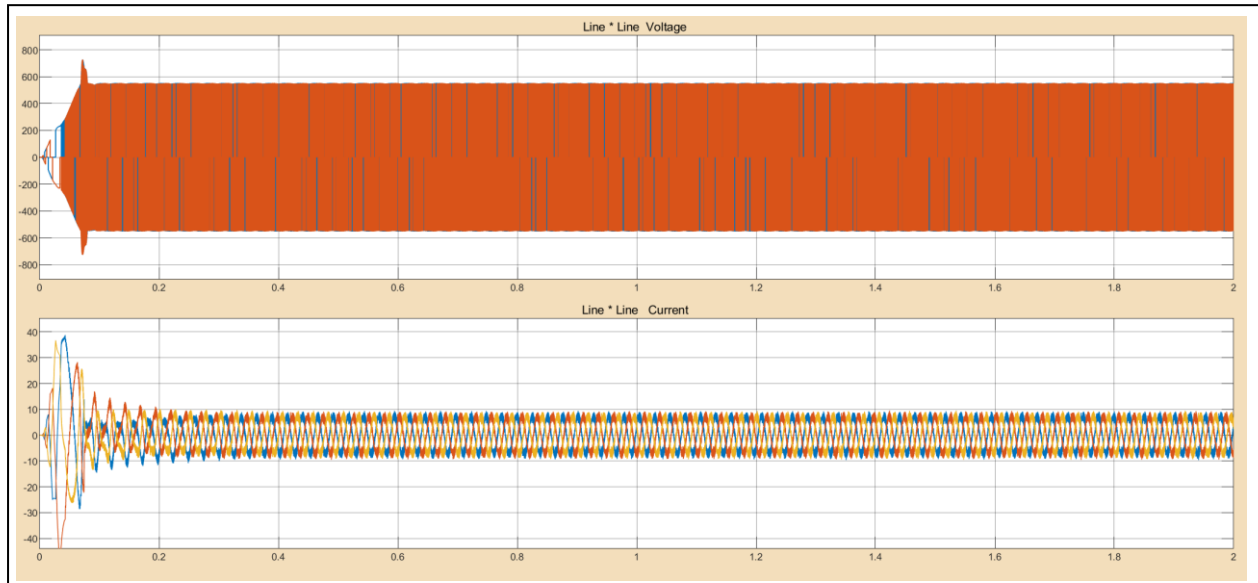

Fig IV-13: Line to line voltage and current curves "No-load start"

Fig IV-13 shows that during the load connection there is a current's call up to 8 A
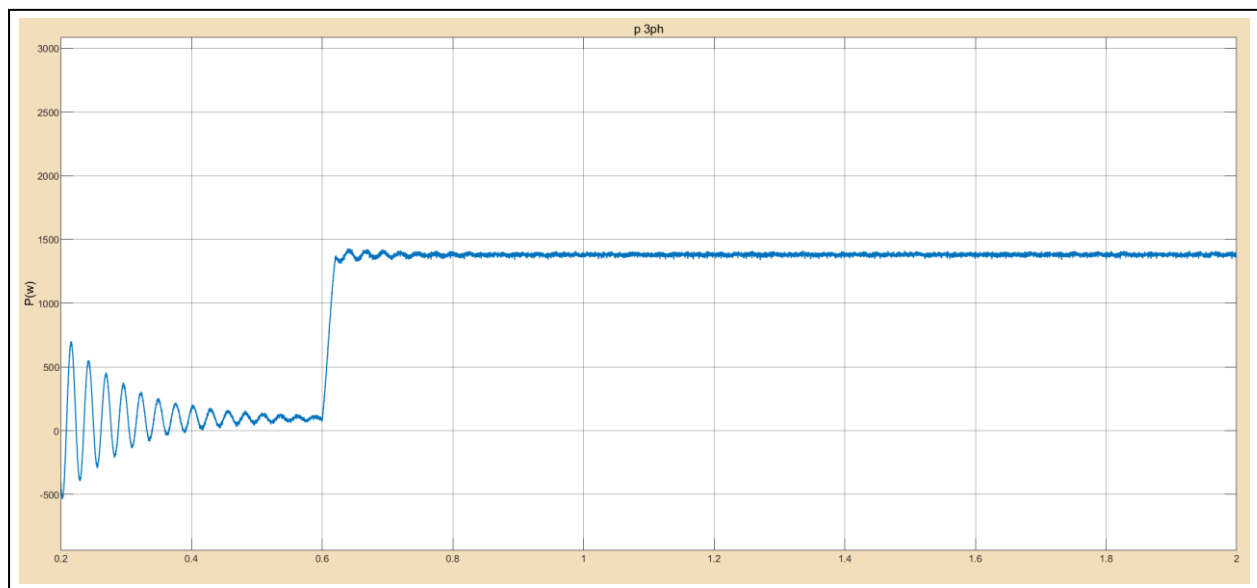
Fig IV-14: AC active power curve"No-load start"
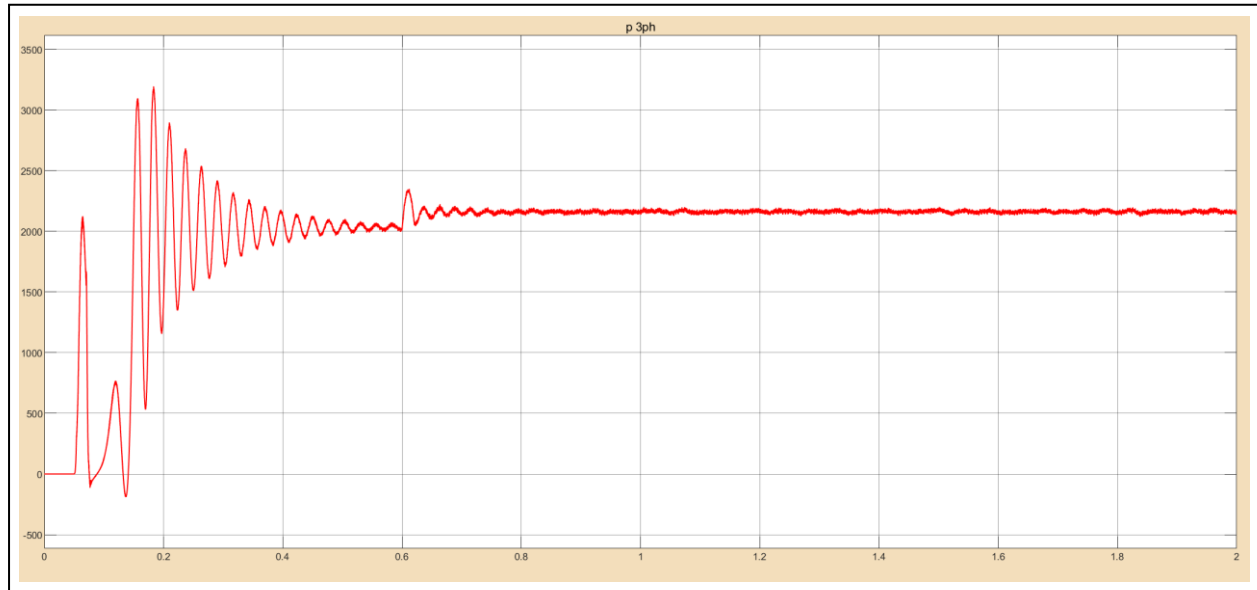
Fig IV-15: AC reactive power curve"No-load start".

From Fig IV-14 and Fig IV-15 we can notice that before adding the load (before 0.6 s) the ASM the active power has very low value in another side he consumes reactive one , this confirms that a motor looks like a transformer in no-load case.

Power reactive part changes little (200 VAr) according to the load, but the active part varies a lot.
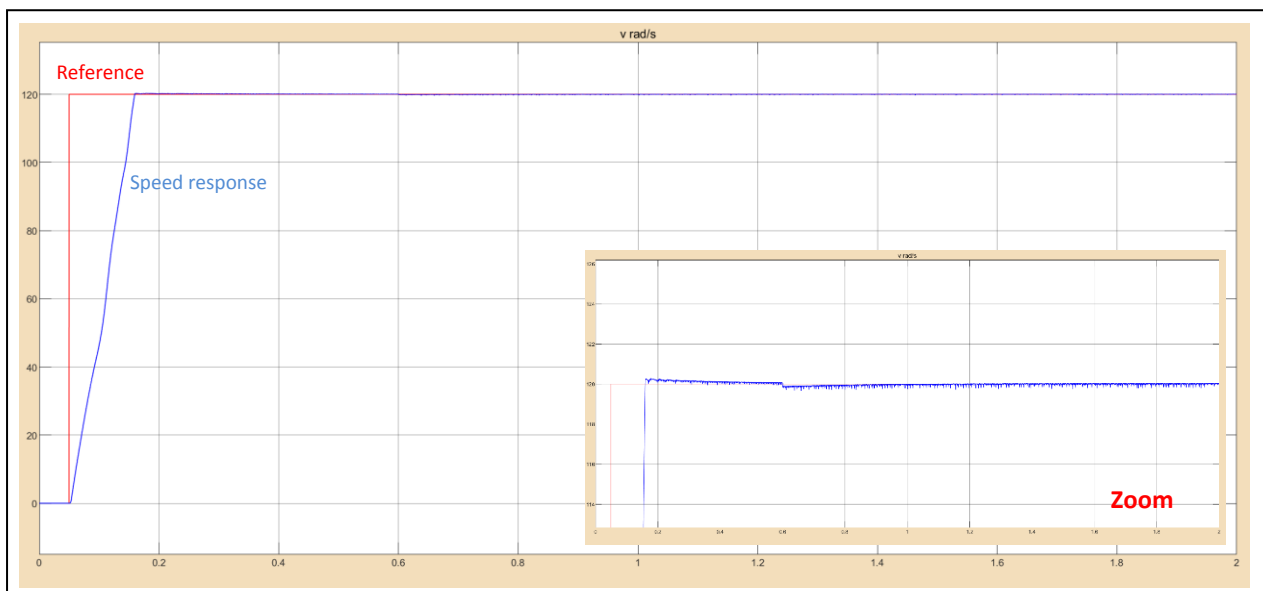
Fig IV-16: motor's speed response with reference speed curve"No-load start".

From Fig IV-16 the speed increases linearly with time up to a point of stability then it decreases by adding load after that it remains stable at the desired value.
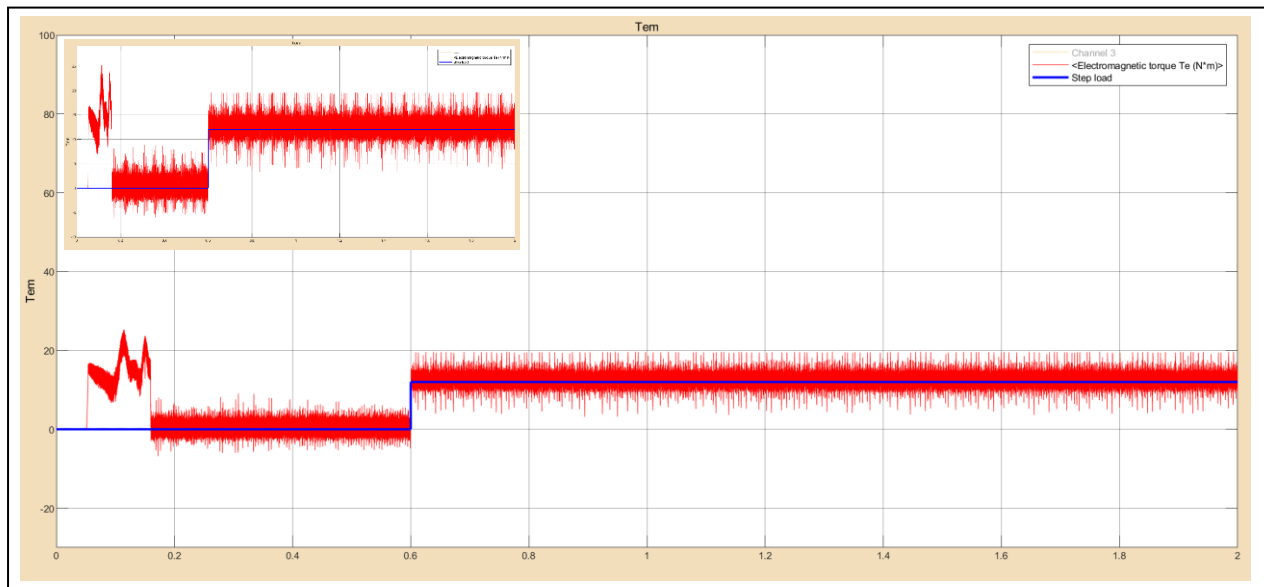
Fig IV-17: Motor's Electromagnetic torque with load torque "No-load start".

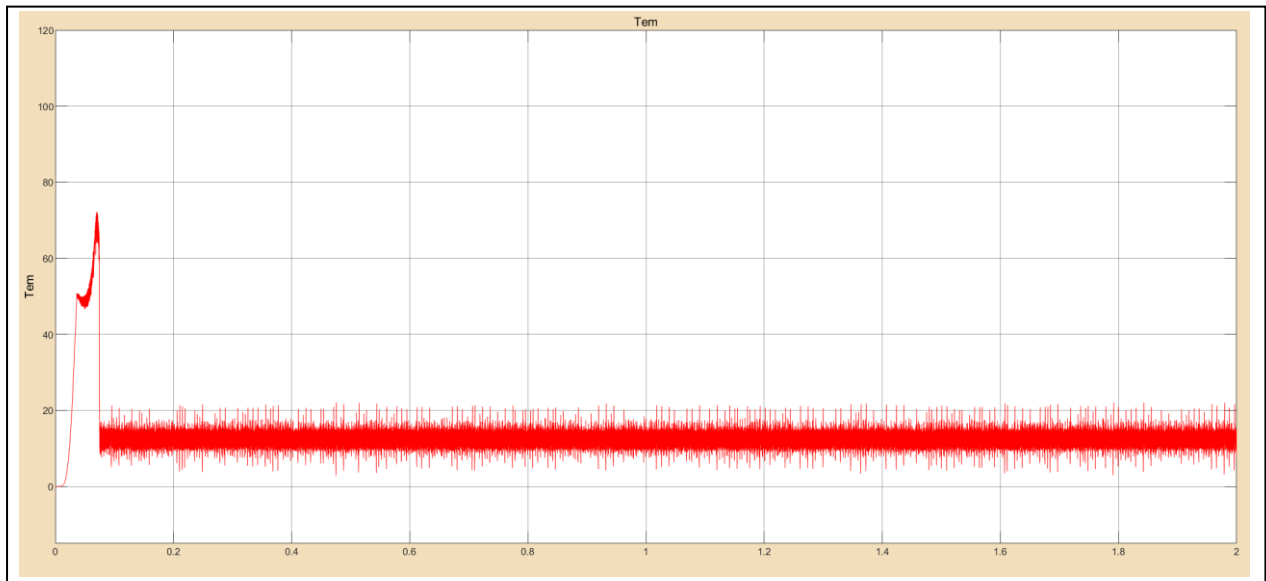On start-up, the electromagnetic torque reaches its maximum value of 22N.m and stabilizes at a practically zero value in steady-state mode after a starting time of 0.17s then stabilizes for a final value of 12N.m with a significant oscillation for load torque 12N.m. The flux path draws a circle as shown in Fig IV-18
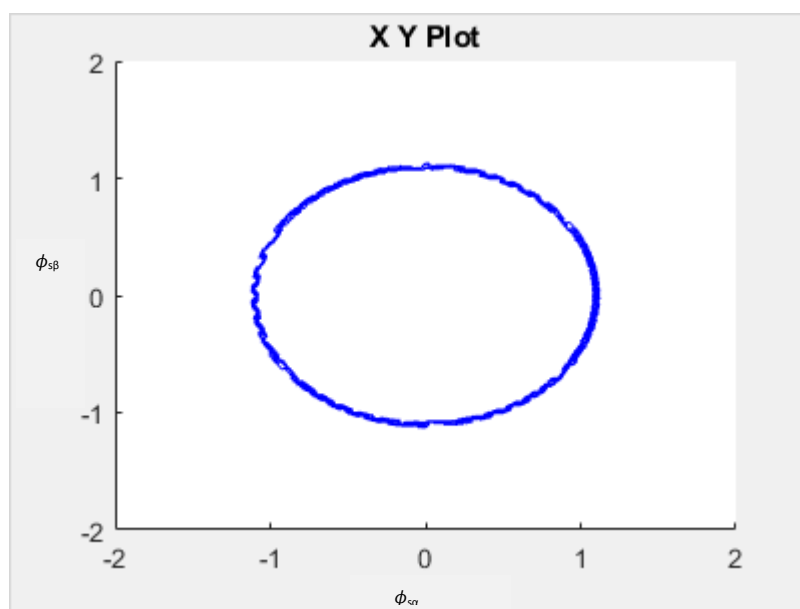
Fig IV-18: path of flux (αβ) "No-load start".

IV.4.2 Load-start

The figures below show the simulation results over 2s with the application of load torque at 0 (s) equal to 12N.m and a reference flux of 1.1Wb. The width of the hysteresis band of the torque comparator is in this case fixed at ± 0.2 N.m and that of the flux comparator at ± 0.02Wb.

Fig IV-19: Line to line voltage and current curves with load-start.

We can see that the starting currents have very high values this is what it corresponds to high value of active power as shown in Fig IV-20.
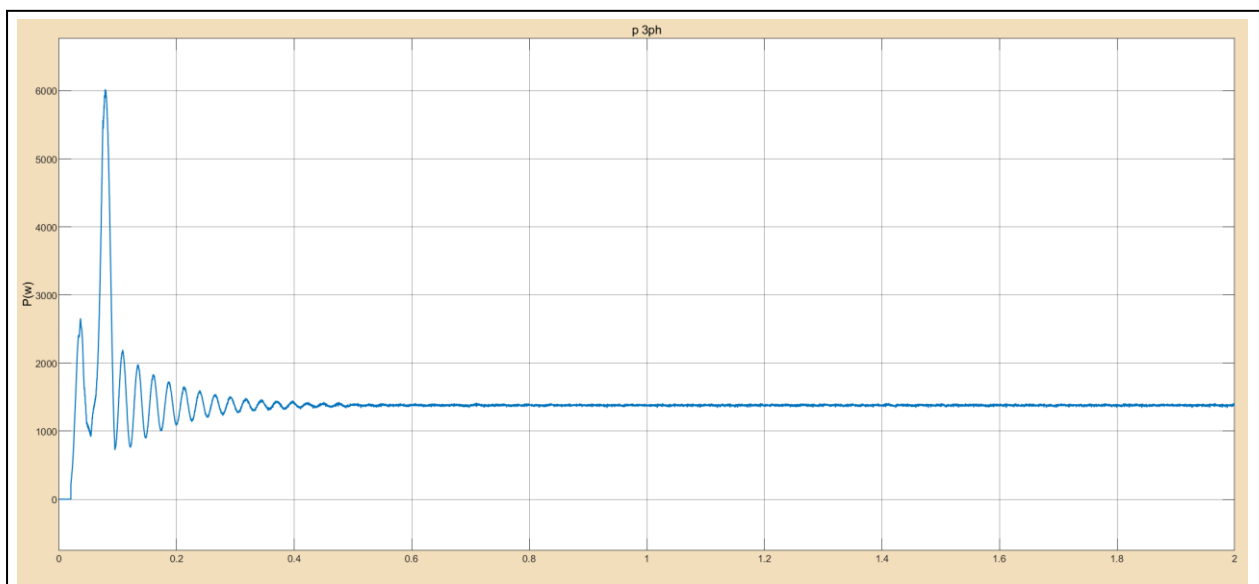
Fig IV-20: AC active power curve with load-start.
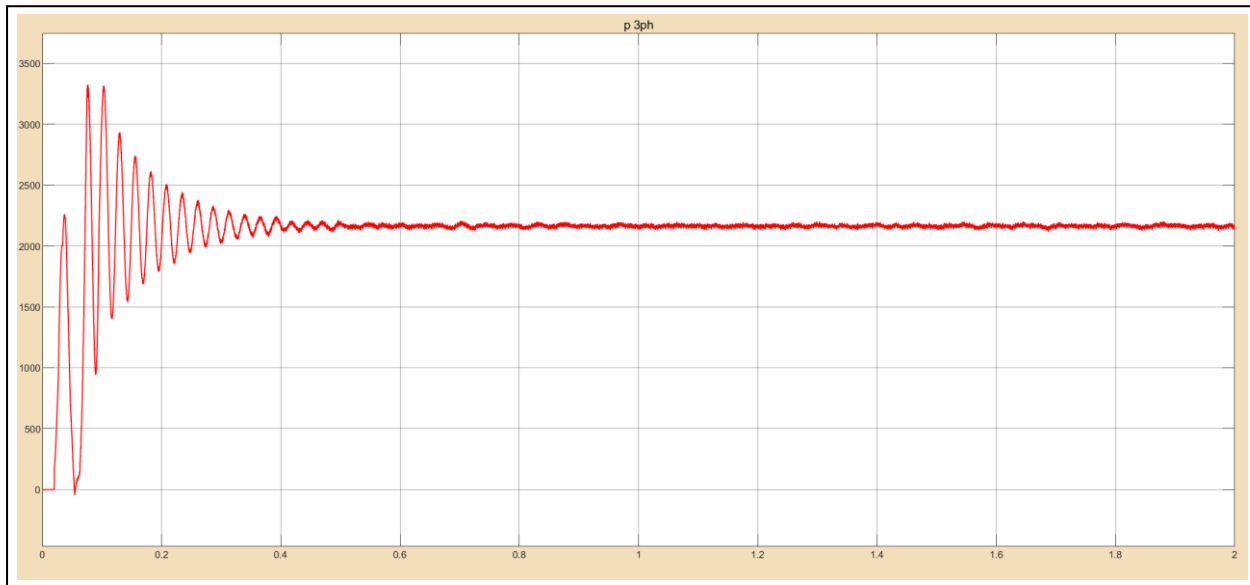
Fig IV-21: AC reactive power curve with load-start.
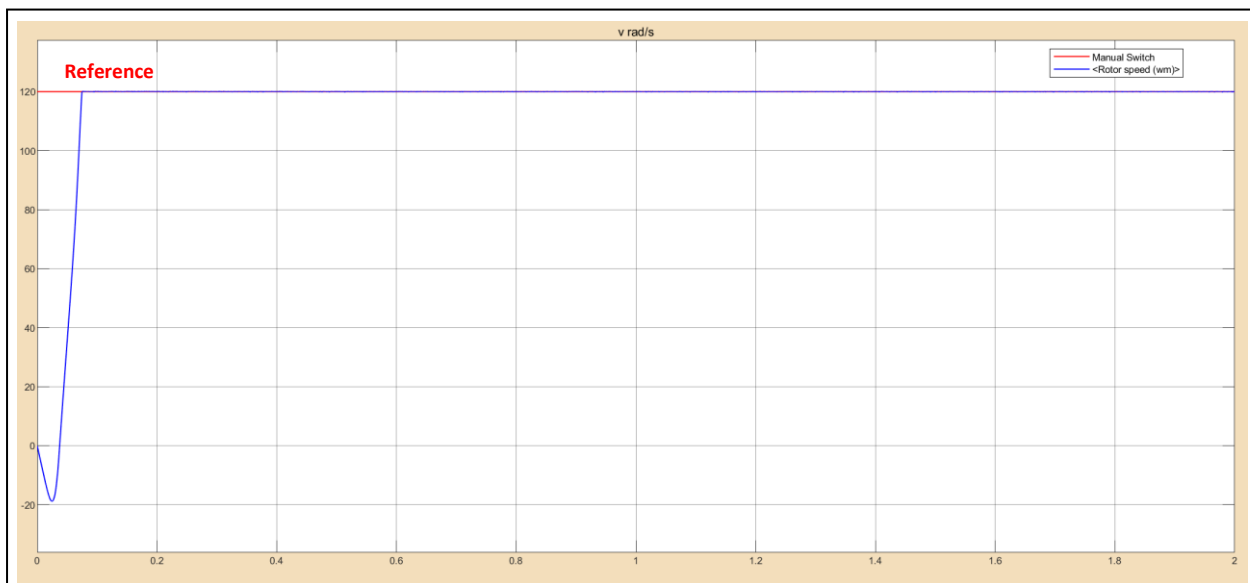
Fig IV-22: Speed and reference curves.

We can see that there is a negative peak at startup because of the load torque application at instant 0(s) and that confirms the torque equation mentioned in (II-54)

Fig IV-23: Motor's Electromagnetic torque with load torque "load-start".

On start-up, the electromagnetic torque reaches its maximum value of 70N.m and then stabilizes for a final value of 12N.m with a significant oscillation for load torque 12N.m
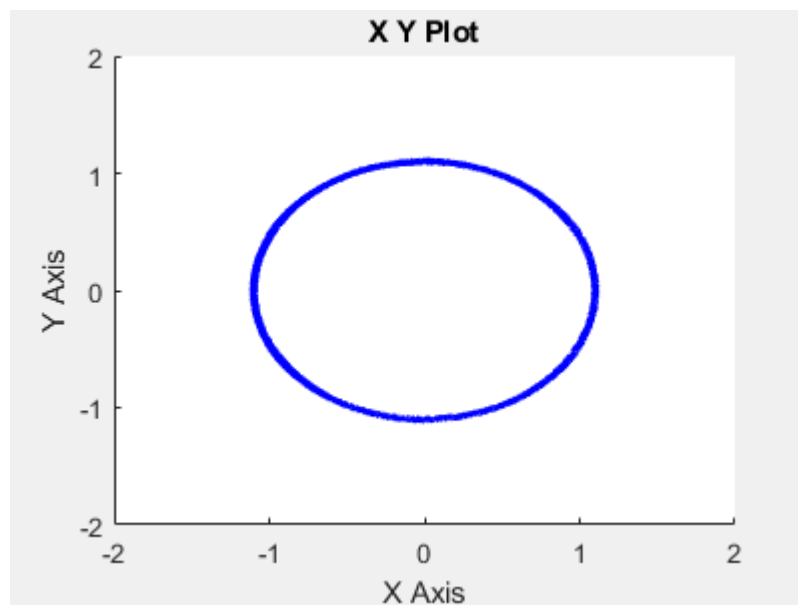
Fig IV-24: Path of flux (αβ) with load-start.

IV.4.3 Reversing the direction of rotation

Reversing the direction of rotation by reversing the speed reference from 100 rad/s to 100 rad/s at 0.5 s without load .
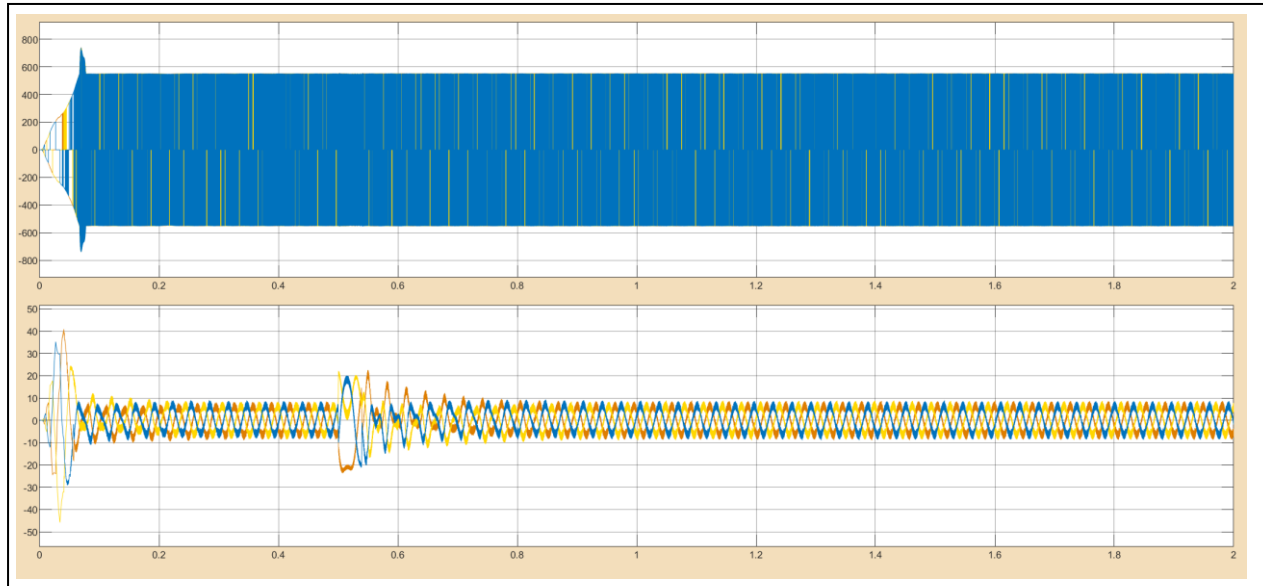

Fig IV-25: Line to line current and voltage curves "reversing direction without T_r".

The currents have sinusoidal shape with peak of 20 A due to the restart in the reverse direction at 0.5 (s).
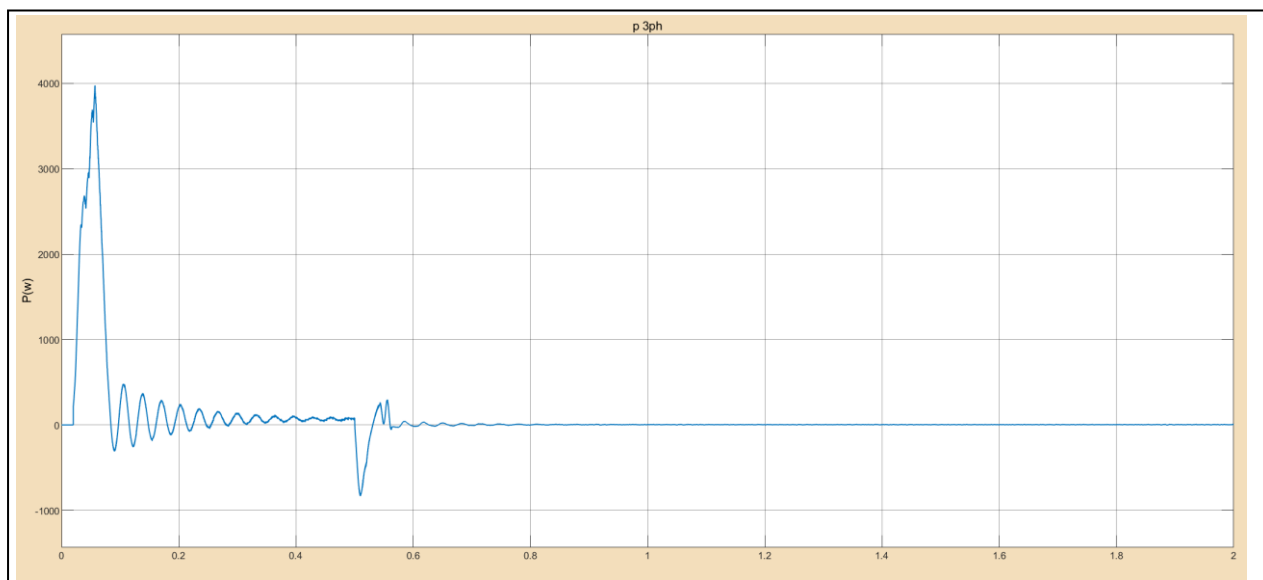

Fig IV-26: AC active power curve "reversing direction without T_r".

Active power are typically 0 w because of load absence but we can notice the negative part at 0.5 (s) which remains that the machine works in generator mode during braking period.
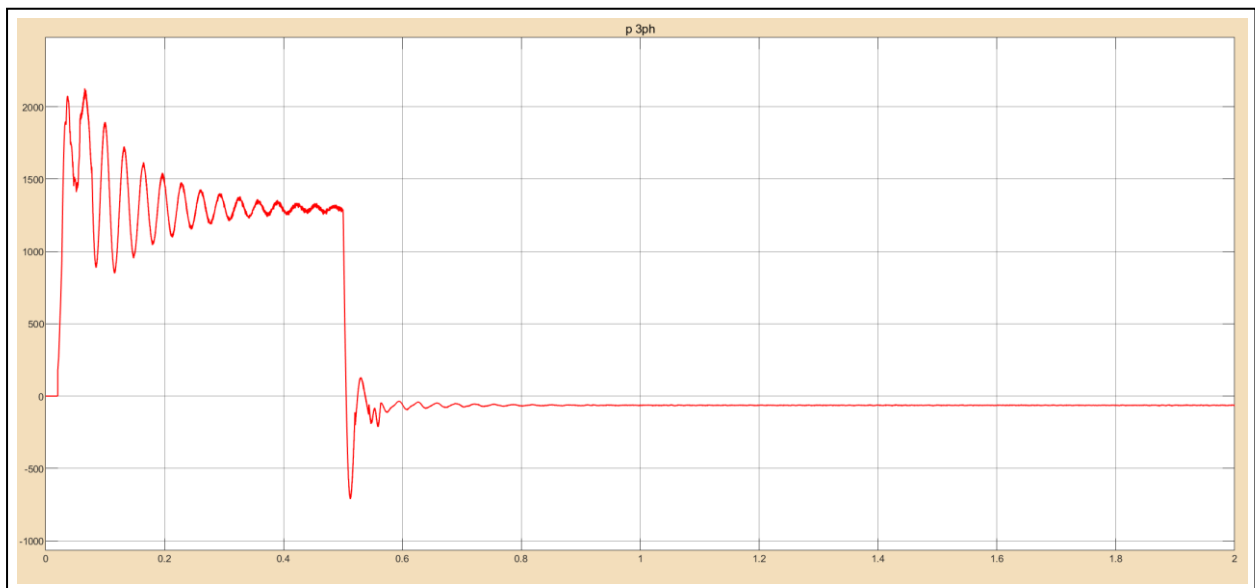

Fig IV-27: AC reactive power curve "reversing direction without T_r".

As we saw before reactive power doesn't has big change between load and no-load case , but after reversing direction it generate reactive power during braking period then it has small constant value.
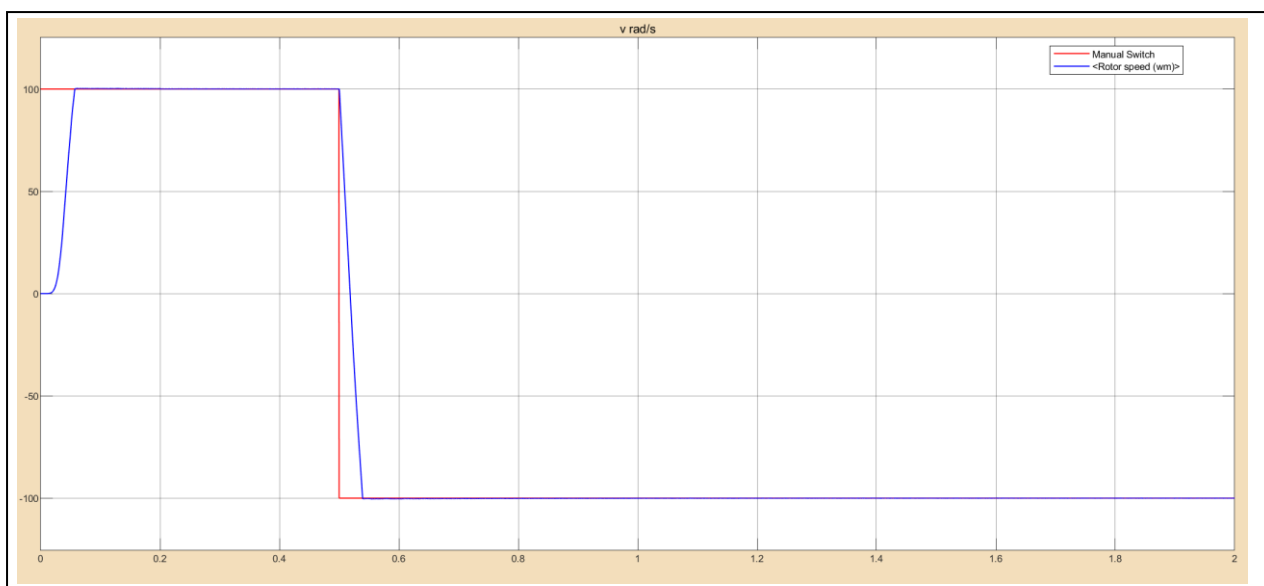

Fig IV-28: speed and reference curves "reversing direction without T_r".

We Note that the system responds positively to this test, the speed follows its new reference -100 rad/s after 0.53(s) without static error,
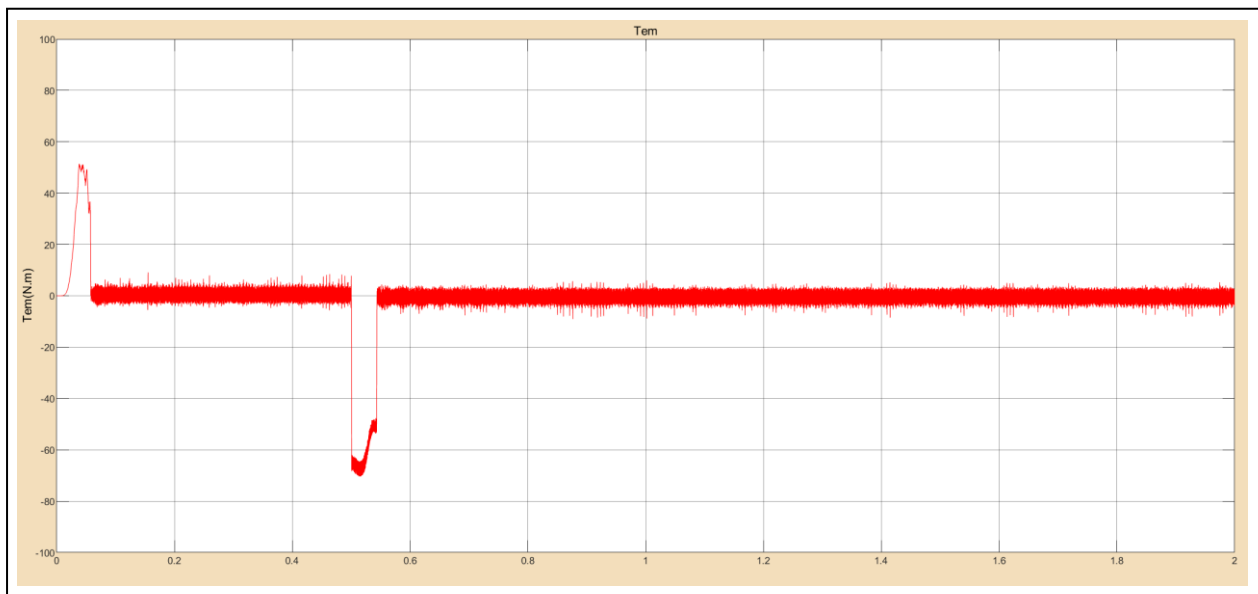

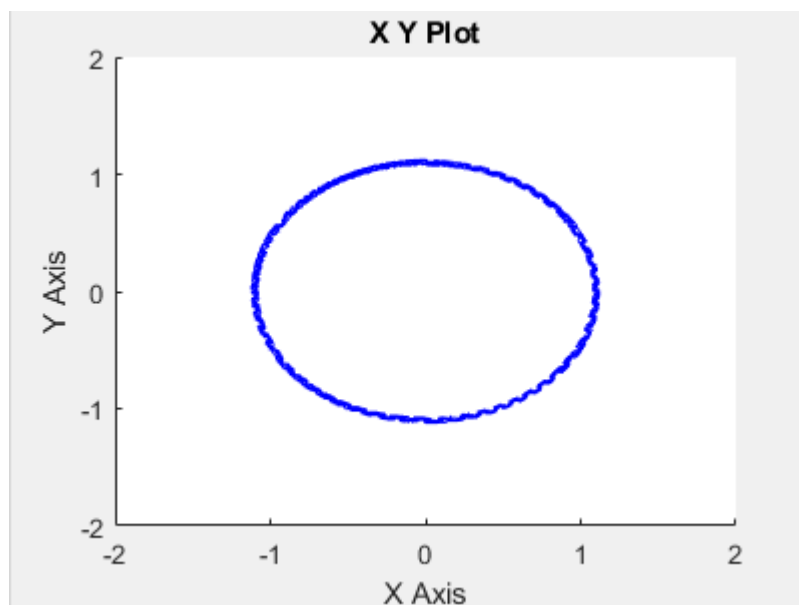Fig IV-29: Motor's Electromagnetic torque "reversing direction without T_r".

Fig IV-30: Path of flux (αβ) "reversing direction without T_r".

The electromagnetic torque stabilized in the vicinity of 0 N.m because there is no load then decreased after 0.5s, i.e. the application of the reference speed variation and stabilized at 0N.m again.

The path of the stator flux is practically circular.

The figures bellow shows the simulation results over 2s with reversing of speed direction at 1 s with applying a resistant torque.
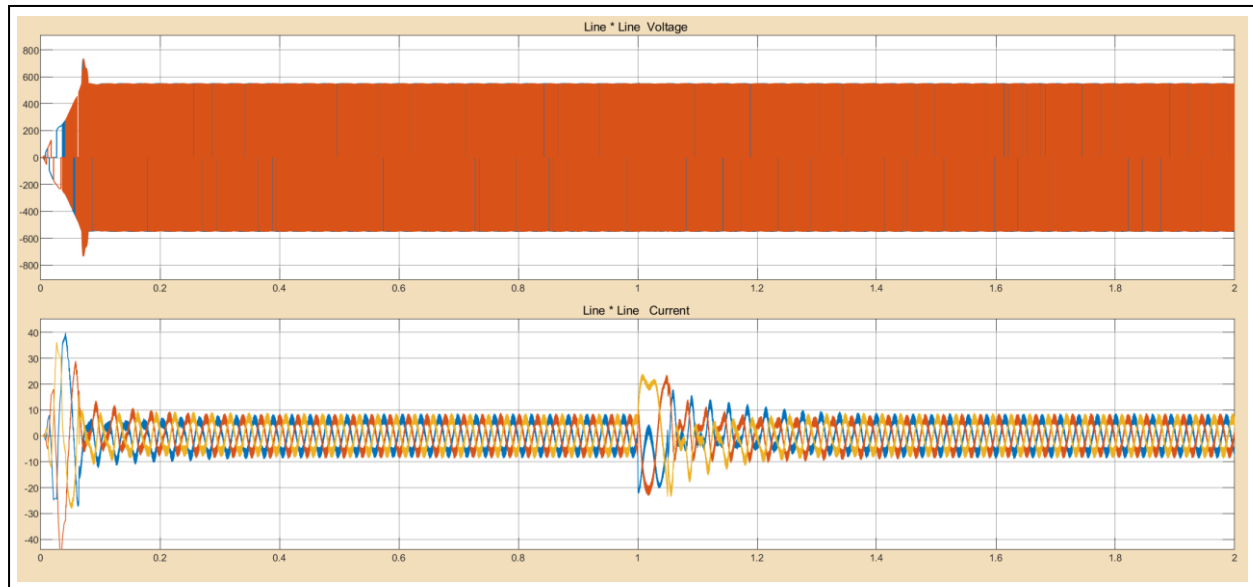

Fig IV-31: Line to line current and voltage curves "reversing direction with T_r".

It's clearly from Fig IV-31 that stator currents are influenced by the speed variation
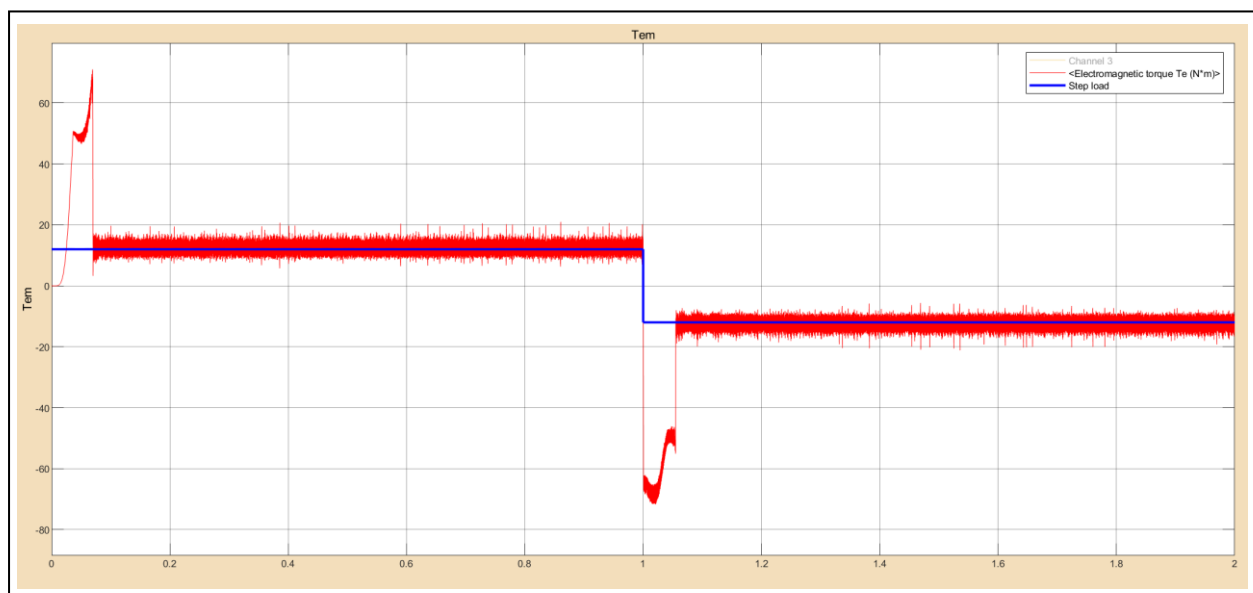

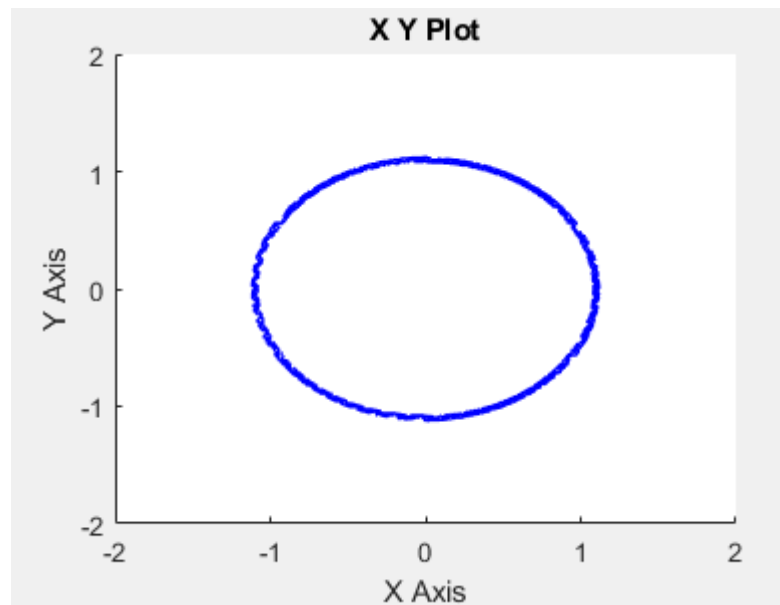Fig IV-32: Motor's Electromagnetic torque "reversing direction with T_r".

Fig IV-33: Path of flux (αβ) "reversing direction with T$_r$".

IV.4.4 Low speed test

The figures below show the simulation results of a start at 0.05 (s) and over 1s with the application of load torque at 0.06 (s) equal to 12N.m and a reference flux of 1.1Wb. The width of the hysteresis band of the torque comparator is in this case fixed at ± 0.2 N.m and that of the flux comparator at ± 0.02Wb
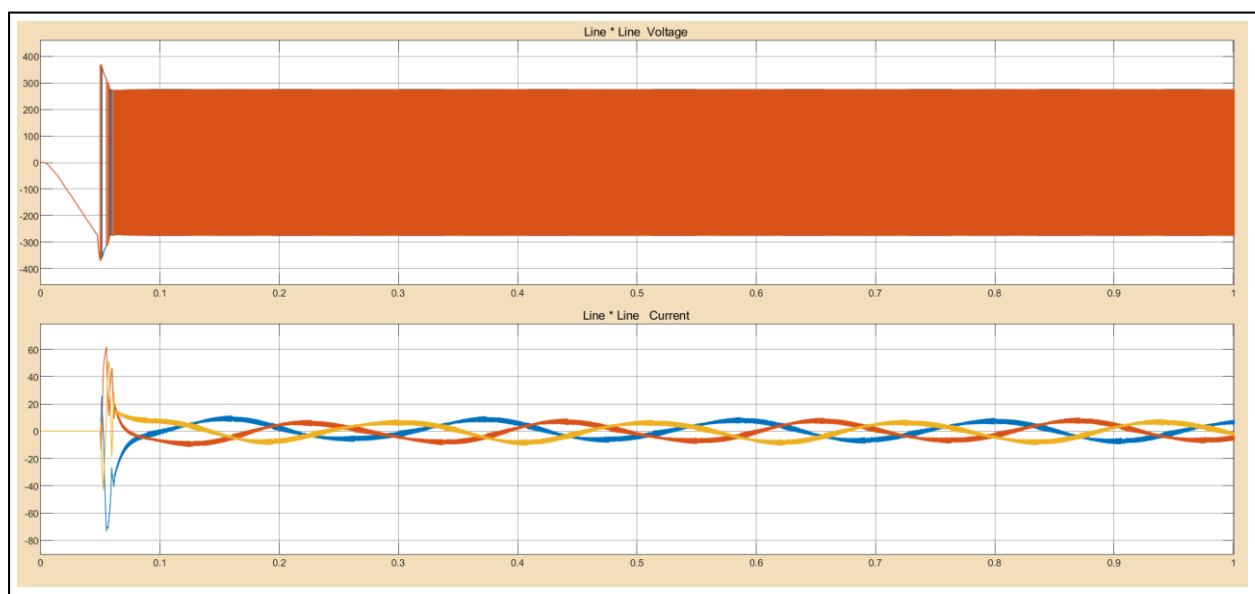

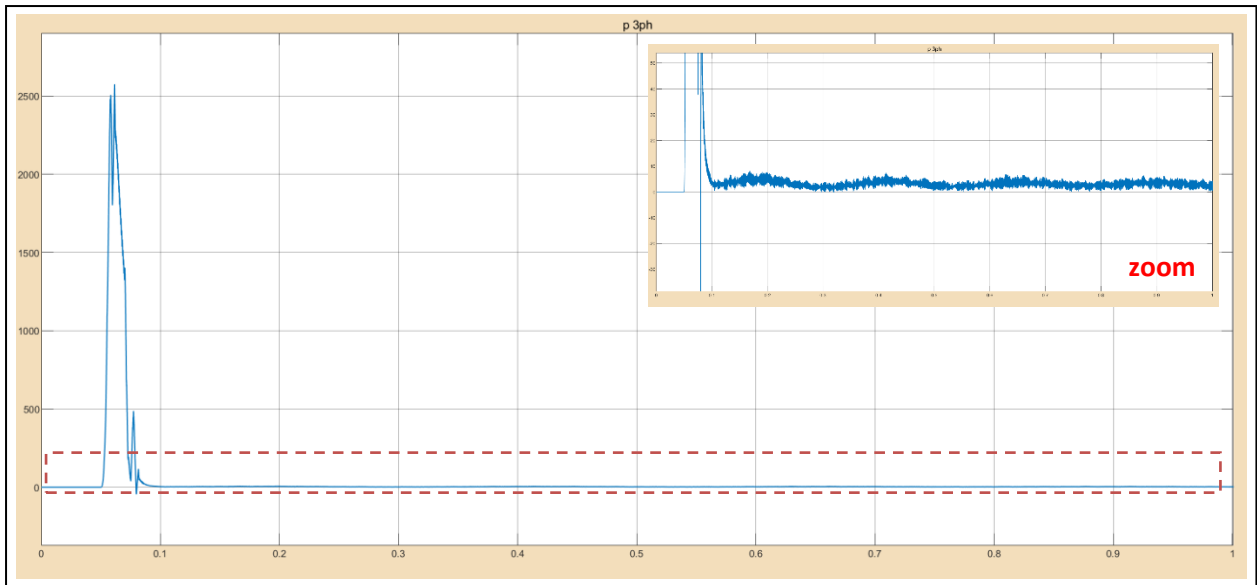Fig IV-34: Line-line current and voltage response curves for low speed test.

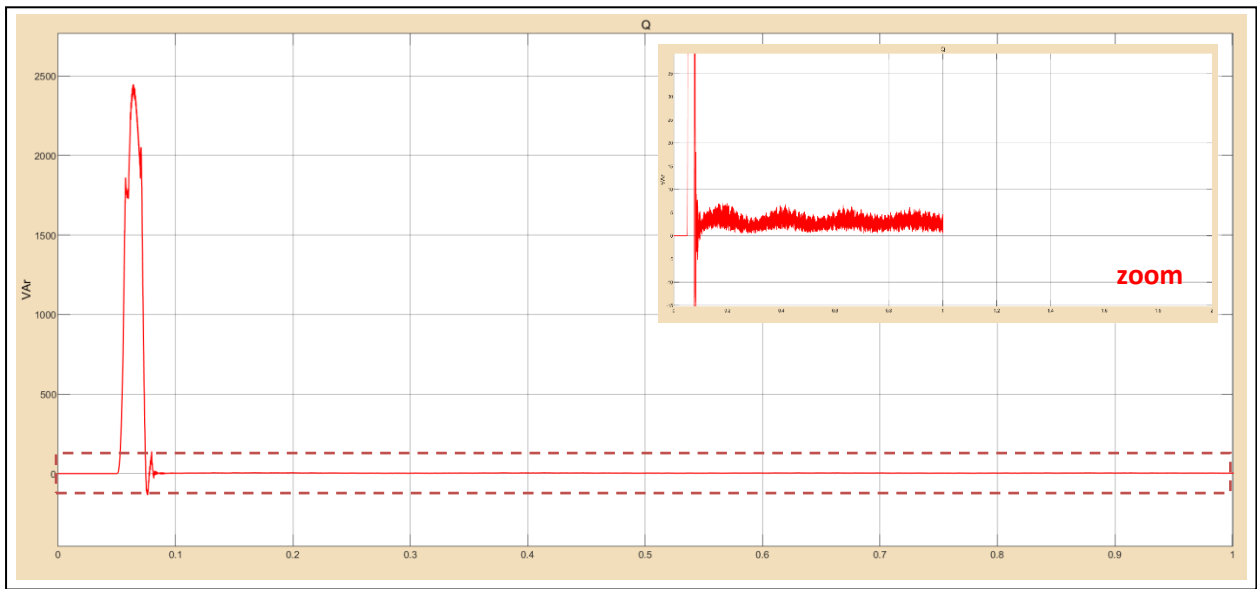Fig IV-35: AC active power curve for low speed test..

Fig IV-36: AC reactive power curve for low speed test.
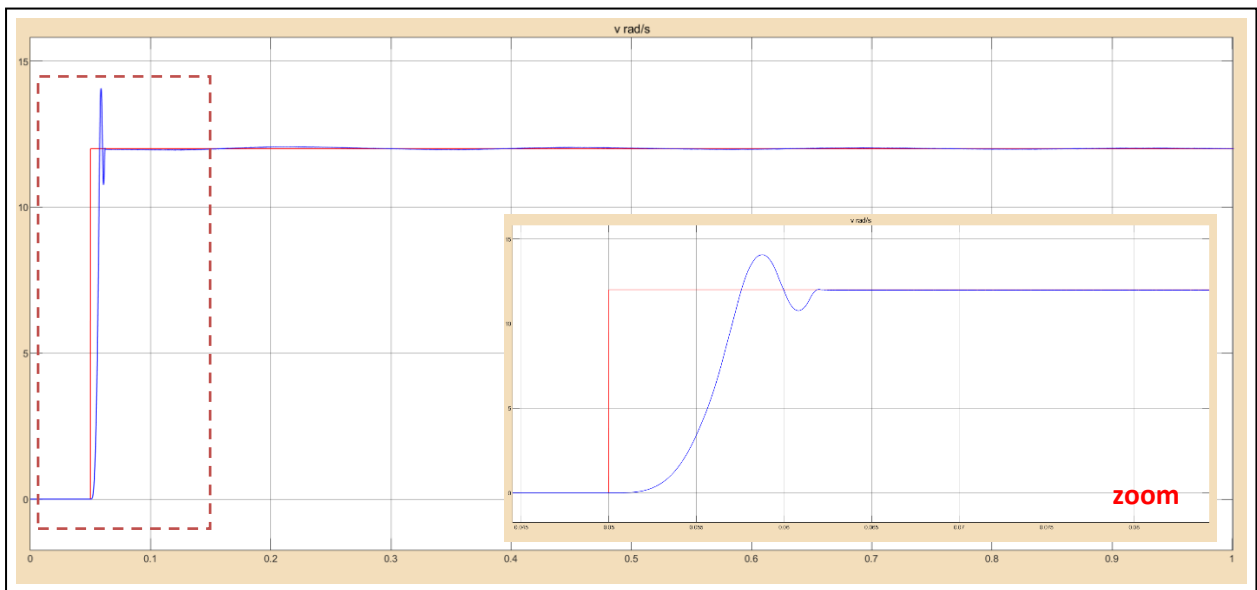
Fig IV-37: Speed and reference curves for low speed test.
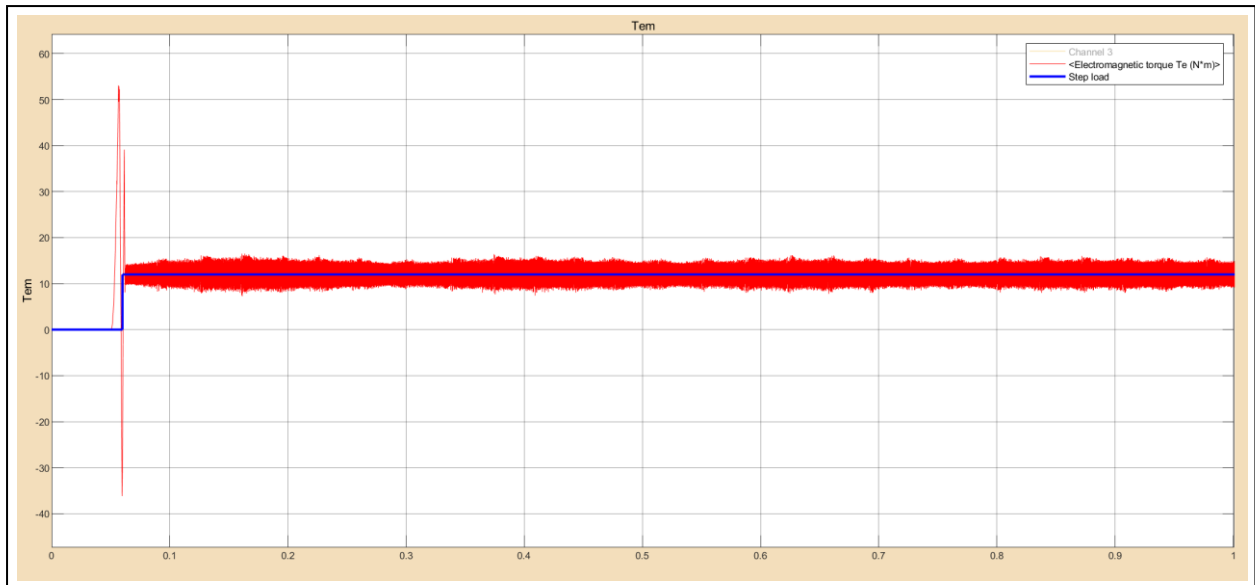
Fig IV-38: Motor's Electromagnetic and reference torques for low speed test.
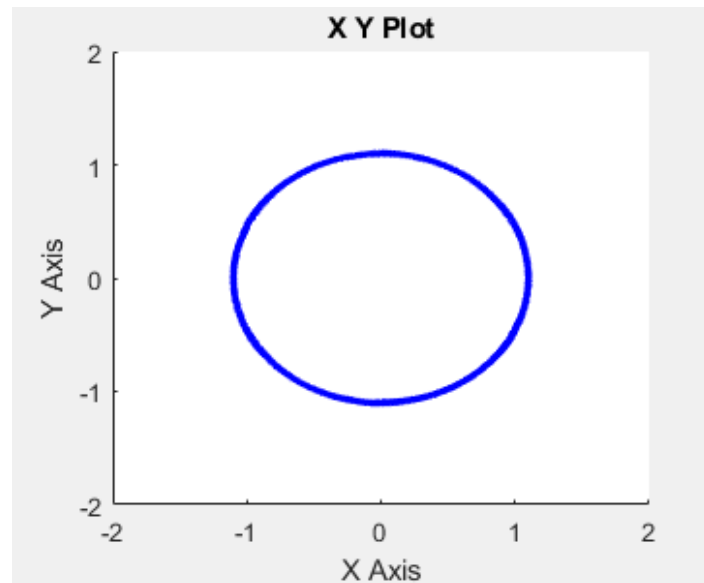
Fig IV-39: Path of flux (αβ) for low speed test.

The system responds positively to this test, the speed follows its new reference with small exceeding, despite the oscillation the electromagnetic torque stabilized in the vicinity of the value of the load.

We note from the results obtained that working in low speed slightly affects the performance of the control, that is to say that the control reacts so as to eliminate this effects .

IV.5 System results

From the previous simulation results, we can say that our control system is robust because it has responded positively to the various robustness tests and that the DTC has good dynamic, static torque and flux performance. As a result of that we submitted the system vehicle drive train to real driving cycle reference (NEDC) and fixed torque (12 N.m) in this case vehicle speed is controlled directly, and second part we will fix the reference to 60 rad /s and connect the mechanic model to electric model ,in this work we will control vehicle speed indirectly by controlling the motor so it will be deduced.

The results of Vehicle dynamic and system simulation are in this part

IV.5.1 Results for NEDC reference
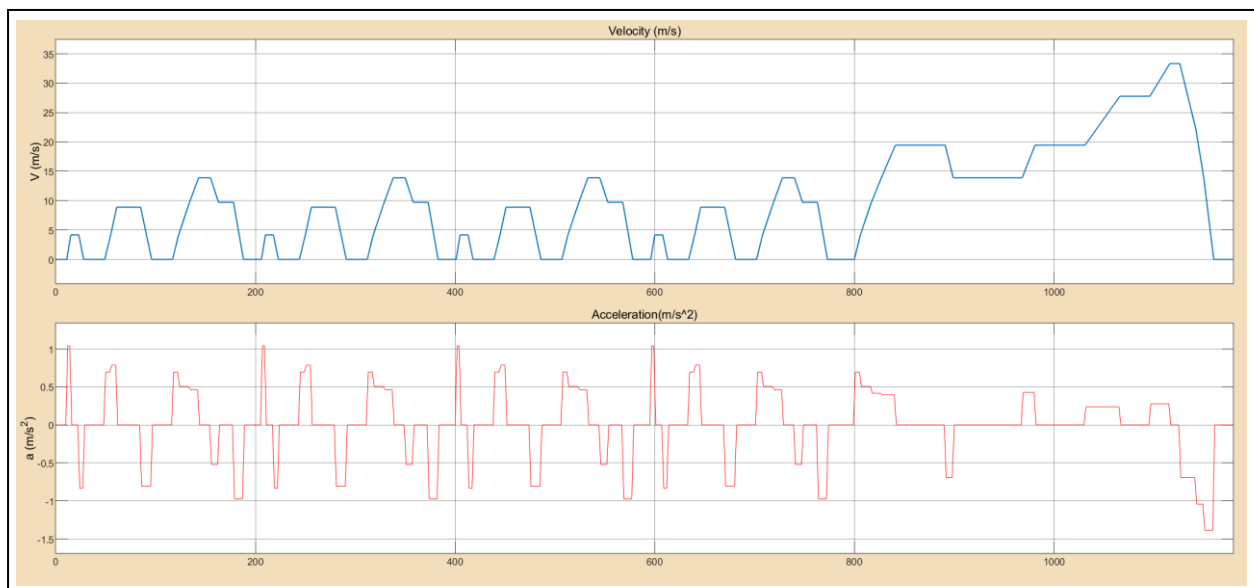
Fig IV-40: Velocity and acceleration curves on NEDC
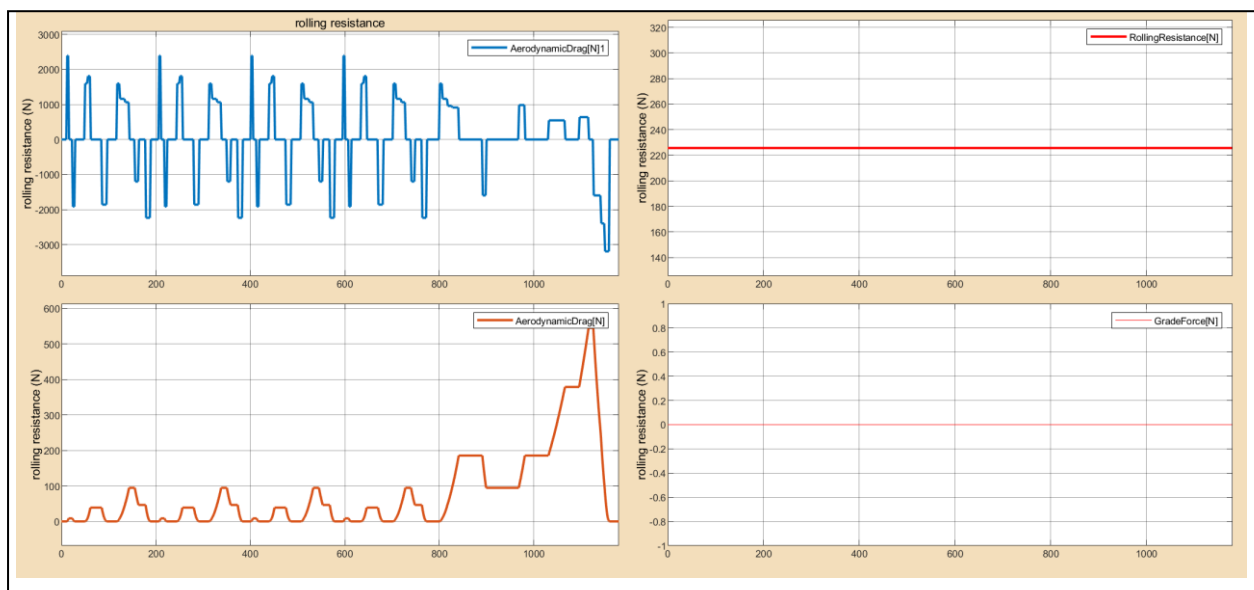
Fig IV-41: Different forces applied to the vehicle (α=0°).
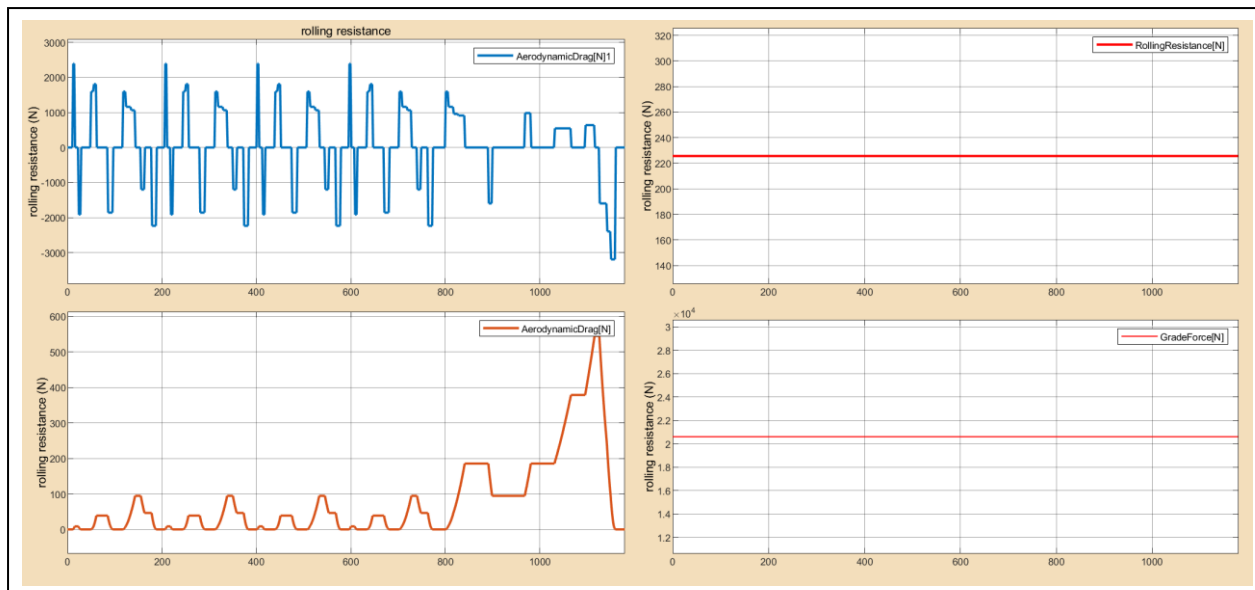
Fig IV-42: Different forces applied to the vehicle (α=20°).
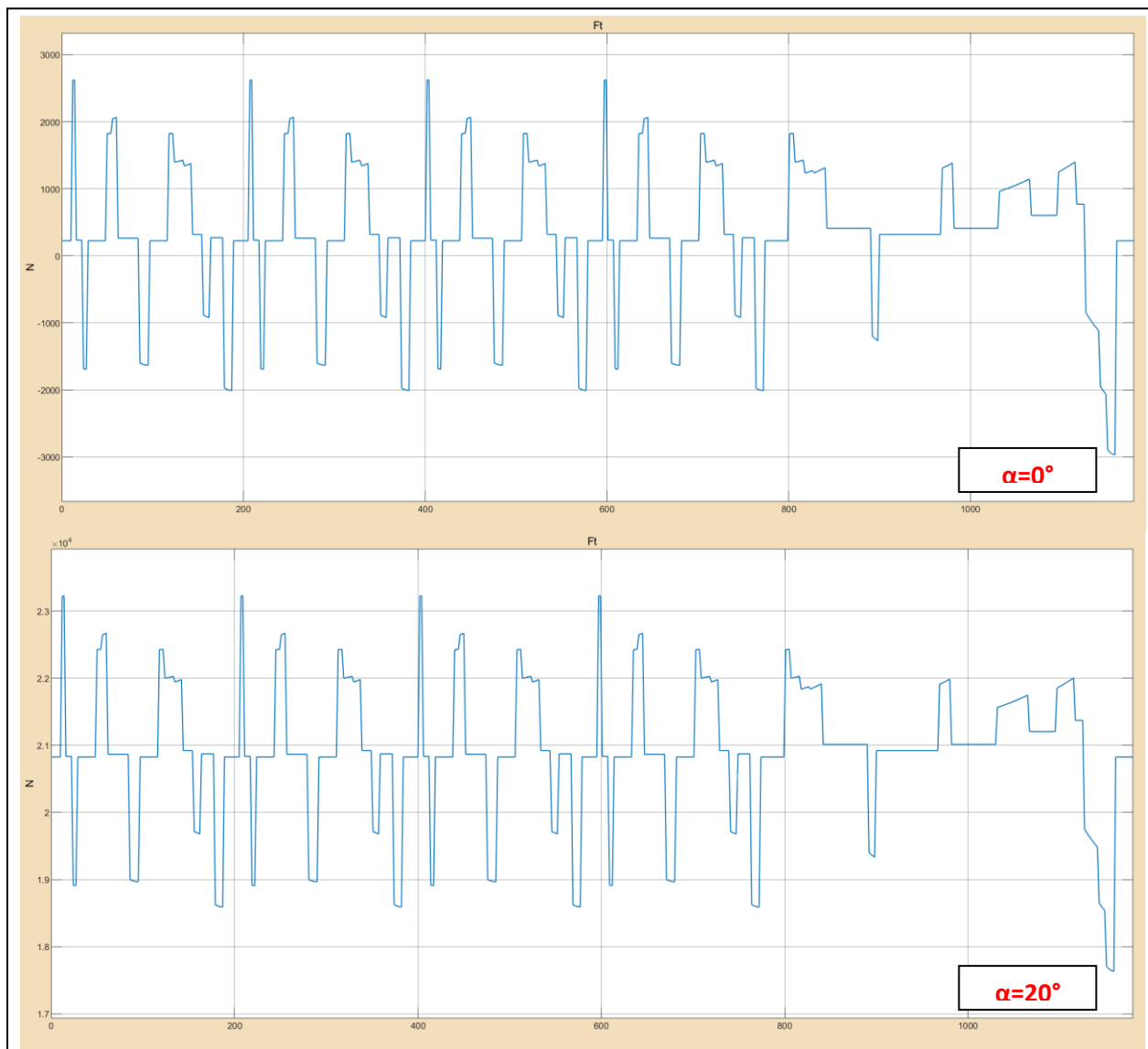
Fig IV-43: Tractive force curve for α=0° and α=20°.
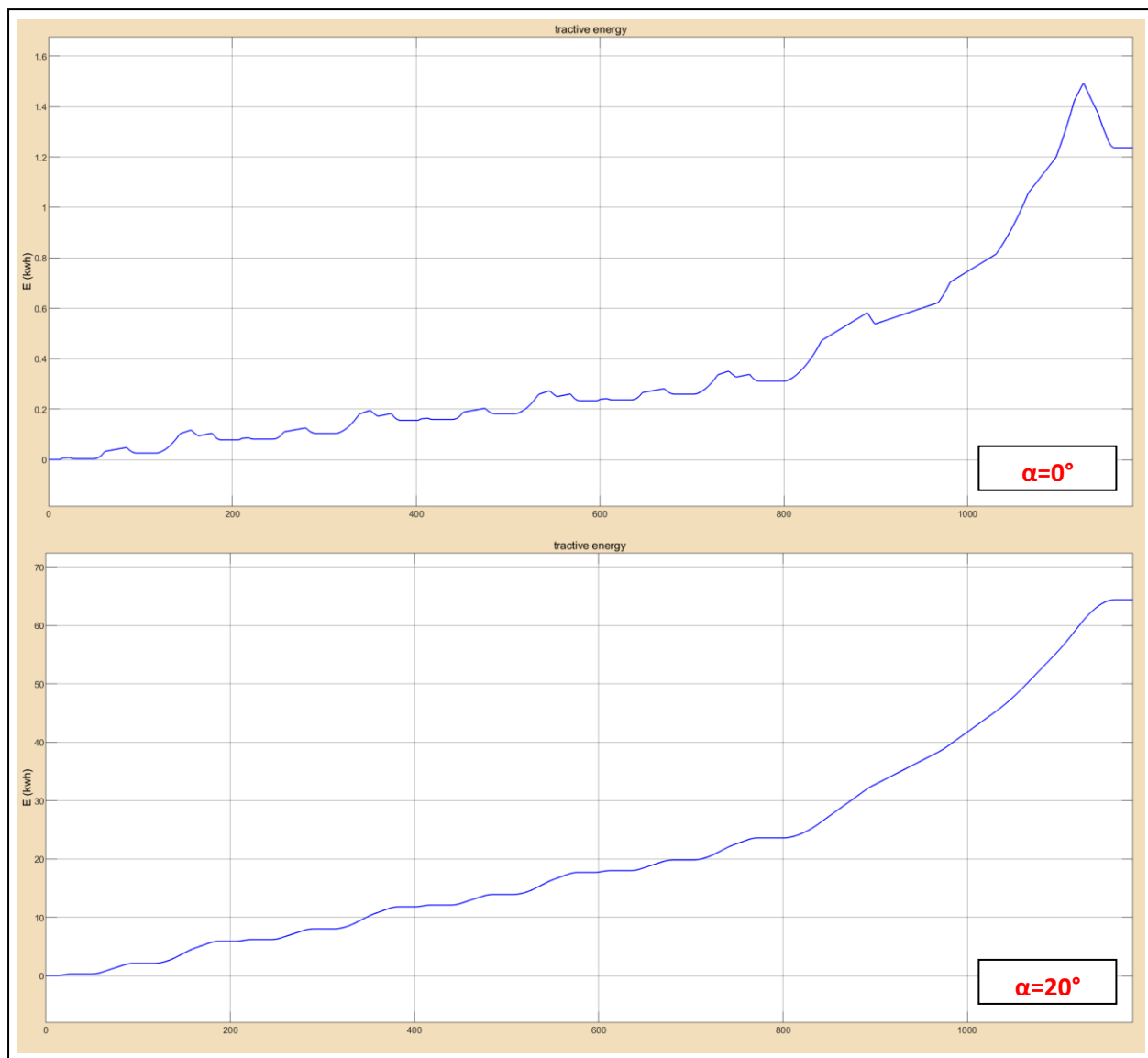
Fig IV-44: Tractive energy curves for α=0° and α=20°.

We can see froù (Fig IV-44) that total tractive force and tractive energy are more bigger when α=20° Than values when α=0° because the grad force is absent in the second one.
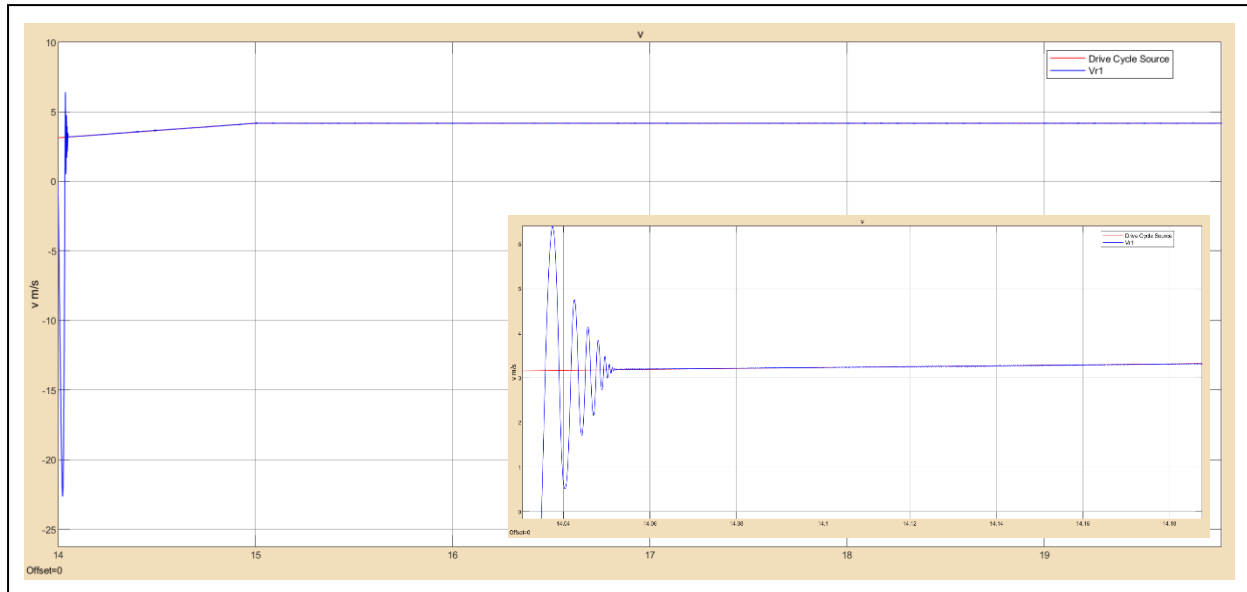
Fig IV-45: Vehicle speed with NEDC reference(m/s) [14-20 s]

We can see from (Fig IV-45) that vehicle speed has oscillation at first time then it followed its reference.

IV.5.2 Results for constant speed reference

For this simulation part we suppose vehicle runing in straight road from 0 to 1 s then it rises by 2 % until 2s , the reference speed is 60 rad/s
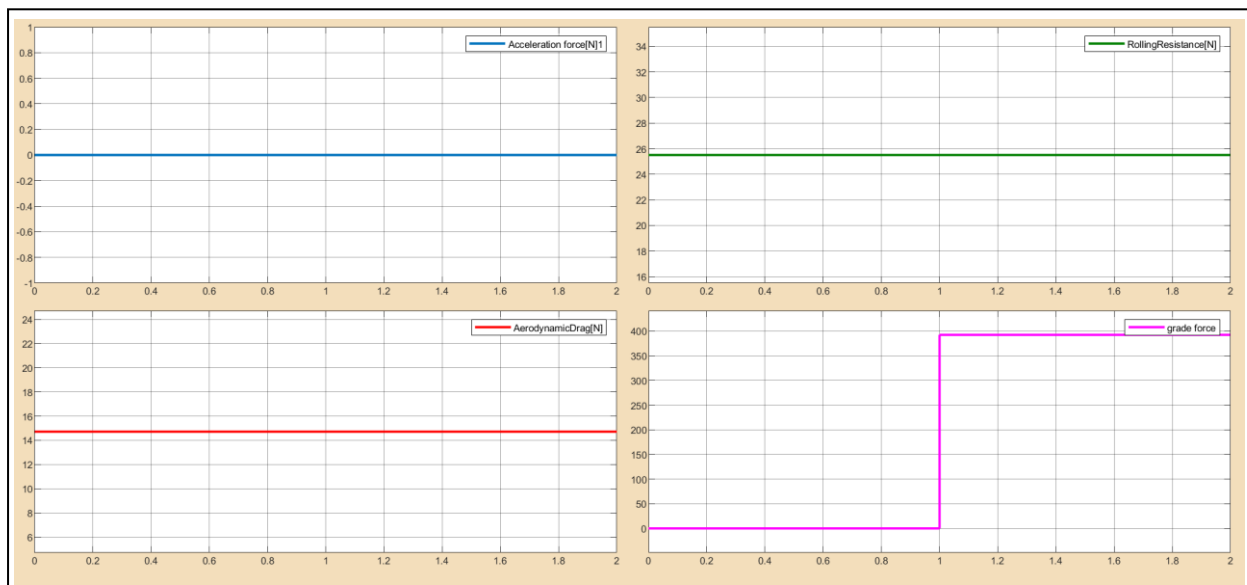
Fig IV-46: Different forces applied to the vehicle "Constant speed reference"
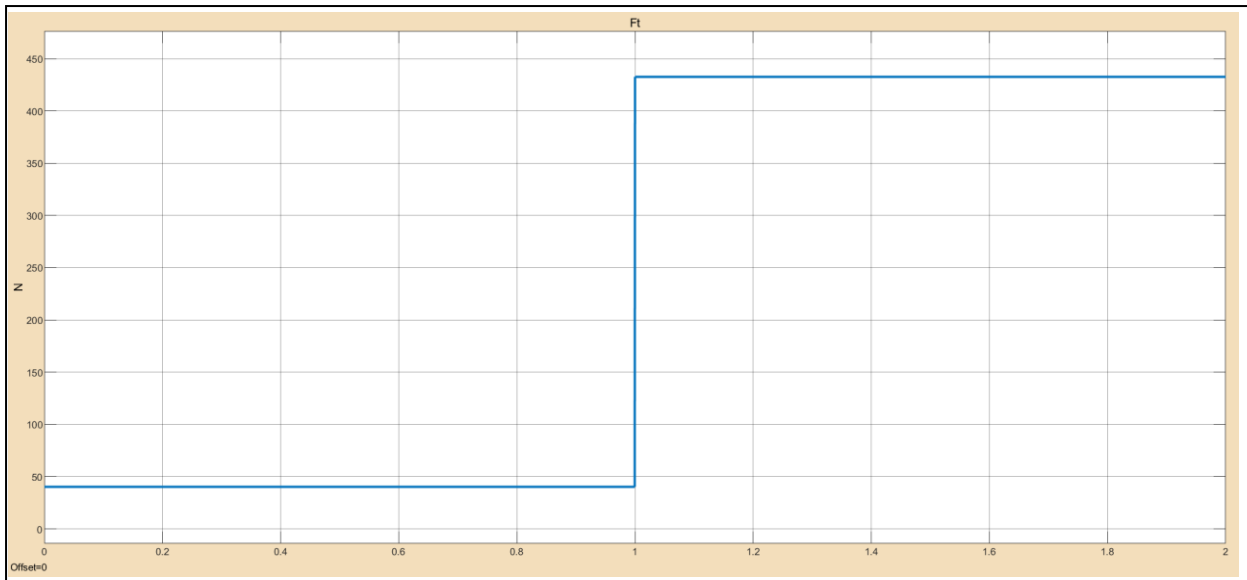
Fig IV-47: Tractive force curve"Constant speed reference"
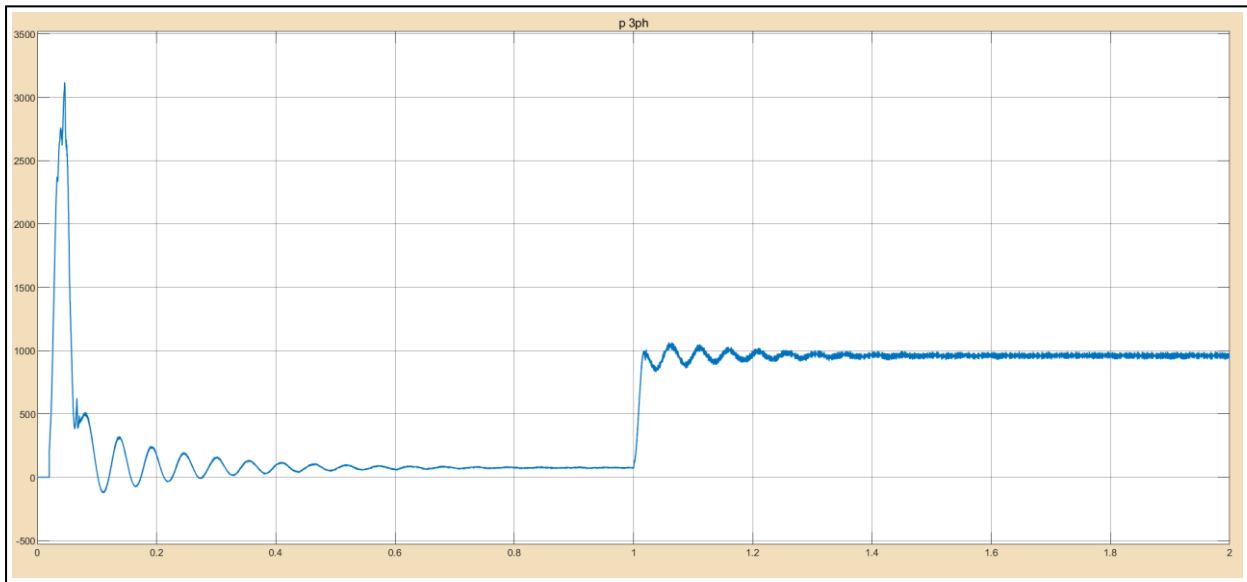
Fig IV-48: AC active power "Constant speed reference"
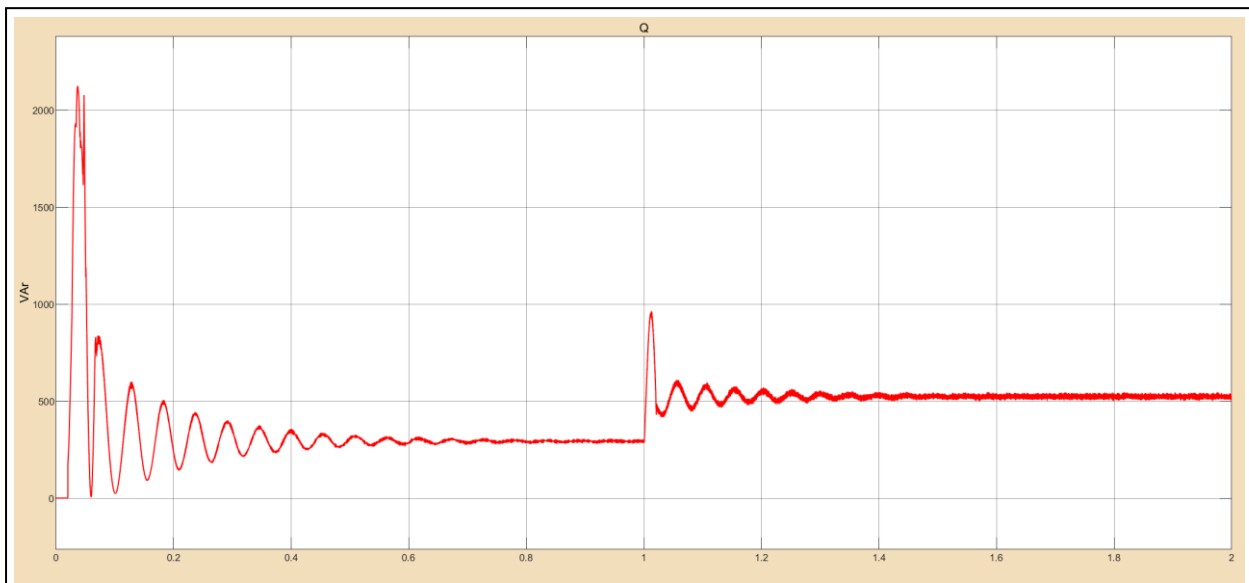
Fig IV-49: AC reactive power "Constant speed reference"
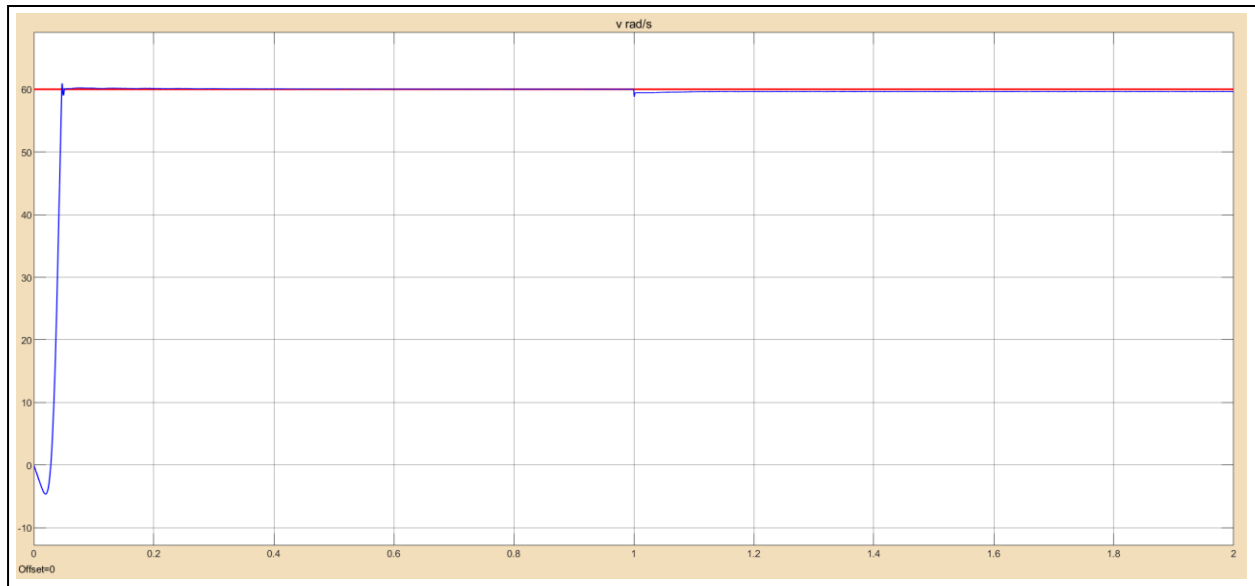
Fig IV-50: Motor and reference speed "Constant speed reference"

Fig IV-50 shows that the speed follow the reference from 0 to 1 (s) then there is pic and a very small error 0.3 rad/s .
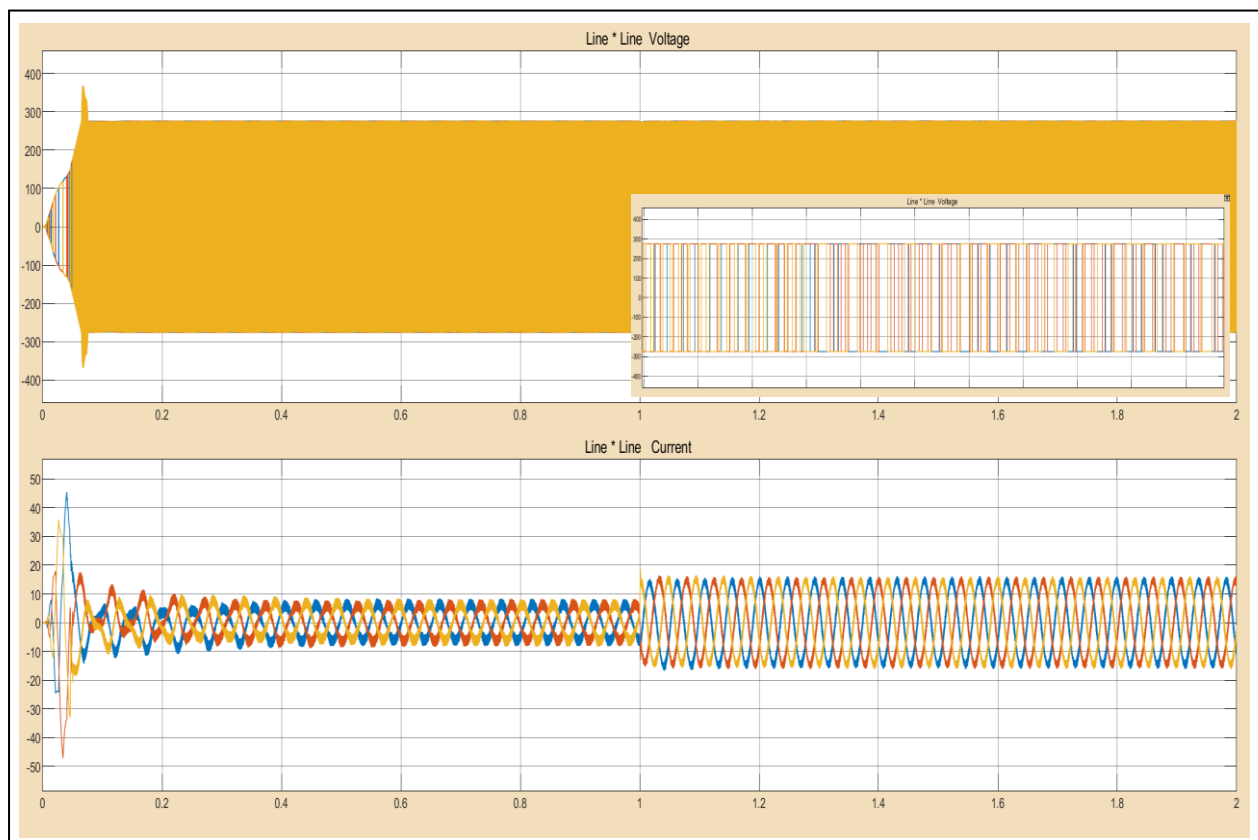
Fig IV-51: Line to line voltage and current curves "Constant speed reference"

Ater the road's height at 1(s) we can see that the current increase
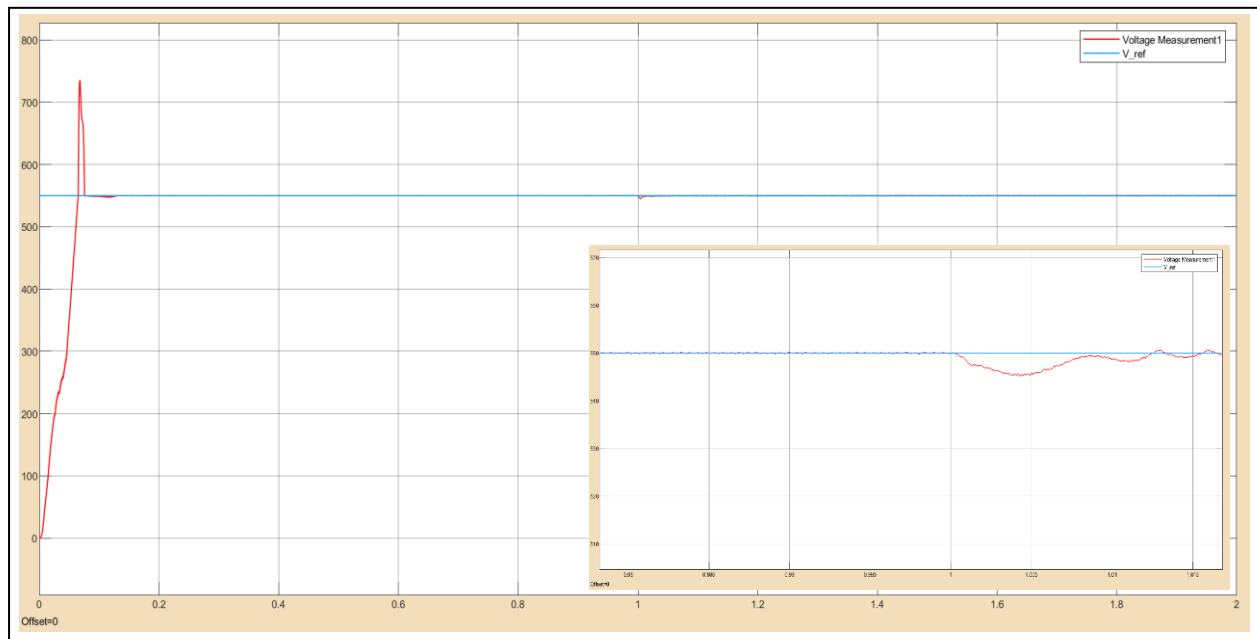
Fig IV-52: DC bus voltage "Constant speed reference"
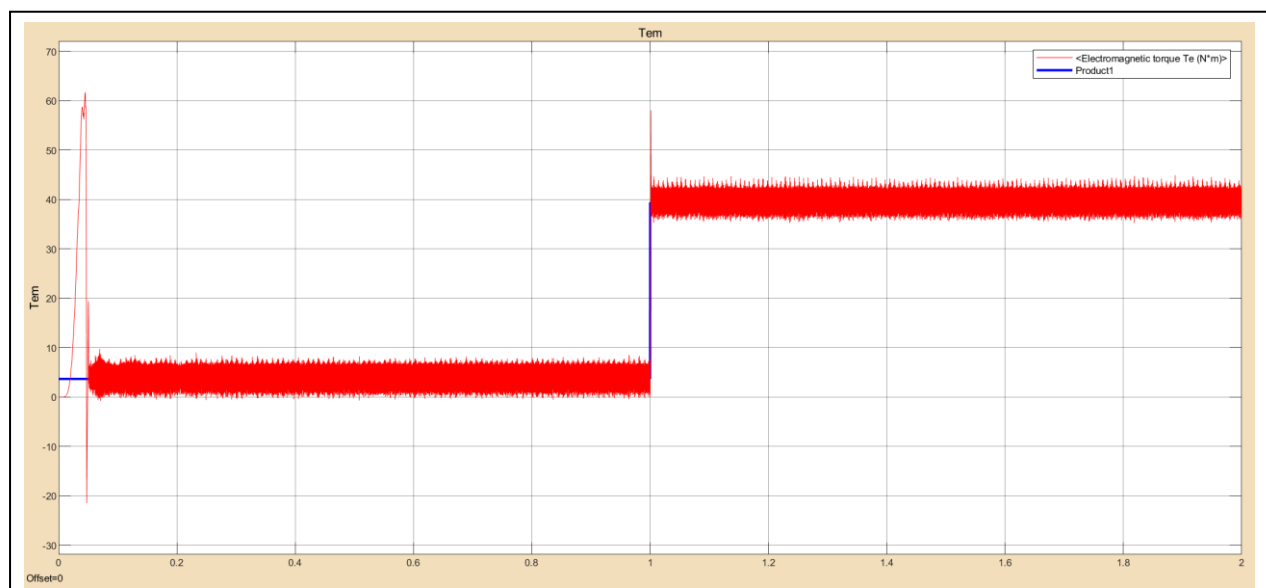
Fig IV-53: Electromagnetic and load torque "Constant speed reference"

From this figure (Fig IV-53) we can see that vehicle load is 3.6N.m for the first phase and 39.4 N.m for the second, electromagnetic torque is bigger than vehicle load which make the vehicle move.

IV.6 Conclusion

In this chapter we have presented the results of simulations of electric vehicle system (fuel cell , battery , ASM and vehicle dynamic) where the DC bus was controlled with PI regulator and the motor speed (likewise vehicle speed) by direct torque control.

To control the DC bus voltage "with storage" method gives a good response and the battery enters into perturbation situations and start-up and can control the voltage drop between the reference and measured DC bus voltage (error).

Despite the current peaks generated by speed changes in some cases are very dangerous and can lead to the destruction of the used motor and that the presence of hysteresis regulators leads to a variable switching frequency and oscillations in the torque which constitutes the major problem of the classic DTC ,but after studying the robustness of this control the simulation results showed that the DTC has good dynamic and static flux performance and the system responds positively to the tests with low performance in low speed..

The system followed all the changes hat thas been done and we saw that the angle of inclination of the road affects to the value of tractive energy and power.

Finally we can say that we reached our goal of speed control using DTC control and DC bus regulation using the propsed strategy.

General conclusion

General conclusion

In this thesis, we have presented and studied a model of an electric vehicle powered by a hybrid source (fuel cell , battery) in fact the source part control laws have targeted to regulate the DC bus voltage , and with the use of the asynchronous propulsion engine control based on the classic DTC we could adjust the speed according to a given reference speed.

At first, we made a general view on electric vehicles their history, the different architectures and the various constituents that are part of this system and we compared between them according to their characteristics, this allowed us to specify the types of system components and fixing the vehicle configuration. So our suggestion settled on choosing hybrid vehicle with fuel cell where the electric motor of asynchronous type is powered by a proton exchange membrane fuel cell assisted by a lithium ion battery as secondary source in order to control and fix the DC bus voltage at 550 v.

In the second chapter, a modelization of the different constituents of the proposed system was made and we focused more on the electrical part and some influences were neglected in order to facilitate the work like the effect of temperature on fuel cell,This modelization allowed us to know the exact components of the system and we expect its responses.

In the third chapter, we presented the different control approaches where choppers were controlled with PI regulator using hysteresis bloc , the first chopper attached to fuel cell to boost its voltage and the second buck-boost work with specific condition in order to control the DC bus voltage, in another hand , the principles of DTC strategy were presented in detail, with an explanation of the principle of flux and electromagnetic torque adjustment. this strategy is based on the determination of the vector control applied to the inverter by the use of hysteresis regulators and a stswitching table whose function is to control the stator flux amplitude and the torque. the proposed strategy is applied to the motor and the end to whole vehicle, taking into account its aerodynamics. We finished that with a simulation tests to validate the feasibility of the techniques used and study the whole system on general.

After gathering information from specialized research, that was carefully selected and according to our simulation results we can conclude that the PEMFC is suitable as a main source for electric vehicles because of its high performances operating temperature, storage strategy is a good solution for DC bus regulation because of its simplicity and efficiency, also we conclude that the DTC solved inconvenience of vector controls based on the orientation of the rotor flux which is relatively sensitive to parametric uncertainties and our smulation results showed that the DTC has greater simplicity and robustness against parametric variations , and followed the different trajectory , the disturbance is rejected in a very short time, fast response and the overshoot is negligible .However, it has some drawbacks most notably torque and current ripples and the difficulty in estimating the reference torque at low speeds.

This work allowed us on the one hand to know the basic principles of knowledge system modeling, power supply techniques, control and adjustment of the speed of the asynchronous machine using DTC , Check out the different types of EV's and their dynamics.

At the end of this work we affirmed that a large part of the objective set has been achieved, for the continuity of this work it occurs to us to define the lines of research which are encouraging . for the development of EVs in view of their performance and autonomy :

- ✓ The use of multi-level inverters, controlled by artificial intelligence techniques (neural network and genetic algorithms). to increase the number of useful voltage vectors and minimize disturbances.
- ✓ The use of a third source (supercapacitor) with intelligent supervisor to optimize the energy produced.
- ✓ Make a comparative study of a vehicle with two or 4 engines.

Bibliography

Bibliography

[1] : Farid Khoucha, Abdelkader Khoudiri, Mohamed Benbouzid, Abdelaziz Kheloui. Commande DTC d'une propulsion moteur asynchrone / onduleur multiniveaux asymétrique pour un véhicule électrique. European Journal of Electrical Engineering, Lavoisier, 2011, 14 (2-3), pp.237-254. ffhal-00728314f

[2]: S.ANTOINE et A.DURET (1974),Vers une deuxième génération les véhicules électriques,France-Paris , La Documentation Française

[3]: A.Nouh , Contribution au développement d'un simulateur pour les véhicules électriques routiers, doctoral thesis , University of technology Belfort-Montbéliard and Franche-Comté universty, March 2008.

[4]: I.MARIF & H.ABDAT , La commande en vitesse d'un véhicule électrique , MASTER thesis, University of Tlemcen , july 2019.

[5]: http://www.avere-france.org/Site/Article/?article_id=7851&from_espace_adherent=0

[6] : Z.Guirong et al, The Driving Control of Pure Electric Vehicle,3rd International Conference on Environmental Science and Information Application Technology pp.433 − 438 Shandong Jiaotong University, China,2011

[7]: B.Mok Types of Batteries Used for Electric Vehicles, coursework for PH240, Stanford University, October 2017.

[8] : B.Daan, Battery Electric Vehicles Performance, CO2 emissions, lifecycle costs and advanced battery technology development, Master thesis in Sustainable Development, Energy and Resources ,University of Utrecht, augest 2010

[9]: Vidyanandan, K.V.. (2018). Overview of Electric and Hybrid Vehicles. Energy Scan (A House Journal of Corporate Planning, NTPC Ltd., India). III. 7-14.

[10]: E.HELEREA et al, Batteries and supercapacitors for power systemes used in transport,international conference on electromechanicak and power systems, University of BrasovOctober 8-9, 2009

[11]: Leccese, Fabio. (2013). Fuel Cells: Technologies and Applications. The Open Fuel Cells Journal. 6. 1-20. 10.2174/1875932720130719001.

[12]: H.BENARIBA,Contribution à la commande d'un véhicule électrique , doctoral thesis in electrical engineering, University of Aboubakr Belkaïd Tlemcen , december 2018.

[13]: D.Murray-Smith,(2019). A Review of Developments in Electrical Battery, Fuel Cell and Energy Recovery Systems for Railway Applications, A report for the Scottish Association for Public Transport, November 2019
http://eprints.gla.ac.uk/204435/1/204435.pdf

[14]: Zarma, Tahir & Galadima, Ahmadu & Maruf, Aminu. (2019). Review of Motors for Electrical Vehicles. Journal of Scientific Research and Reports. 1-6. 10.9734/jsrr/2019/v24i630170.

[15]: Lukman, Grace & Hieu, Pham & Jeong, Kwang-Il & Ahn, Jin-Woo. (2018). Characteristics Analysis and Comparison of High-Speed 4/2 and Hybrid 4/4 Poles Switched Reluctance Motor. Machines. 6. 4. 10.3390/machines6010004.

[16]: H.Chetouane and A.Benamira, Etude paramétrique d'une machine synchrone à aimants par logiciel ANSYS Maxwell ,Master thesis, University of Jijel ,2019

[17]: Kamel, Khechiba.(2016).Design and implementation of microcontroller based controller for direction and speed of a robot using ARDUINO. 10.13140/RG.2.2.22462.69447.

[18]: A.Ferhat and S.TOUAHRI , Etude et simulation d'un système redresseur MLI – onduleur Pour l'entrainement de la MAS, Master thesis, University of Ouargla September 2015.

[19]: A.BOUKAROURA, Modélisation et Diagnostic d'un Onduleur Triphasé par l'Approche Bond-Graph,, Magister thesis ,Electrotechnical department university of SETIF December 2009

[20]: L.CHEBBI, Etude et simulation d'une pile a combustible de type PEM , master thesis in Mechanical Engineering Akli Mohand Oulhadjde university of Bouira , june 2016

[21] : S.SAKER,Modélisation et Contrôle du système Pile à Combustible, convertisseurs et Super condensateur Magister thesis in industrial electricity , Mohamed Khider university of Biskra, October 2016

[22]: A.YOUCEFI B.TELEMÇANI , Modélisation d'une pile à combustible de type PEM, Master thesis, Mohamed Boudiaf university of M'SILA , 2016/2017

[23]: N. Benchouia , A.E. Hadjadj , A. Derghal , L. Khochemane ,and B. Mahmah (2013) Modeling and validation of fuel cell PEMFC , Revue des Energies Renouvelables Vol. 16 N°2 365 – 377 365.

[24]: Dimitar, Spirov & Lazarov, Vladimir & Daniel, Roye & Zarkov, Zahari & Mansouri, Omar. (2009). MODELISATION DES CONVERTISSEURS STATIQUES DC-DC POUR DES APPLICATIONS DANS LES ENERGIES RENOUVELABLES EN UTILISANT MATLAB/SIMULINK ®.

[25]: Naffouti, Seif Eddine. (2012). Dimensionnement et commande d'un hacheur parallèle alimenté par une source photovoltaïque. 10.13140/RG.2.1.1409.7682/1.

[26]: M.BAGHLI and O.M.BOUDIA, Commande d'un moteur asynchrone triphasé basée sur l'approche des modes glissants avec observateurs de flux et de vitesse, Master thesis in Machine Control , Abou Bekr Belkaid university of Tlemcen ,2013

[27]: Kıyaklı, Ahmet & Solmaz, Hamit. (2019). Modeling of an Electric Vehicle with MATLAB/Simulink. International Journal of Automotive Science And Technology. 9-15. 10.30939/ijastech..475477.

[28] : Noëlle Janiaud. Modélisation du système de puissance du véhicule électrique en régime transitoireen vue de l'optimisation de l'autonomie, des performances et des coûts associés.. Energie électrique.Supélec, 2011. Français. tel-00660749v1

[29]: Ianko Valero Exposito. INTERFAÇAGE ET CONTROLE COMMANDE DE PILES A COM-BUSTIBLE POUR APPLICATIONS STATIONNAIRES ET TRANSPORT. Sciences de l'ingénieur[physics]. Université Joseph-Fourier - Grenoble I, 2004. Français. tel-00397448.

[30]: Naffouti, Seif Eddine. (2012). Dimensionnement et commande d'un hacheur parallèle alimenté par une source photovoltaïque. 10.13140/RG.2.1.1409.7682/1.

[31]: A.MENADI ,Commande Par Les Techniques Intelligentes D'un Système Photovoltaïque Connecté Au Réseau, Doctoral thesis , Department of Electrical Engineering Mohamed Khider university of Biskra ,2016.

[32]: A.H. ZAIDOU ,Stratégies de commande et réglage des bus continus dédiés aux systèmes de production d'énergies éolienne et solaire, engineering in industrial electronics and computing,Polytechnic School of Antsiranana Madagascar ,2007- https://www.memoireonline.com/09/13/7351/m_Strategies-de-commande-et-reglage- des-bus-continus-dedies-aux-systemes-de-production-denerg2.html

[33]: Hika, Brahim & Khakha, Ismail & Kadri, Farid. (2010). La commande DTC par logique floue d'un moteur à induction alimenté par un onduleur de tension multi niveaux. 10.13140/RG.2.2.27803.98081.

[34]: M.L Nechma ,Modélisation, Commande et Simulation d'un Moteur Asynchrone à cage,master thesis in Electromechanical, Badji Mokhtar university of Annaba, 2019

[35]: Habib BENBOUHENI , Régulateurs PI-flou pour la Commande DTC neuronale sans vecteurs nuls à 12 secteurs d'une MAS de forte puissance, Nature & Technology Journal, Class A Fundamental and Engineering Sciences, 19 (2018) 37-48: http://www.univ-chlef.dz/revuenatec/issue-19/Article_A/Article_479.pdf

[36]: Feroura, Hamza. (2015). commande Directe de couple à fréquence de commutation .constante de la machine asynchrone

[37]: Dehane, Mohamed & Boukhris, Mohamed & Kadri, Farid. (2014). Régulation de vitesse d'une machine asynchrone commandée par DTC. 10.13140/RG.2.2.20945.63845.

Annexes

Annex.A

➢ Fuel cell characteristic's program

```matlab
R = 8.314; % Ideal gas constant (J/molK)
F = 96487; % Faraday's constant (Coulombs)
Tc = 80; % Temperature in degrees C
P_H2 = 3; % Hydrogen pressure in atm
P_air = 3; % Air pressure in atm
A_cell=100; % Area of cell
N_cells=90; % Number of Cells
r = 0.19; % Internal Resistance (Ohm-cm^2)
Alpha = 0.5; % Transfer coeffi cient
Alpha1 = 0.085; % Amplifi cation constant
io = 10^-6.912; % Exchange Current Density (A/cm^2)
il = 1.4; % Limiting current density (A/cm2)
Gf_liq =-228170; % Gibbs function in liquid form (J/mol)
k = 1.1; % Constant k used in mass transport
%%%%%%%%%%%%%%%%%%%%%%%%%%%%%%%%%%%
% Convert degrees C to K
Tk = Tc + 273.15;
% Create loop for current
loop = 1;
i = 0;
for N = 0:150
i = i + 0.01;
% Calculation of Partial Pressures
x = -2.1794+0.02953.*Tc-9.1837.*(10.^-5).*(Tc.^2)+1.4454.*(10.^-7).*
(Tc.^3);
% Calculation of saturation pressure of water
P_H2O = (10.^x);
% Calculation of partial pressure of hydrogen
pp_H2 = 0.5 .* ((P_H2)./(exp(1.653 .* i./(Tk.^1.334)))-P_H2O);
% Calculation of partial pressure of oxygen
pp_O2 = (P_air./exp(4.192 .* i/(Tk.^1.334)))-P_H2O;
% Activation Losses
b = R .* Tk./(2 .* Alpha .* F);
V_act = -b .* log10(i./io); % Tafel equation
% Ohmic Losses
V_ohmic = -(i .* r);
% Mass Transport Losses
term = (1-(i./il));
if term > 0
V_conc = Alpha1 .* (i.^k) .* log(1-(i./il));
else
V_conc = 0;
end
% Calculation of Nernst voltage
E_nernst = -Gf_liq./(2 .* F) - ((R .* Tk) .* log(P_H2O./(pp_H2 .*
(pp_O2.^0.5))))./(2 .* F);
% Calculation of output voltage
V_out = E_nernst + V_ohmic + V_act + V_conc;
if term < 0
V_conc = 0;
break
end
if V_out < 0
V_out = 0;
break
```

```matlab
end

figure(1)
title('Fuel cell polarization curve')
xlabel('Current density (A/cm^2)');
ylabel('Output voltage (Volts)');
plot(i,V_out,'.');axis([0 2 0 1.3]);
grid on
hold on
disp(V_out)
% Calculation of power
P_out = N_cells .* V_out .* i .* A_cell;
figure(2)
title('Fuel cell power')
xlabel('Current density (A/cm^2)');
ylabel('Power(Watts)');
plot(i,P_out,'*');
grid on
hold on
disp(P_out);
end
```

Annex.B

➢ Vehicle parameters

- o **Vehicle mass** m = 2000 kg .
- o **Wheel radius** r = 0.34 m .
- o **CD*A$_f$** = 0.8.
- o **Cr** = 0.013.

➢ Chopper parameters

- o **L$_b$, L$_p$** = 4.5 ×10^-3
- o **C$_b$, C$_p$** =1200 ×10^-6
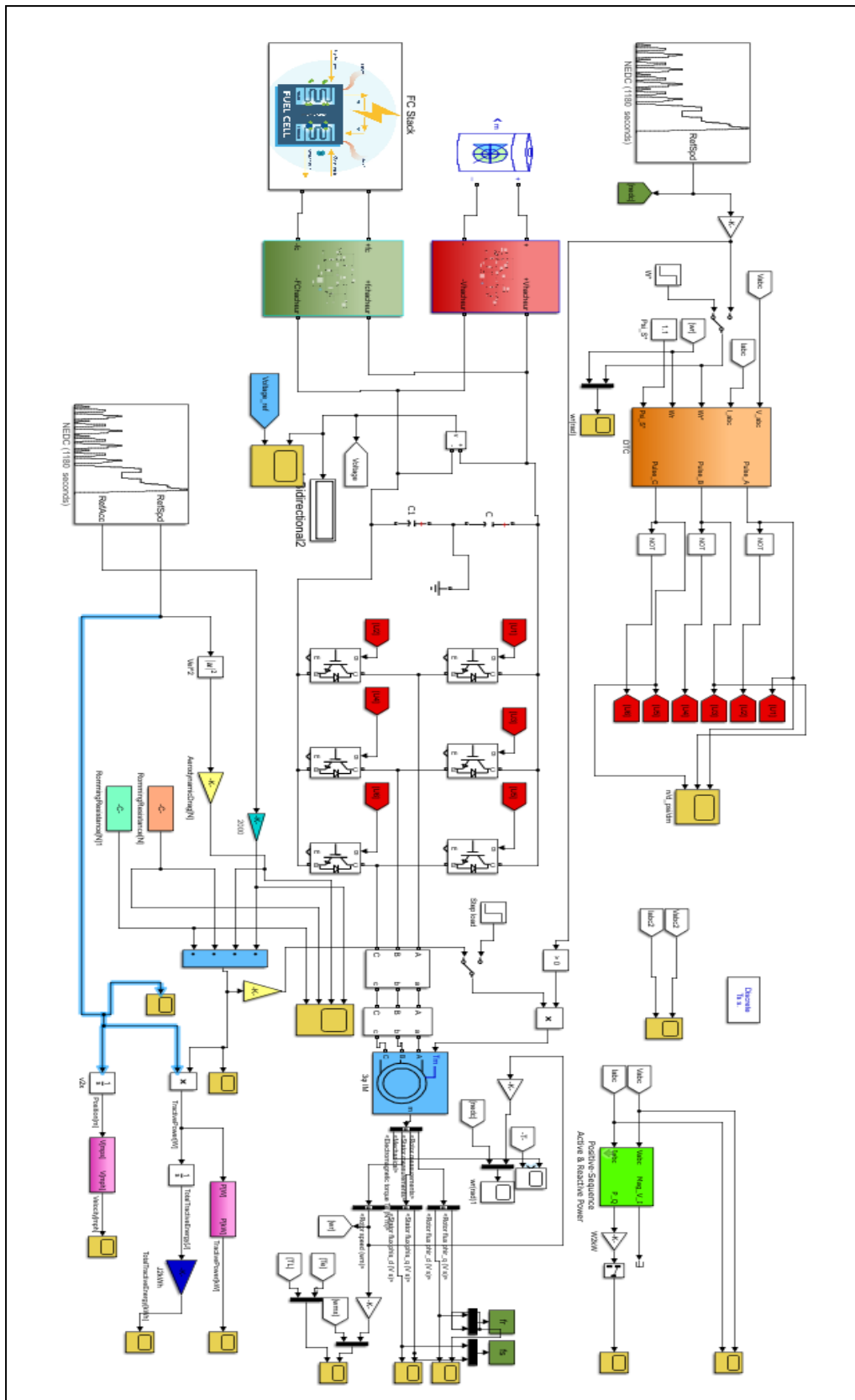- o **C$_{1bus}$, C$_{2bus}$** =2300 10^-6

Annex.C

Fig-1 : Simulation model of the complete system in MATLAB / SIMULINK®